INVESTIGATING PREDICTED WATER RESERVES IN PORTIONS OF THE OGALLALA AQUIFER OF THE TEXAS PANHANDLE USING CONCEPTUAL MODELS

By

Robert Glen Green, III

A Dissertation Submitted in Partial Fulfillment

of the Requirements for the Degree

DOCTOR OF PHILOSOPHY

West Texas A&M University

Canyon, Texas

December 2016

Approved:

_____ _____

Dr. Robert DeOtte
Chairman, Dissertation Committee Date

_____ _____

Dr. Bob Stewart
Member, Dissertation Committee Date

_____ _____

Dr. Brent Auvermann
Member, Dissertation Committee Date

_____ _____

Dr. Ty Lawrence
Member, Dissertation Committee Date

_____ _____

Dr. Lal Almas
Member, Dissertation Committee Date

_____ _____

Dr. Lance Kieth
Head, Major Department Date

_____ _____

Dr. Dean Hawkins
Dean, Major Department Date

_____ _____

Dr. Angela Spaulding
Dean, Graduate School Date

PREFACE

Throughout this paper the term "Ogallala aquifer" is used. Gutentag and others (1984) proposed using the term High Plains aquifer and provided two main reasons. As summarized by Dutton (2001), "first, groundwater can move between the Ogallala formation and adjacent Permian, Mesozoic, and Quarternary formations, so the term Ogallala aquifer is inadequate to refer to the whole aquifer system. Second, not all of the Ogallala Formation is saturated. The term "High Plains aquifer" addresses these issues and avoids use of a formational name that is also an aquifer name."

The use of the term "Ogallala aquifer" is used throughout this document since this is still the most recognized name of the water bearing zone.

Exhaustive efforts were made while researching the material for this document to ensure references using either "Ogallala aquifer" or "High Plains aquifer" were found and proper credit and reference given.

Images used in this document are used with permission from the USGS, USDA and TWDB provided proper credit is cited.

ABSTRACT

The Ogallala aquifer is a vital source of water for the Texas High Plains. Irrigated crop production is primarily dependent upon water mined from the aquifer. State water policy requires establishing desired future conditions for groundwater management areas. In order to accurately estimate the water remaining in storage, groundwater models are used to monitor aquifer drawdown. Current models are based upon the Well Measurement Approach (WMA). This approach utilizes field measurements to determine the water surface elevation. Models are then constructed to match the surface elevations from year to year. Once calibration is complete, these models are then used to project future water remaining water levels.

Observations of additional water in the aquifer using the Agronomic Water Mass Balance Approach (AWMBA) led to the hypothesis that additional water remains between wells after pumping. The additional water suggested by the AWMBA indicates that more water may be available than models based upon the WMA indicates. Further, this implies that new water surface elevations are not fully established when normal field measurements are taken. A conceptual model using two wells was developed to evaluate the output of the software. Two additional models using portions of both the Northern and Southern groundwater availability models were then studied to determine whether mounded water would be present between pumped wells. The wells used in the model

were allowed to pump for 120 days per year and rebound for the remainder of the year. The models used in this study did not allow for recharge of the aquifer as this is not believed to be a viable source to explain the differences between the Well Measurement Approach and the Agronomic Water Mass Balance Approach.

Results of the study indicate that mounded water does exist between pumped wells. This is due to the delay of the aquifer to return to a flat water table condition between pumping cycles. Complete well rebound takes as many as seven years. Well measurements do not allow for complete rebound and thus do not accurately measure the actual amount of water remaining in the aquifer.

As a result of the proposed mounds in the Agronomic Mass Balance Approach, more water may be available in the Ogallala aquifer than previously reported. The scope of this study was not to provide an accurate account of the additional remaining water but the results do indicate further study along this line would provide a better estimate of the water remaining in storage.

ACKNOWLEDGEMENTS

I would like to thank Dr. Robert DeOtte for his help, guidance and unending patience through this process. I would also like to thank Dr. Brent Auvermann, Dr. Bob Stewart, Dr. Ty Lawrence and Dr. Lal Almas for their support and for serving as committee members for this project.

I also want to thank my wife Tammie and my children for their love, support, encouragement and patience. It has been a long road. I know you have all sacrificed a lot for this.

I would also like to thank Brandon Steinle in the West Texas A&M graphics department for all of the images produced.

Finally I would like to thank Todd Wood with Aquaveo for the training he provided on GMS.

This research was support in part by the Ogallala Aquifer Program, a research-education consortium seeking solutions to problems arising from declining water availability from the Ogallala Aquifer. The program is led by ARS-USDA and includes Kansas State, Texas Tech, Texas A&M and West Texas A&M universities.

TABLE OF CONTENTS

LIST OF TABLES

LIST OF FIGURES

Chapter I

INTRODUCTION

Water in Texas is a critical and valuable resource. The present status of water resources and future demands placed upon these resources are vital to the future of the state. Current water law allowing the pumping of groundwater beneath owned property is an attractive prospect for business and industry looking to relocate. This provides economic diversification to the state. However, the Rule of Capture adhered to by the State of Texas presents certain problems, particularly regarding the availability of groundwater. The concept of Rule of Capture allows a landowner to pump as much groundwater as desired from beneath the property that he owned. Under current practices, nonrenewable groundwater resources, such as that in the Ogallala aquifer, Figure 1.1, are being used at an ever-increasing rate.

Based on English Common Law, the Rule of Capture law was established in Texas by the Texas Supreme Court in 1904 in *Houston & T.C. Ry. Co. v East*, 81 S.W. 279 (Texas 1904). This court case provided two reasons for the decision. First, the court stated that the "secret, occult, and concealed" attributes of groundwater and the movement of groundwater made it impossible to regulate. Second, the court decided that allocations of groundwater would discourage future water development projects.

Groundwater modeling has provided insight that was not available when the accepted capture law was implemented. Improved models continue to shed more light upon the current status of the Ogallala. The purpose of this work is to continue the advancement of the modeling effort and to support the proposal that, quantitatively, there is more water remaining in the Ogallala than currently estimated.

Since the original court decision, many changes have been made to the laws regulating groundwater. Article 16, Section 59 of the Texas statutes provides for legislative power to pass laws related to the conservation of all natural resources of the state (Texas Constitution 1917). It is not the intent of this project to extensively explore water law. However, from that legislation numerous other decisions have been made and laws passed regarding groundwater, the use of groundwater, and the future conditions of aquifers. We begin with an introduction to Groundwater Conservation Districts (GCD).

The Texas Legislature authorized the creation of GCDs throughout the state in 1949. State lawmakers believed that local control of groundwater was a more reasonable approach than statewide laws that could become complicated because of the variations in hydrology and geology. The districts are charged with implementing water regulation including the development of an effective groundwater management plan within the respective district. Most districts are also required to develop water-surface decline maps. The maps created for GCDs responsible for monitoring non-renewable aquifers were used to determine property depreciation. Districts are governed by a board of directors elected from the counties comprising the GCD. Decision-making authority is

granted to the GCD to work in lieu of the Rule of Capture. The 84th session of the Texas Legislature passed a law stating that groundwater is owned by the property owner and allows for the production of the groundwater beneath the owned property (Texas Legislature Online 2016). Further, in Bragg v Edwards Aquifer Authority (EAA), the Supreme Court of Texas ruled that, by denying the well permit application and amounts requested by Bragg, this action constituted regulatory "taking" by the Authority (Bragg v EAA 2002). The Texas Constitution in Article 1 Section 17 expressly provides that no person's property can be taken without adequate compensation (Texas Constitution Online 2016). As a result of the denial of one well permit and a reduced allowance of production of a second permit, the Authority was ordered to provide monetary compensation or allow for the originally requested production. While water districts work to slow the irreversible decline of the Ogallala aquifer, court decisions continue to rule that landowners own the groundwater beneath their land. The High Plains Underground Water Conservation District, based in Lubbock, was the first groundwater conservation district established in 1951. The North Plains Groundwater Conservation District, based in Dumas, followed in 1955. These are the two groundwater conservation districts within which this modeling effort is based.

Based upon predevelopment conditions McGuire (2014) states that by 2013 there was a "10 percent decrease in 25 percent of the area, 25 percent decrease in 15 percent of the area, 50 percent decrease in 5 percent of the area, an increase of 10 percent or more in 1 percent of the area, and between a rise of 10 percent and a decline of 10 percent in 74 percent of the area." Complicating matters further, the GCDs have been tasked with

maintaining a desired future condition as defined by the Texas Administrative Code, Title 31, Part 10, Chapter 356, Subchapter A, Rule 356.10 (7) (Texas Administrative Code Online 2016). Those future conditions are defined as "the desired, quantified condition of groundwater resources (such as water levels, spring flows, or volumes) within a management area at one or more specified future times as defined by participating groundwater conservation districts within a groundwater management area as part of a joint planning process" (TAC Online 2016). Districts have the latitude to implement modifications to this required storage.

The plans to preserve groundwater while stating that the landowner owns the water in place generated some tense situations regarding use of the water. This is noted primarily in the North Plains Groundwater Conservation District (NPGCD). The western four counties (Dallam, Hartley, Sherman and Moore) are large, corn-producing counties in the Texas Panhandle. Rules adopted by the NPGCD allow for the preservation of forty percent of the groundwater in those counties. Other counties within the district decided to retain more than fifty percent of the available groundwater. The result is that the overall average groundwater remaining in the aquifer in the NPGCD is fifty percent. The preservation of the groundwater coupled with district metering requirements to ensure the groundwater is retained has put pressure on major corn producers. Some producers believe that reduced pumping will limit crop production.

Figure 1.1. Location of the Ogallala aquifer showing the aquifer boundary by the US Geological Survey (2015). Used with permission.

Groundwater conservation districts granting well-drilling permits to landowners have been responsible for monitoring groundwater levels, have provided data to the Texas Water Development Board, and are monitoring groundwater withdrawal by landowners through metering programs. GCDs are responsible for developing and maintaining a Groundwater Management Plan. This is accomplished through education programs,

issuing rules regarding groundwater withdrawal, and other services provided by the districts. The GCD plans are then incorporated into a broader, regional plan.

Senate Bill 1 passed by the 75th Texas Legislative Session in 1997 (Texas Legislature Online 1997) established regional water planning groups charged with preparing regional water planning strategies to meet the future needs of all Texans. The Panhandle Water Planning Group (PWPG) encompasses the northern Ogallala aquifer region designated as Groundwater Management Area 1 and is shown in Figure 1.2. The PWPG is directed to develop the Panhandle Water Planning Area (PWPA) regional plan. The regional plan evaluates all major stakeholders' interests and provides a regional water plan to the state for inclusion into the state water plan. The plans that were adopted in 2001 are some of the most extensive plans established regarding water resources in Texas (PWPG 2015).

In order for the water planning areas to develop regional water plans, it was necessary to develop more comprehensive and detailed groundwater models. Modeling of the Ogallala aquifer in Texas has progressed through many iterations. The chronological process of early model development has been well documented by Mace and Dutton (1998). A chronological illustration of these model efforts is shown in Figure 1.3. Models have continued to undergo refinement through the years as additional understanding of the aquifer is gained and as the modeling tools have improved.

One of the first recognized efforts to develop an accepted comprehensive Groundwater Availability Model (GAM) for the northern Ogallala aquifer was undertaken by Dutton,

Reddy, and Mace under contract to the PWPG (Dutton 2001). The model was then refined to improve calibration (Dutton 2004) and was accepted by the Texas Water Development Board as the official GAM for the northern portion of the Ogallala aquifer in 2001. Additional model revisions were provided and accepted in 2004 and 2010.

The simulation proposed by Dutton was the initial effort to quantify the water in the Ogallala in the Texas Panhandle. Recent work on a mass-balance approach suggests that the estimated quantities of water remaining in the saturated zone projected in the accepted GAM may miss some important detail (Ouapo, et al. 2014). The mass-balance approach implies that using well-water surface elevations may underestimate the water in storage. Figure 1.4 is a conceptual drawing of the suggested mounding of water between two pumping wells. Data used to support the argument show that some wells have an increase in water elevations. While some might argue that this represents recharge, it seems more likely that this may be attributed to rebound.

Rebound occurs when wells are pumped and then shut off. The pumping creates a cone of depression about the well. Over time, water will fill the cone. As the cone fills, a new water table condition will be approached. The resulting water surface elevation will be lower than the previous level due to the removal of a quantity of water from the aquifer. Further, this study suggests that prolonged, economically-viable irrigation has continued longer than models suggest should be feasible. For this reason, the hypothesis is proposed that there is additional water in storage in mounds between measured wells. The mounded water supplies the water which results in the aforementioned rebound. As

this water moves from the mounded water between wells, some wells may show increased water elevations, especially if the well has been decommissioned. Further, the time required for the aquifer to approach a new water table condition after a series of pumping events is very long. This total recovery rebound time is not taken into account prior to water elevation measurements. The total estimated rebound time will be illustrated further.

Problem Statement

The work by Ouapo, et al. (2014) suggests that an effort to model the storage and observe the mounds of water between wells as it moves toward the wells during pumping and rebound periods would yield valuable new information. According to the Agronomic Water Mass Balance Approach theory (AWMBA), more water has been withdrawn from the aquifer for irrigation than suggested by depletion estimates derived from the water level measurements in wells. Ouapo, et al. (2014) used AWMBA to estimate water removed from the Ogallala aquifer. This was compared to the well measurement approach used by the Texas Tech University Center for Geospatial Technology (TTUCGT). For the Southern Cluster of counties (Castro, Deaf Smith, Parmer, and Swisher) the AWMBA indicates a greater withdrawal of water than does the WMA; however, for the Northern Cluster (Dallam, Hartley, Moore, and Sherman) the results are similar. The WMA is based upon the measurement of the water surface elevations within a network of wells in the GCD.

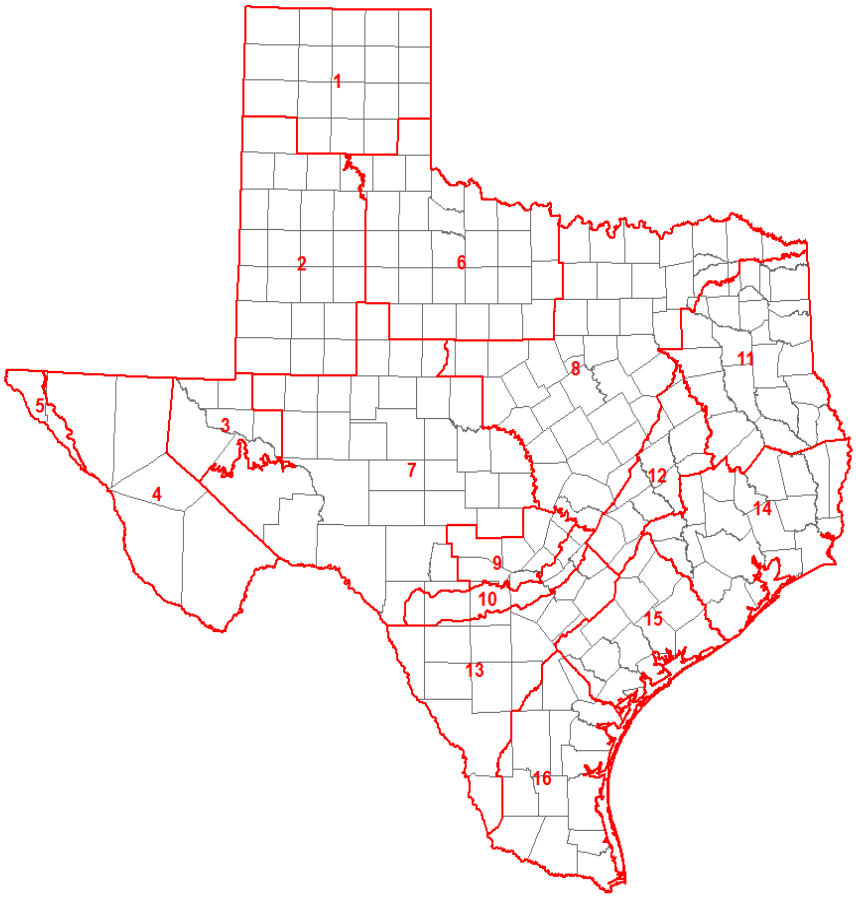

Figure 1.2. Groundwater Management Areas from TWDB (2016). Used with permission.

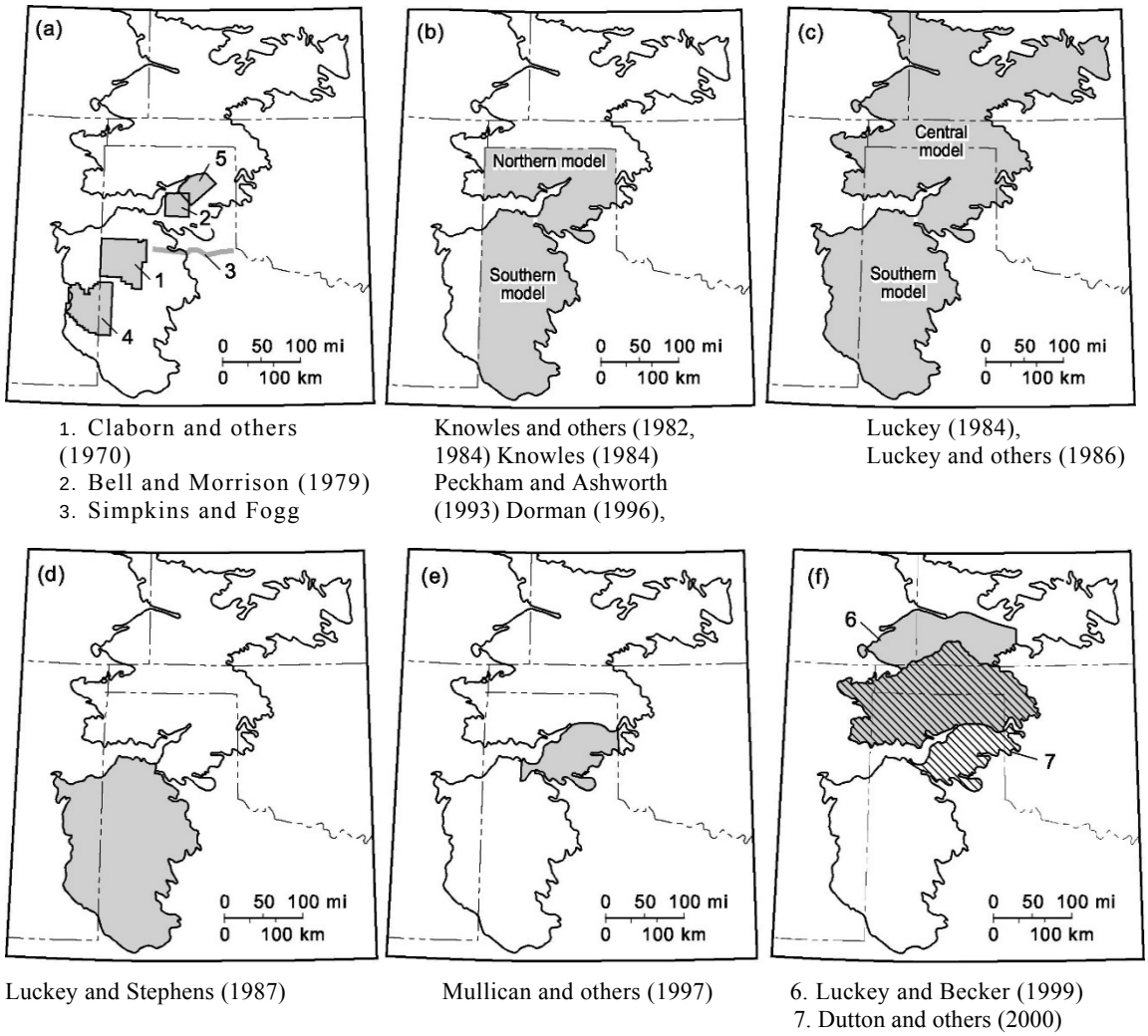

1. Claborn and others (1970)
2. Bell and Morrison (1979)
3. Simpkins and Fogg

Knowles and others (1982, 1984) Knowles (1984) Peckham and Ashworth (1993) Dorman (1996),

Luckey (1984), Luckey and others (1986)

Luckey and Stephens (1987)

Mullican and others (1997)

6. Luckey and Becker (1999)
7. Dutton and others (2000)

Figure 1.3. Location and area of coverage of models of the Ogallala aquifer in Texas. From Mace 1998 and Dutton 2001.

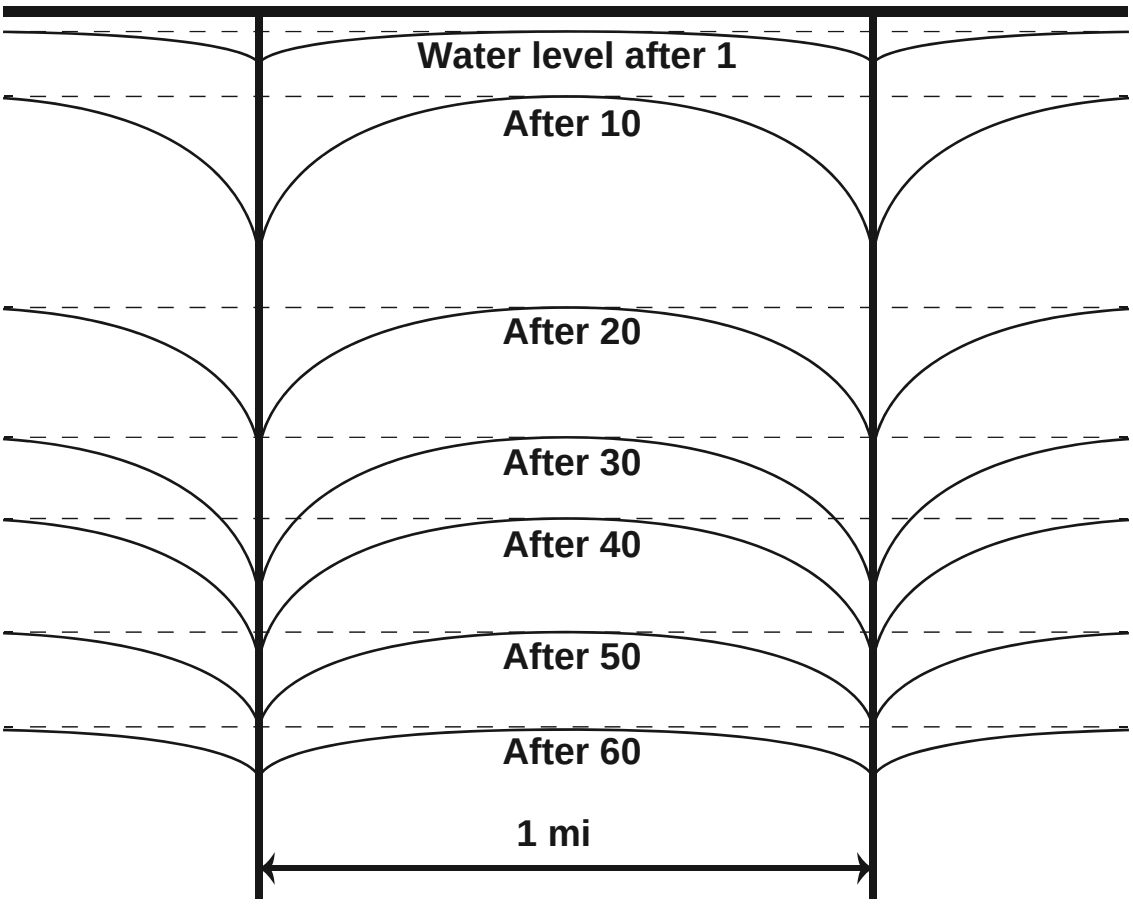

Figure 1.4. Conceptual model of the development of cones of depression about wells and overall decline of aquifer levels in succeeding years.

Water remaining in the aquifer is then estimated based upon extrapolation of water surface elevations between measured wells and calculation of the saturated thickness.

Natural recharge of the Ogallala aquifer has been estimated to be between 0.5-0.8 inches per year (Theis 1937, Barnes 1949, Havens 1966, HPGWCD 2005). Bell (1981) proposed a recharge rate of 0.5 inches based upon changes in the soil and land surfaces associated with current agricultural practices. The practices believed to alter recharge

rates are clearing the land of deep rooted native vegetation, deep plowing of fields, plowing of playa lake sides and bottoms, leveling, contouring and terracing of farmland, maintaining a higher soil moisture content as a result of irrigation prior to rainfall events, and increased humus from the plowing under of residual crop residue. Bell then added ten percent to this amount to account for return flow of irrigation water. Return flow water is water applied as irrigation water that percolated back to the aquifer. However, estimating reliable recharge rates is challenging. Further, current withdrawal rates far exceed any significant recharge potential. Recharge of the aquifer does not appear to be an adequate source necessary to balance the AWMBA with the WMA. The High Plains is a semi-arid region with most of the rainfall occurring during the growing season. This also corresponds to the time period when higher evapotranspiration rates occur. For recharge to be a possible source of water to balance the AWMBA and the WMA, sufficient rainfall would have to occur to meet evapotranspiration rates and allow for infiltration of the water that must ultimately reach the aquifer.

One might postulate return flow from row and furrow irrigation as a potential source of water that might help explain the differences between the WMA and AWMBA methods. Estimating return flow is particularly difficult due to the water application being non-uniform across an irrigated field. Further, changes in irrigation practices from row and furrow irrigation to center-pivot irrigation systems over the last several decades have led to more uniform application of irrigation water. The precision application through center-pivot irrigation and lack of excessive application, which occurred with row and

furrow applications, would not be sufficient to contribute significantly to the return flow of water to the aquifer.

The current estimates of water remaining within the saturated thickness of the aquifer are based upon a well measurement approach (WMA). Water surface elevation data is collected during the non-pumping season which is usually January and February of a given year. These measured water levels are interpolated using splines to provide estimated saturated thicknesses between wells and to provide a county-wide estimate of remaining available water. This implies that the aquifer will return to a smooth "water table" in a relatively short period of time. Although this may be the best method for generating a significant amount of data with which to work, modeling efforts show the WMA may underestimate the amount of water remaining within the aquifer.

The goal of this project is to develop a groundwater model using MODFLOW to determine how pumping influences groundwater withdrawal and whether or not mounds of water may remain between pumping wells. As a well is pumped, a "cone of depression," as seen in Figure 1.5, is created in the groundwater table surrounding the well. The most pronounced depression effect is immediately adjacent to the well and declines as one moves away from the well. The cone results in a decreased saturated thickness nearest the well. In order for the well to maintain output, the flow of water through the depression must increase. Conversely, there is a mound of water at the outer edges of the cone. Because the cylinder at radius r_m is greater than the radius r_d nearer the well, the area at r_m is greater therefore the water velocity is lower and the depth of

saturated thickness necessary to replenish the water in the cone of depression. However, as the cone begins to rebound, the rate of rebound declines resulting in a persisting cone of depression and a mound of water between the wells.

The models developed here attempt to observe local well recovery based on inflow from the boundary of the cone of depression. The model runs encompasses multiple years of well operation, simulating observed normal irrigation practices. When the pumping of the wells is stopped, successive calculations performed by the model will allow water to move through the saturated thickness to allow the well to rebound to whatever level it may achieve prior to the next pumping cycle.

Modeling efforts are based on the groundwater availability model (GAM) developed by Dutton (2004) and accepted by the Texas Water Development Board. This model used the parameters incorporated into Dutton's model, except for specific yield, (the ratio of the amount of water a soil will yield by gravity drainage to the volume of the soil). Deeds (2015) suggests higher variability of the specific yield of the aquifer in particular regions. Based upon the locations of the two models developed in this work, the specific yield was adjusted accordingly. The well measurement approach is used in Dutton's model to generate the current status of the aquifer and then the model is allowed to operate for multiple years into the future to simulate remaining water levels in the saturated thickness. The aquifer is assumed to be isotropic in both vertical and horizontal directions.

The modeling effort undertaken as an extension of the work by Ouapo, et al. (2014) strives to explain the deviation between the current GAM and the AWMBA. All hydraulic parameters used in the accepted GAM remain the same in this model, except specific yield. The goal is to observe if the cones of depression can be generated and to observe the resulting mound of water remaining between wells. This will provide a model-based foundation to support the theory that there is more water remaining in the Ogallala than previously estimated.

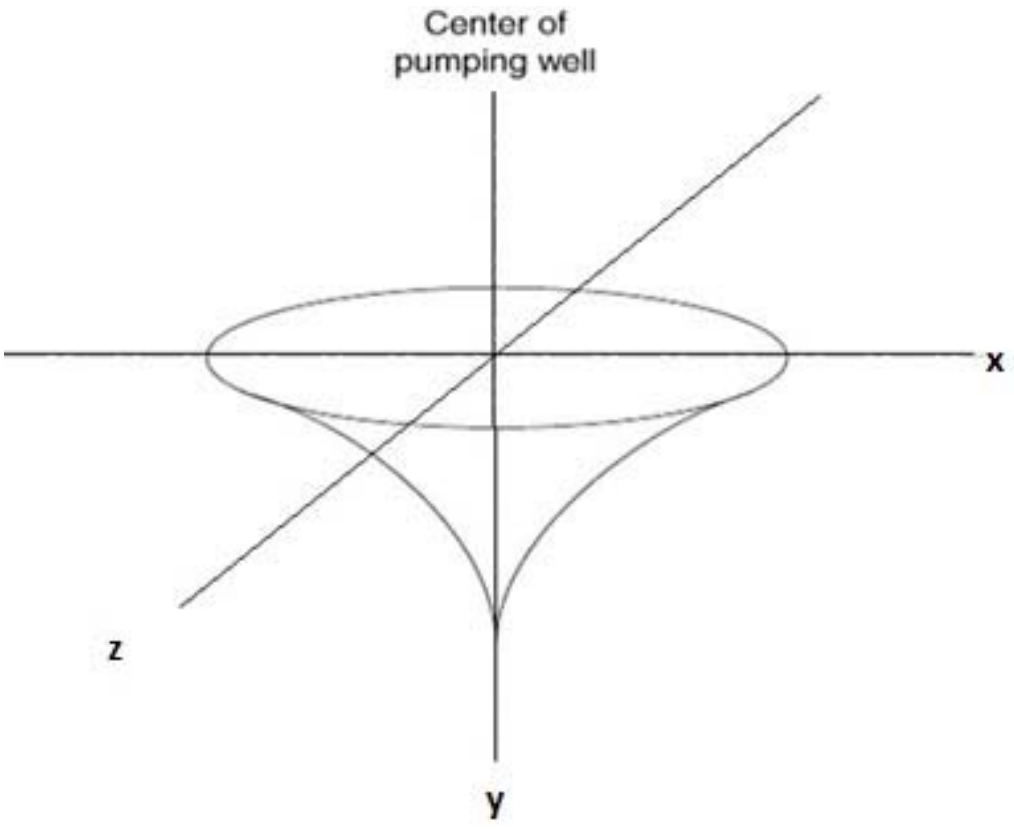

Figure 1.5. Cone of depression associated with a pumping well in a homogeneous aquifer (From Alley 1999). Used with permission.

Recently, producers have begun drilling wells to much greater depths. This is more costly, but given the value of the crop and risk of reduced crop production due to a shortage of irrigation water, many consider the cost justified. These wells are being completed in the Dockum, in some locations referred to as the Santa Rosa, and Rita Blanca aquifers which underlie some parts of the northwestern counties of the Texas Panhandle. Hydraulic connections between the Ogallala with the Dockum and the Rita Blanca Aquifers are not well established; however, it is very likely these aquifers are interconnected (Dutton 2001). Should the two aquifers share significant interconnectivity, two things are evident: one, the flow of water from the Dockum and Rita Blanca into the overlying Ogallala formation could help explain some of the differences between the AWMBA and WMA approaches. If there is the potential for water flow between the two aquifers, some water could move from the upper Ogallala to the lower aquifers. This would explain the lower water amounts seen in the WMA as opposed to the AWMBA. Questions arise about the depths of completion of some wells. Subsurface geology suggests that some wells once assumed to be completed in the Ogallala may actually be completed in the Dockum. The thickness of a confining layer is not clearly defined. Older well logs indicating that a "redbed" or confining layer were penetrated point to the possibility that some wells were drilled and completed in a lower aquifer. In such cases, withdrawal of water from the Dockum would be accounted as having derived from Ogallala water. This may explain some of the discrepancy between the WMA and the AWMBA. Should water from both aquifers be pumped from a well, there is no way to distinguish the source of the water and this would imply that there is significantly more water available to pump than previously understood. Additionally, if

there is adequate potential for water to move from the underlying Dockum aquifer to the upper aquifer, presuming at such locations the Dockum is artesian, this could explain why the AWMBA approach indicates there is more water available than the WMA approach indicates.

In order from water to flow from the Dockum or Rita Blanca, shown in Figure 1.6, into the Ogallala aquifer, Figure 1.7, there must first be a hydraulic gradient established between aquifers. Both of these aquifers underlie portions of the Ogallala. This would imply that for water-flow to be established from the Dockum to the Ogallala, the water would need to flow uphill, which can happen as long as the gradient declines in the direction of flow. Figure 1.8 is a cross-sectional view of the Texas Panhandle from West to East. In this illustration the drop in elevation from West to East across the region would be substantial enough to establish a gradient and allow water to flow from the underlying aquifers into the Ogallala. Estimating a drop in elevation from West to East of 2500 feet across approximately 165 miles of the Texas Panhandle, the average elevation drop would be 15 feet per mile. Where the Dockum and Rita Blanca underlie the Ogallala to the West, the respective elevations would approach the water surface elevation of the Ogallala and allow them to feed water to the East into the Ogallala.

The focus of this effort is to develop a conceptual model to see if mounds of water between pumped are a reasonable possibility, as suggested by Oupao et al (2014). This would provide evidence that would help explain the differences between the Well Measurement Approach (WMA) and the Agronomic Water Mass Balance Approach (AWMBA) methods of estimating water remaining in the Ogallala aquifer. Existence of

these mounds may explain why wells have remained productive as long as they have and why rebound has been noted in wells previously reported as “dry”. Wells that are considered “dry” are economically unviable for production agriculture or wells that can no longer be pumped. In at least some locations, wells that remain inactive for a number of years appear to gain water. The apparent gain in water surface elevation could be the result of the mounded water slowly filling in a cone of depression about the well and the establishment of a new water table. Water mounded between wells may also explain some of the errors reported in other modeling efforts (Dutton, 2004).

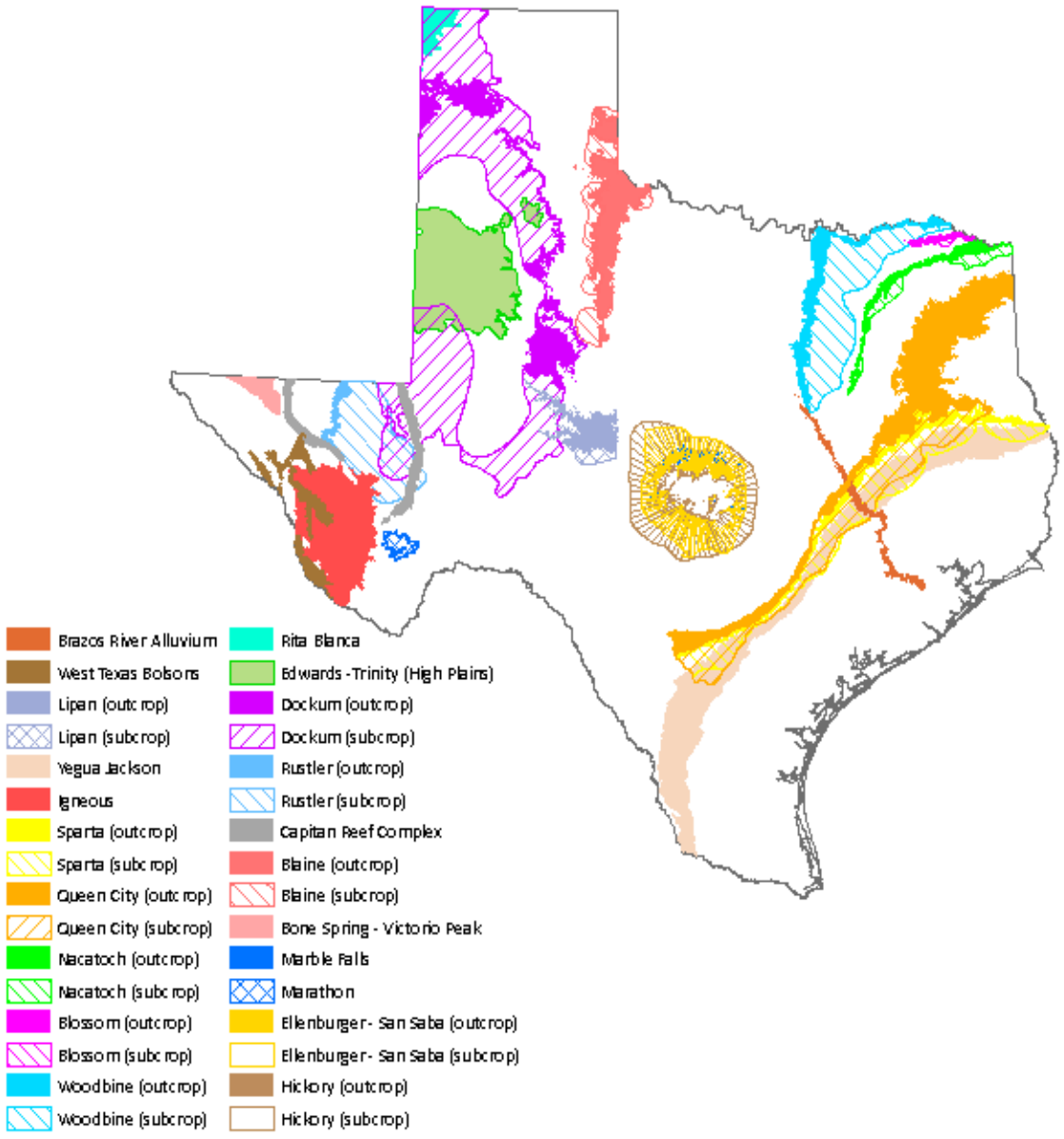

Figure 1.6. Minor Aquifers in Texas. From TWDB website http://www.twdb.texas.gov/groundwater/aquifer/minor.asp (2016). Used with permission.

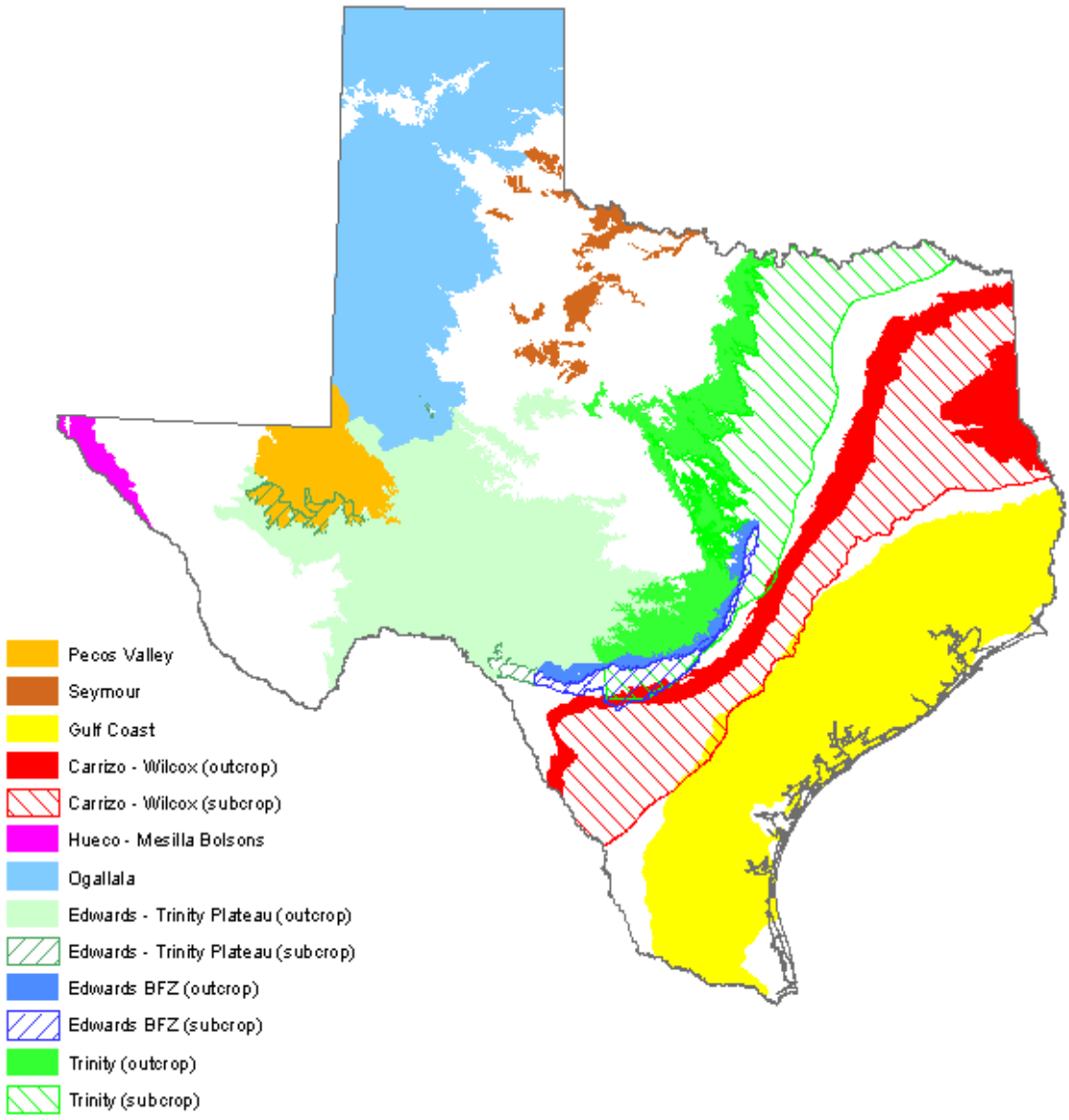

Figure 1.7. Major Aquifers in Texas. From TWDB website http://www.twdb.texas.gov/groundwater/aquifer/major.asp (2016). Used with permission.

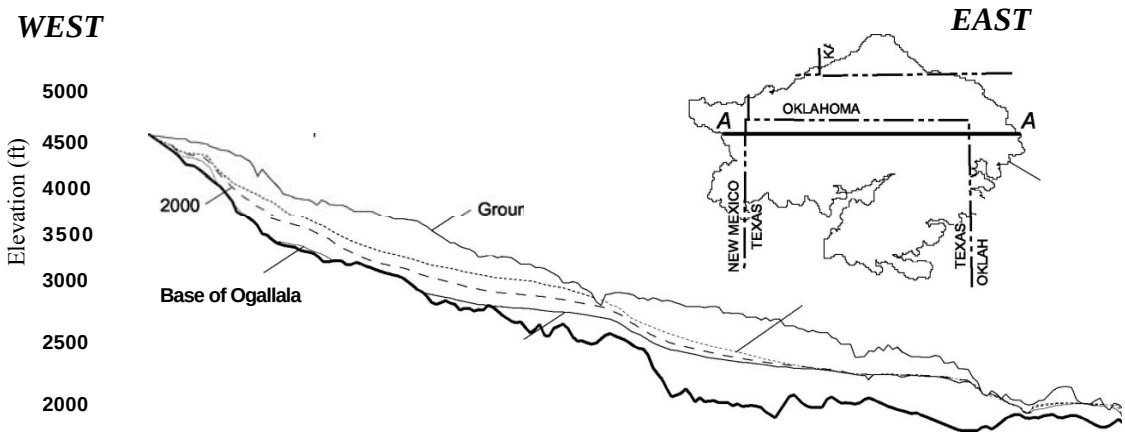

Figure 1.8.West-east cross section illustrating relationship between ground surface, aquifer base, and the changing water table in the Ogallala aquifer (modified from Dutton 2001). Used with permission.

Chapter II

LITERATURE REVIEW

The Ogallala is a vast, unconfined aquifer underlying parts of eight states and covering an estimated area of 174,000 mi^2 as shown in Figure 1.1. The aquifer serves as the primary source of water in the High Plains, a largely agricultural region of the United States (Gutentag, et al., 1984). Water withdrawals for irrigation vastly exceed any recharge for large portions of the aquifer. The result of this is essentially a mining process of the saturated thickness of the aquifer. There will be a point in time where the stock can no longer supply the demand flow.

The Ogallala aquifer is comprised of one or more hydraulically connected geographic units of later Tertiary or Quaternary age. The actual Ogallala formation underlies approximately 174,000 square miles with a maximum saturated thickness of 700 feet (Gutentag, et al., 1984). The depositional process resulting in the Ogallala formation has generally been accepted as a transport of erosion debris from west to east (Gilbert 1896, Johnson, 1901, Frye, 1970, Schultz, 1977, Gutentag, et al., 1984). Deposition of the erosion debris was brought about by both stream and wind erosion. Table 2.2 provides the generalized geologic sections of the Ogallala aquifer and underlying formations.

Table 2.2. Generalized description of geologic units that compose (blue shading) and underlie (gray shading) the Ogallala aquifer. (From Weeks and Gutentag, 1981.) USGS used with permission.

Series	Geologic unit	Thickness, in feet	Physical characteristics
Pleistocene and Holocene	Valley-fill deposits	0 to 60	Stream-laid deposits of gravel, sand, silt, and clay associated with the most recent cycle of erosion and deposition along present streams. Forms part of the High Plains aquifer where saturated and hydraulically connected to underlying Quaternary and Tertiary deposits.
	Dune sand	0 to 300	Fine to medium sand with small amounts of clay, silt, and coarse sand formed into hills and ridges by the wind. Forms part of the High Plains aquifer where
	Loess	0 to 250	Silt with lesser amounts of very fine sand and clay deposited as windblown dust.
Pleistocene	Unconsolidated alluvial deposits	0 to 550	Stream-laid deposits of gravel, sand, silt, and clay locally cemented by calcium carbonate into caliche or mortar beds. Forms part of High Plains aquifer where hydraulically connected laterally or vertically to deposits of Tertiary age.
Miocene	Ogallala Formation	0 to 700	Poorly sorted clay, silt, sand, and gravel generally unconsolidated; forms caliche layers or mortar beds where cemented by calcium carbonate. The Ogallala where saturated composes a large part of the High Plains aquifer.
	Arikaree Group	0 to 1,000	Predominantly massive very fine to fine-grained sandstone with localized beds of volcanic ash, silty sand, siltstone, claystone, sandy clay, limestone, marl, and mortar beds. Considered part of the High Plains aquifer.
Oligocene	White River Group: Brule Formation	0 to 700	Upper unit, Brule Formation, predominantly massive siltstone containing sand- stone beds and channel deposits of sandstone with localized lenticular beds of volcanic ash, claystone, and fine sand. The Brule Formation is considered part of the High Plains aquifer only where it contains saturated sandstones or interconnected fractures. Lower unit, Chadron Formation, mainly consists of varicolored, bentonitic, loosely to moderately cemented clay and silt that contains channel deposits of sandstone and
	White River Group: Chadron Formation		
Upper Cretaceous	Undifferentiated rocks	0 to 8,000	Shales, chalks, limestone, and sandstones. Upper part may contain lignite and coal beds.
Lower Cretaceous	Undifferentiated rocks	0 to 700	Fine- to medium-grained, thin-bedded to massive, cliff-forming sandstone inter- bedded with shale. Black and varicolored shale to thin- to thick-bedded lime- stone.
Middle and Upper Jurassic	Undifferentiated rocks	0 to 600	Varicolored shale, fine- to very coarse-grained sandstone, limestone, dolomite, and conglomerate.
Upper Triassic	Dockum Group	0 to 2,000	Upper unit, varicolored siltstone, claystone, conglomerate, fine-grained sand- stone, limestone. Lower unit, varicolored fine- to medium-grained sandstone with some claystone and interbedded shale.
Lower and Upper Permian	Undifferentiated rocks	300 to 3,000	Interbedded predominantly red-shale, siltstone, sandstone, gypsum, anhydrite, dolomite, bedded salt, and local limestone beds.

Computer modeling of aquifers has advanced significantly over the years. Numerous software packages are now available with which to view the results of model runs. MODFLOW, according to the USGS the most accepted software package for modeling groundwater (USGS 1997, Harbaugh, 2005) was initially developed in 1984 (McDonald and Harbaugh, 1984). Several upgrades and packages have been developed to support MODFLOW through the years. Computer generated models have become vital in attempting to understand and explain the characteristics of groundwater, including hydraulic conductivity (a proportionality describing the rate at which water can move through a permeable medium), specific yield, quantity remaining in storage, stress on the aquifer caused by withdrawal, and natural inflow and outflow to the aquifer. Of primary importance is the ability to appraise the water remaining in storage. The consequences of underestimating or overestimating the available water in storage could have significant impact on legislation which could drive policies designed to influence the rate of decline of the aquifer.

Concerns about access to water are universal. Currently 11 percent of the global population lacks an improved source of drinking water (UN 2012). Numerous groundwater studies have been conducted worldwide, many of which would be similar to those conducted on the Ogallala aquifer. According to Rossman (2013), Van der Heijde et al. (1985) extensively reviewed nearly 400 modeling efforts around the world and found that 188 models had simulated water flow and been applied to field problems.

One of the most studied aquifers in the world, the Ogallala underlies about 174,000 mi^2 in eight states and is shown in Figure 1.1. Gollehon (2013) reported that the revenue generated from the sales of crops irrigated with Ogallala aquifer water totaled more than $7.2 billion in 2007. This accounts for approximately 60 per cent of the crop sales in the eight-state region and over 10 percent of the national irrigated crop sales. The 215 counties dependent upon the Ogallala aquifer are shown in Figure 2.1. Thirty percent of the groundwater withdrawn in the United States for irrigation comes from this aquifer. As many as 32,000 farms depend on this source of water for irrigation (Gollehon, 2013). Qi (2010) states that about $20 billion per year of the agricultural industry in the United States is supported by the withdrawals from the Ogallala. Amosson, et al., (2015) reports that irrigated agriculture in the Texas High Plains results in approximately $4.8 billion in industry output and $8.1 billion in regional economic impact.

Gutentag (1984) reported that there were over 170,000 wells withdrawing water from the aquifer. Mace (1998) reported there were about 70,000 wells withdrawing water in the Texas portion of the Ogallala. USGS data indicated approximately 75,000 wells in Texas with as many as 30,000 located within Castro, Crosby, Floyd, Hale, Lubbock, Parmer, and Swisher counties (Ryder, 1996). A recent survey of groundwater districts located in the Texas Panhandle indicated there are nearly 80,000 irrigation wells completed in the Ogallala aquifer (Bennett 2016, Coleman 2016, Guthrie 2016, Ward 2016). This survey indicates wells continue to be drilled into the Ogallala for irrigation.

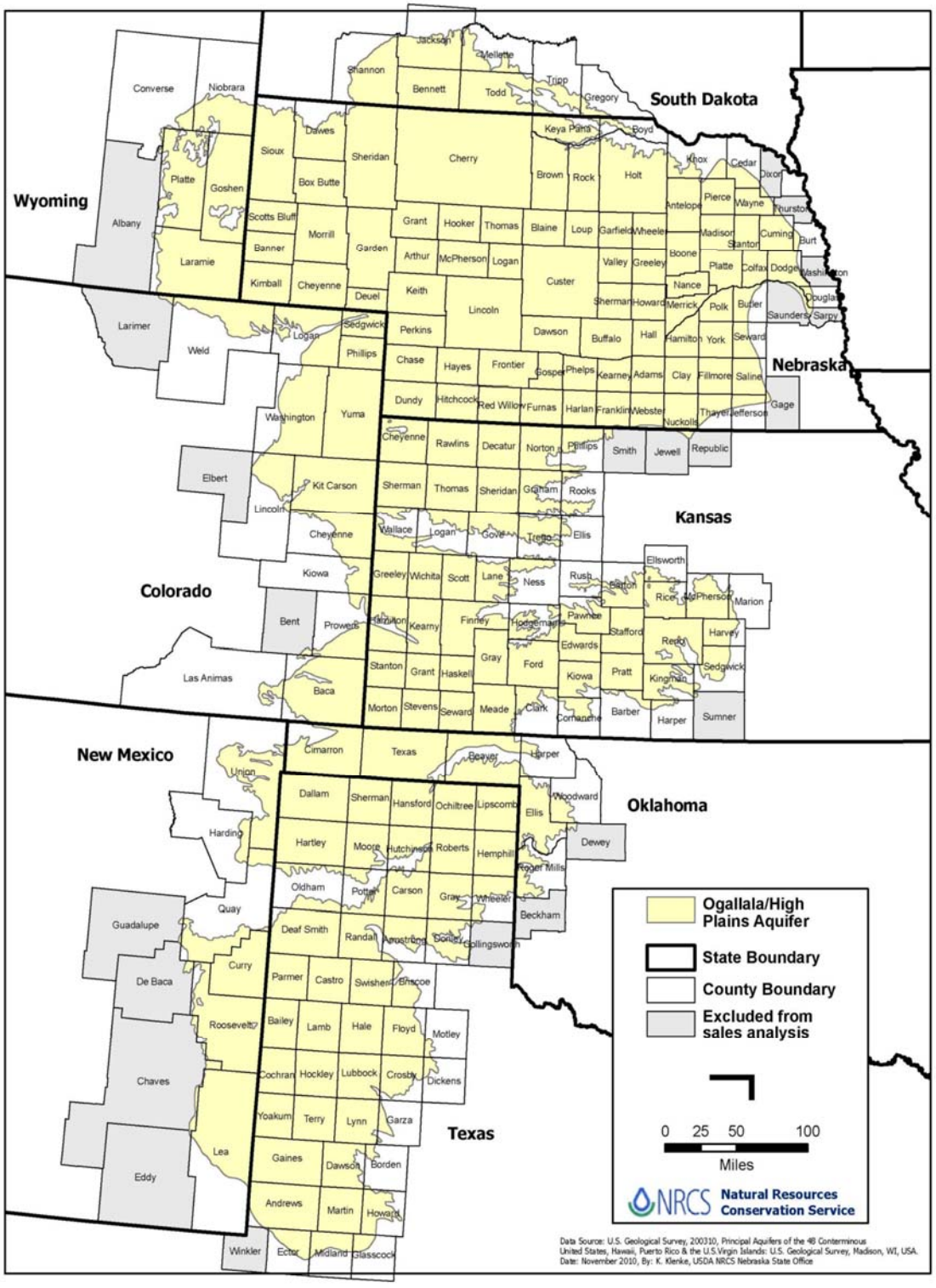

Figure 2.1. Counties overlying the Ogallala Aquifer (Gollehon, 2013). Used with permission.

To attempt to gain a better understanding of the Ogallala aquifer, Table 2.1 lists many of the models that have been developed. Initial attempts were developed but lacked a significant amount of data to fully explain the aquifer (Claborn 1970). Additionally, computing time and resources then were not as readily available or as fast as those of today. These models were the foundations of the modeling work to follow, including this effort. Several of the models listed in Table 2.1 are small-scale models (Bell 1979, Andrews 1984, Mullican 1995 and 1997, Luckey 1999); some are updates to previously developed models (Knowles 1982 and 1984, McAda 1984, Luckey 1987, Peckham 1993, Dorman 1996, Harkins 1998, Dutton 2000 and 2004, Stovall 2001, Deeds 2015); two investigate sub-Ogallala hydrology (Andrews 1984, Wirojanagud 1986); and one was used to investigate a salt-dissolution zone (Simpkins 1982). Following are brief summaries of the previous modeling efforts which focus on the Ogallala aquifer and the water available within the saturated thickness.

Claborn and others (1970) used a polygonal finite-difference code developed by E. M. Weber of the California Department of Water Resources. The area of study is identified in Figure 1.3. The joint effort between Texas Tech and the High Plains Underground Water Conservation District No. 1 focused primarily on the Ogallala aquifer in the southern portion of the Texas Panhandle. This effort demonstrated the value of numerical modeling as a management tool for the aquifer. However, this effort also identified a lack of quality data for model construction (Dutton 2001).

Models developed by Knowles (1984) and Knowles and others (1982, 1984) were the first attempts to model the entirety of the Ogallala aquifer. A tremendous amount of data was collected about the aquifer in order to construct the model. This included gathering information about the water table elevation and aquifer base elevation to improve the accuracy of the estimated saturated thickness. Specific yield and permeability (a function of the size of openings through which fluid moves) maps were created based upon lithologic descriptions of the aquifer. The specific yield of the aquifer was determined to be 16 percent. Knowles divided his model into two portions: the northern section and the southern section of the Ogallala. The division of the model occurred along the valley of the Canadian River and the Prairie Dog Town Fork of the Red River. This was a natural dividing boundary since the erosion of the river has essentially cut the Texas portion of the Ogallala into two separate aquifer bodies. Knowles concluded that, given projected demands, groundwater supplies in the southern model would be inadequate by 2030 (Dutton 2001).

Results obtained by Peckham and Ashworth (1993) were similar to those found by Knowles (1984). Slight increases in water availability were noted over previous modeling studies but the overall continued decline of the aquifer was confirmed (Peckam and Ashworth 1993).

The USGS Regional Aquifer-System Analysis (RASA) project was mandated by Congress, with direction to develop quantitative assessments of the major groundwater systems within the United States (Weeks et al, 1988). The Ogallala aquifer was recognized as a vital agricultural and economic resource to the area overlying it (Colorado, Kansas, Nebraska, New Mexico, Oklahoma, South Dakota, Texas, and Wyoming). Significant declines in saturated thickness are primarily noted in Texas, New Mexico and Kansas, with the southern plains of Texas showing the most decline. Almost all states show declines in saturated thickness where large- scale irrigation development is prevalent. Some areas of Kansas, Oklahoma and particularly Nebraska show some increases to the saturated thickness although heavily irrigated in some locations. This prompted an extremely large study encompassing the entirety of the Ogallala aquifer. The objectives of the study were to collect geologic, hydrologic, and geochemical information, to analyze, to develop and understand the system, and to develop predictive capabilities that contribute to the effective management of the system (Weeks et. al, 1988). Model projections out to 2020 showed significant declines in well yields in the southern portion of the Ogallala and a resulting decrease in irrigated agriculture in Colorado, Kansas, New Mexico, Oklahoma, and Texas. As a result of the available water, irrigated agriculture is expected to increase in Nebraska.

The next major step in the model evolution was completed by Dorman (1996) when the model used previously by the Texas Water Development Board (TWDB) was converted from a GWSIM-III to a MODFLOW-based simulation. Prior to incorporating them into MODFLOW, Dorman had to develop several computer programs to adjust pumping rates

from GWSIM-III. Validation of the conversion process was completed by showing that simulated volume in storage was similar to that published by the TWDB by Peckham and Ashworth (1993).

Four pumping scenarios were evaluated by Dorman to simulate the aquifer response from 1990 to 2040. The pumping data provided by Peckham and Ashworth (1993) and a demand forecast developed by the TWDB in 1995 were used for all four scenarios. The results provided by Dorman indicated continued declines of the saturated thickness but also a reduced rate of decline in conservation scenarios that use more efficient irrigation delivery systems.

Harkins et al. (1998) used a modified version of MODFLOW to portray groundwater levels. The modifications allowed the model to internally calculate pumping rate adjustments using transmissivity and saturated thickness constraints. Additional modifications included the calculation of saturated thickness, volume in storage, and the ratio of adjusted to predicted pumpage (Stovall 2001). The goal of Harkins' work was to provide a modeling tool for groundwater conservation districts and to support part of the High Plains Ogallala Area Regional Water Management Plan. Referencing the GWSIM-III model, validation of Harkins' model was accomplished by using the same finite grids, aquifer parameters, and pumping estimates as the TWDB. Numerous scenarios were explored by Harkins including the following:

- the modeling of altered irrigation rates,
- pumping scenarios under prolonged drought conditions,

- irrigation reductions of 25 percent and 50 percent,
- reduced withdrawal rate impacts on the aquifer, and
- recharge simulations.

Conclusions reached by Harkins were that groundwater withdrawal would continue to deplete the aquifer. Conservation practices would reduce the rate of decline and prolong the useful life of the aquifer. Harkins proposed that the central counties of the Southern High Plains of Texas could be depleted by 2020 and further proposed that less irrigation, more efficient irrigation delivery systems, conservation practices, and other water-saving measures should be implemented.

Modifying the model developed by Harkins, Stovall (2001) developed a new regional model for the southern portion of the Ogallala in Texas. Stovall's goals included reporting groundwater storage by county, converting hydrologic maps for use in computer simulations, improving accuracy of calculations of water in storage, discretizing model cells using 1 mi^2 cells, developing datasets for input to MODFLOW, and simulating future water withdrawals and impacts on regional water supply.

Modifications incorporated by Stovall (2001) into the Harkins model included changes to the discretization, model domain, boundary conditions, physical parameters, hydrologic parameters, and initial conditions. The discretization was changed to meet the TWDB size requirements. The model domain was updated to include the portion of the Ogallala lying in western New Mexico. No-flow boundaries were set for the northern, western

and southern edges while the eastern boundary was set as a constant head boundary. The eastern boundary conditions were designated by Knowles (1984) as constant head boundaries. Knowles changed the eastern boundary from a no-flow boundary to a constant head boundary to prevent "ponding" of the water along the eastern edge during trial runs. Efforts were made to improve the elevation of the base of the aquifer by applying known elevations to a grid system. Pumpage demands of the modeled area were based upon historical estimates provided by the TWDB for the counties in Region O. Calibration of the initial model conditions was based upon water-surface elevations from 1985 and target and future conditions were based upon water-surface elevations for 1995. Several recharge scenarios were evaluated, and the best were selected based upon the calibration statistics and used in later phases of calibration. To determine aquifer responses the model was then tested under various conditions in which recharge and distribution of pumping were parameters adjusted during calibration of the model. Once the model outputs matched water-surface elevations for 1985 and 1995 then future withdrawals were evaluated. Results suggest that in Region O 79 percent of the available groundwater measured in 1995 would remain in 2050. Some of the water is attributed to using a higher than previously reported recharge rate and water that is located under non-irrigable land. Higher recharge rates are possibly due to return flow of irrigation water to the aquifer. Return flow is excess irrigation water that percolated back to the saturated zone. Here a distinction must be made between recharge and return flow. Recharge is infiltration of water, generally from rainfall. Return flow is water previously pumped from the aquifer. By adding return flow as recharge this water is being counted twice in the model. This would lead to overestimating water as mentioned by Stovall. Further,

model simulations indicated a significant increase in groundwater storage over the initial calibration levels and saturated thickness in Crosby, Dawson, and Dickens counties. Results from the baseline simulation representing the most likely scenario of water use indicate that 79 percent of the volume in storage in 1995 would be available in 2050 while only 65 percent of the 2050 demand would be satisfied in region O. Stovall mentions that estimates of recharge rates are higher than in previous modeling studies performed by the TWDB and Texas Tech University Water Resources Center. Rising water levels were noted in the above mentioned counties during the 1985-1995 period used for calibration. These two factors could cause the model to overestimate the water remaining. Stovall also used simulations to observe the effects of a precipitation enhancement program on the remaining water in the aquifer. Reduced irrigation demand simulations were generated by Stovall. Results show that the impact to water remaining in storage was positive meaning that additional rainfall would add additional water to the aquifer (Stovall 2001). An alternative explanation not explored in this work would be the possibility of mounds of water as opposed to recharge. The restoration of a flat surface of water between pumped wells is assumed in most models to occur prior to water-surface elevation measurements. Calibrations based upon these measurements do not allow adequate time for full rebound of the cone of depression about the wells.

Stovall concluded that a substantial area within the model would have a saturated thickness of less than 20 feet. Irrigation would likely suffer the most from the shortfall. Counties exhibiting apparent groundwater recharge could be showing increasing water table levels due to return flow from irrigation

Dutton and others (2001) developed the groundwater availability model currently accepted by the TWDB. The model was updated by Dutton (2004) to adjust model parameters in order to improve calibration. The most recent update to this model was prepared by Dutton (2010) to support the 2011 state water plan regarding the northern Ogallala aquifer. Dutton's original numerical model was designed to assess the current status of the aquifer as well as to provide predictions of conditions to 2050.

Applying a water-budget method, the pre-development water in place was estimated using data accumulated and stored in a geographic information system (GIS) and water inflow and outflow which were added and subtracted in a spreadsheet (Dutton and Reedy, 2000). Projections based on the water-budget analysis suggested that parts of Dallam, Moore, Oldham, Potter, and Randall Counties will have saturated thickness of less than 50 feet by 2050.

A finite-difference model was constructed and analyzed by Dutton, et al., with MODFLOW calibrated as both a steady state model and a transient model. The steady state model was based upon a "predevelopment" model of the aquifer. The "predevelopment" aquifer levels were those existing up until 1950. To monitor the model responses to pumping, the transient or second calibration used water-surface elevation differences between 1950 and 1988. The model design had one square mile cells for the coverage and one single layer, for a total of 24,242 active cells.

Two conclusions were drawn from the projections. First, there were some areas of the model in which current demand would not be met using current pumping rates due to decreased well production in those areas. Second, there were portions of Carson, Dallam, Hartley, Hutchinson, Moore, Potter, Randall, Roberts, and Sherman counties that would be dewatered. Groundwater withdrawal rates used in the simulations were held constant from 2001-2050. No decreases in withdrawal rates were made versus what the aquifer may be able to sustain over this period. The conclusion was also made that economic irrigation, the ability to irrigate crops adequately, may cease in some areas well ahead of dewatering the aquifer.

Dutton (2004) provided an addendum to the Ogallala report from 2001 in which the base of the aquifer and recharge rates were adjusted to improve model calibration. Aquifer base level changes were the result of new information collected from drilling information in Roberts County, indicating the aquifer was deeper than originally modeled. Other changes were made due to the capabilities of the MODFLOW Drain and General Head Boundary (GHB) packages and some minor changes were made to hydraulic conductivity. Some adjustments to recharge rates were made as well. The overall result was that the root mean square error was reduced by more than 3 feet across the model domain.

The majority of the modeling efforts have been focused on the southern portion of the Ogallala aquifer. This area underwent irrigation development earlier than the northern portion of the Ogallala in Texas and, therefore, has seen more drawdown of the aquifer as

a whole. Interestingly, in every modeling effort to date, both the northern and southern aquifers have been modeled as a single layer aquifer. Dutton (2001) stated that the Ogallala can be modeled as a one-layer model and that no vertical heterogeneity was modeled in this effort. Currently, there is inadequate resolution of the formation to be able to account for vertical heterogeneity.

Deeds (2015) used a multiple layer model for analysis of the aquifers. The Ogallala was the upper layer, while the second layer was comprised of the Rita Blanca and Edwards Trinity aquifers and the upper and lower Dockum were represented as layers 3 and 4. The model used half-mile square grids and is reported to represent an advance in four areas:

1. The Rita Blanca Aquifer is simulated separately from the Ogallala Aquifer
2. A uniform approach to the implementation of input parameters, such as conductivity and recharge, is used.
3. No "overlap areas" exist where two models give conflicting results.
4. Simulation of cross-formational flow between the various aquifers that comprise the system is explicitly accounted for. Simulations supporting water planning will have this interaction "built-in."

Based upon a sensitivity analysis, Deeds reported that horizontal hydraulic conductivity is an important parameter for all aquifers except the Dockum Aquifer. The Dockum was more sensitive to vertical hydraulic conductivity. A sensitivity analysis provides some understanding of how critical the parameters are to the output of the model.

All previous models indicated a decline in water elevations, generally under all simulated conditions. Modifications to irrigation practices had the most impact on model simulations. The evolutionary process of both the northern and southern GAM in Texas seems to be a logical procession from attempt to attempt. All models presented here were

based upon previous work and were calibrated to known conditions before future projections were completed. Errors were reduced to reasonable levels prior to model runs but often parameters such as hydraulic conductivity or recharge had to be adjusted to make the model achieve known measurements.

Darcy's Law provides the mathematical underpinning for description of flow through porous media, including aquifers, and states that the flow of water through a material is proportional to the difference in height of the water between the two ends of the porous medium and inversely proportional to the length of the flow path. He also determined that the quantity of flow is proportional to a coefficient, K – hydraulic conductivity, which is dependent upon the nature of the permeable material.

$$\mathrm{Q} \propto h_A - h_B \quad \text{and} \quad \mathrm{Q} \propto -\frac{1}{\mathrm{L}} \tag{2.1}$$

The water-filled voids of a formation must allow water to move through the pore spaces to create flow otherwise the well would not produce water. This scenario is shown in Figure 2.2. Provided the flow rate through the porous media remains constant, the flow rate would be proportional to the cross-sectional area normal to the flow. Adding a proportionality constant to the equation yields Darcy's law

Table 2.1. Sequential listing of models of the Ogallala aquifer in Texas (modified by author from Mace 1998)

No.	Model Developer(s)	Date	Study Area	Intent of Model	Agency	Numerical Code
1	Claborn and others	1970	Counties of the Southern High Plains	First Modeling of Ogallala	Texas Tech University	Weber, California Water Resources polygonal finite-difference
2	Bell and Morrison	1979	Carson County	Water resource	Texas Dept. of Water Resources[1]	Unknown
3	Simpkins and Fogg	1982	Cross sectional model	Evaluate salt-dissolution zone	Bureau of Economic Geology	FLUMP, finite-element (Neuman and Narasimhan, 1977)
4	Knowles and others Knowles	1982, 1984 1984	Texas portion of the Ogallala	Water resource	Texas Dept. of Water Resources	Modified PLASM (Knowles, 1981)
5	McAda	1984	Parts of the Southern High Plains	Water resource	U.S. Geological Survey	Finite-difference model (Trescott and others, 1976)
6	Luckey Luckey and others	1984 1986	Central United States	Water resource	U.S. Geological Survey	Finite-difference model developed for the study (Luckey and others, 1986, p. 8)
7	Andrews	1984	Palo Duro Basin	Analysis of regional deep-basin flow system	Intera Technologies, Inc.	3D Finite-difference code
8	Wirojanagud and others	1986	Central part of the Southern High Plains	Evaluate cross-formational and deep-basin flow	Bureau of Economic Geology	TRAVEL (Charbeneau and Street, 1978)
9	Luckey and Stephens	1987	Part of Southern High Plains	Sensitivity on grid size	U.S. Geological Survey	Finite-difference model developed for the study (Luckey and others, 1986)
10	Peckham and Ashworth	1993	Texas portion of the Ogallala	Water resource (adjustment of the Knowles [1984] and Knowles and others [1984] model)	Texas Water Development Board	Modified PLASM (Knowles, 1981)
11	Mullican	1995	Roberts and Huthcison counties	Impact of proposed well field	Panhandle Ground Water Conservation District No. 3	MODFLOW (McDonald and Harbaugh, 1988)

Table 2.1, continued. Sequential listing of models of the Ogallala aquifer in Texas (modified by author from Mace 1998)

12	Dorman	1996	Part of the Southern High Plains	Water resource (conversion of the Knowles [1984] and Knowles and other [1984] model to MODFLOW	Texas Tech University (Master's thesis)	MODFLOW (McDonald and Harbaugh, 1988)
13	Mullican and others	1997	North of Palo Duro Creek and south of the Canadian River, Texas	Evaluate recharge rates and advective transport	Bureau of Economic Geology	MODFLOW (McDonald and Harbaugh, 1988)
14	Harkins	1998	Texas portion of the Ogallala	Water resource (conversion of the Knowles [1984] and Knowles and other [1984] model to MODFLOW	Texas Tech University (Ph.D. dissertation)	Modified version of MODFLOW (McDonald and Harbaugh, 1988)
15	Luckey and Becker	1999	Oklahoma portion of the Ogallala (north of the Canadian River and south of the Cimarron River)	Water resource	U. S. Geological Survey	MODFLOW
16	Dutton and others	2000, 2004	18 Texas Panhandle counties in the Panhandle Water Planning Group	Water resource, future conditions	Bureau of Economic Geology	MODFLOW
17	Stovall	2001	Southern portion on of the Ogallala	Water resource	Texas Tech University (Ph.D. dissertation)	MODFLOW
18	Deeds	2015	Ogallala, Rita Blanca, Edwards Trinity, Dockum	Water resource	Intera for the Texas Water Development Board	MODFLOW

1-Now the Texas Water Development Board

$$Q = -KA\left(\frac{h_A - h_B}{L}\right) \quad (2.2)$$

which may be expressed as:

$$Q = -KA\left(\frac{dh}{dl}\right) \quad (2.3)$$

in which dh/dl is known as the hydraulic gradient, dh represents the change in head between two points infinitesimally close together and dl is the minuscule distance between these points. The negative sign indicates the flow is in the direction of decreasing hydraulic head (Fetter, 2001). The first assumption of a model is that Darcy's law is followed in the Ogallala aquifer formation.

Fetter (2001) provides many basic assumptions made about the hydraulic conditions in the aquifer and about the pumping and observation wells:

1. The aquifer is bounded on the bottom by a confining layer.
2. All geologic formations are horizontal and have infinite horizontal extent.
3. The potentiometric surface of the aquifer is horizontal prior to the start of pumping.
4. The potentiometric surface of the aquifer is not changing with time, prior to the start of the pumping.
5. All changes in the position of the potentiometric surface are due to the effect of the pumping well alone.
6. The aquifer is homogeneous and isotropic.
7. All flow is radial toward the well.
8. Groundwater flow is horizontal.

9. Darcy's law is valid.
10. Groundwater has a constant density and viscosity.
11. The pumping well and the observation wells are fully penetrating; that is, they are screened over the entire thickness of the aquifer.
12. The pumping well has an infinitesimal diameter and is 100% efficient with respect to drawdown.

Wells completed in an unconfined aquifer initially behave as Theis wells, and the drawdown can be calculated using the Theis nonequilibrium equation:

$$h_o - h_t = \frac{Q}{4\pi T}\int_u^\infty \frac{e^{-a}}{a}\,da \qquad (2.4)$$

where the argument u is given by:

$$u = \frac{r^2 S}{4Tt} \qquad (2.5)$$

where:

Q is the constant pumping rate (L^3/T, where T = 24 hours or 1 day);

h_t is the time-varying hydraulic head at a given radius, r (L);

h_o is the initial hydraulic head (L);

h_o - h is the drawdown (L);

T is the aquifer transmissivity (L^2/T);

t is the time since pumping began (T);

r is the radial distance from the pumping well (L);

S is the aquifer storativity (dimensionless).

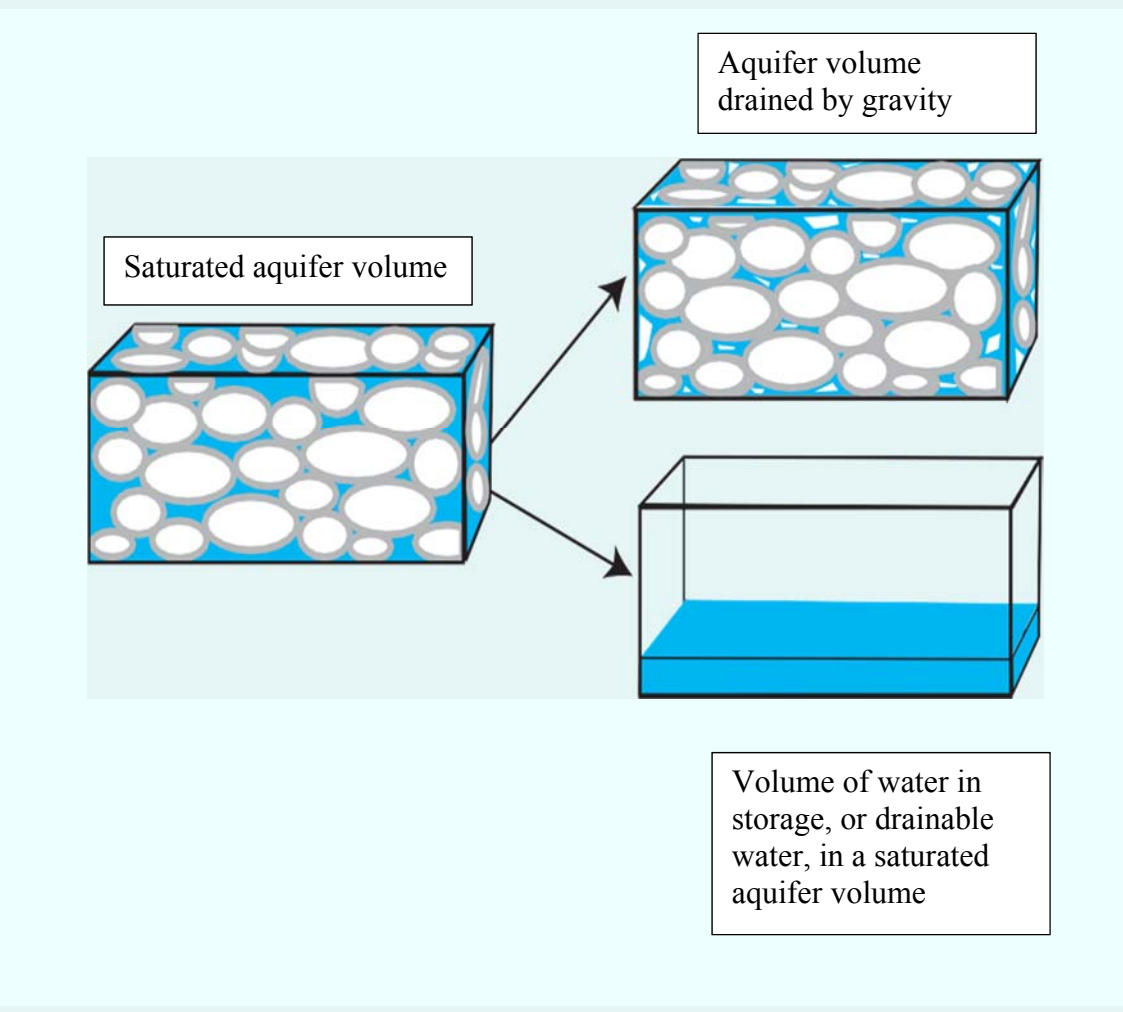

Figure 2.2. Schematic showing the amount of water in storage in a representative volume of the Ogallala aquifer (McGuire 2003). Used with permission.

Storativity is the volume of water released from a vertical column of the aquifer per unit surface area of the aquifer and unit decline in water level (Dutton 2001)

The integral form of the Theis equation is of a form known as an exponential integral, which can be expanded by an infinite series, resulting in the following form of the Theis equation:

$$h_o - h_t = \frac{Q}{4\pi T}\ [-0.5772 - \ln u + u - \frac{u^2}{2 * 2!} + \frac{u^3}{3 * 3!} + \frac{u^4}{4 * 4!} + \cdots] \qquad (2.6)$$

The infinite series term of equation 2.6 is known as the well function and is designated W(u). Substituting the well function notation, the Theis equation becomes:

$$h_o - h_t = \frac{\mathrm{Q}}{4\pi\mathrm{T}}\mathrm{W}(u) \qquad (2.7)$$

Reversing the sign on the values of the Theis drawdown calculated values will provide the calculated cone of depression created by a well. This is shown in Figure 2.3 below.

This is the process that will occur as the water is withdrawn from the saturated thickness of the aquifer. The cone of depression will eventually rebound once the well is no longer being pumped. However, as the well rebounds towards a new equilibrium, the water level will not return to the original level in the aquifer. This would violate assumption number 12 above. The well is not 100% efficient with respect to drawdown. The theoretical drawdown will not match the actual drawdown in the well. Figures 2.4

through 2.8 illustrate the variables that will influence the development of the cone of depression and how the cone will be allowed to rebound.

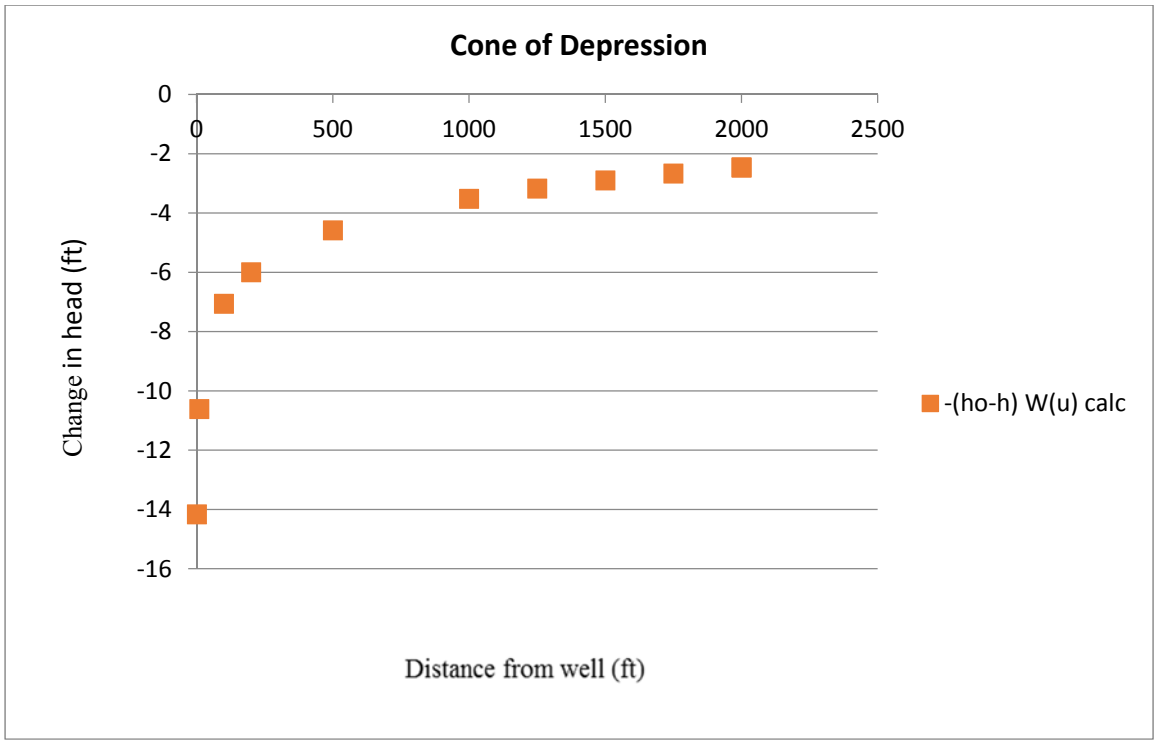

Figure 2.3. Calculated cone of depression for a pumping well in an unconfined aquifer.

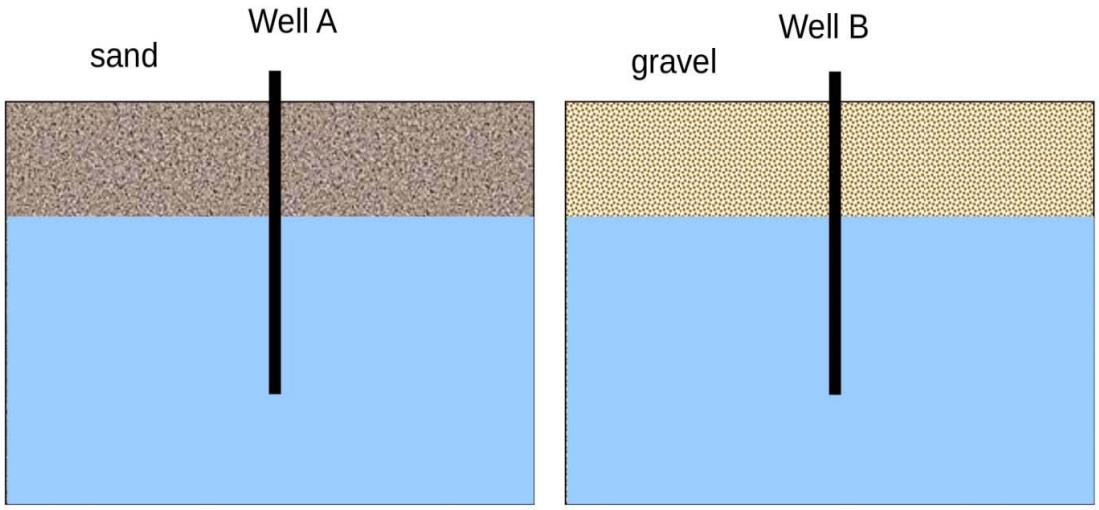

Figure 2.4. Wells completed in sand and gravel modified from R. J. Mitchell, used with permission.

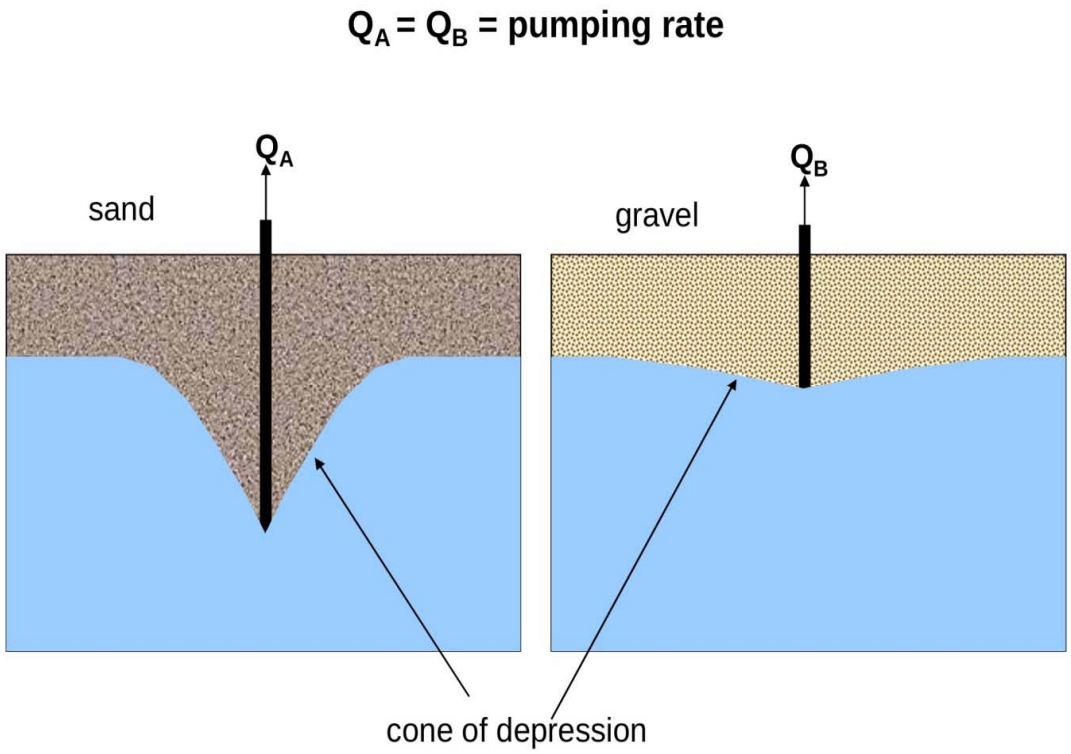

Figure 2.5. Wells illustrating differences in development of cone of depression based upon stationary media, from R. J. Mitchell, used with permission.

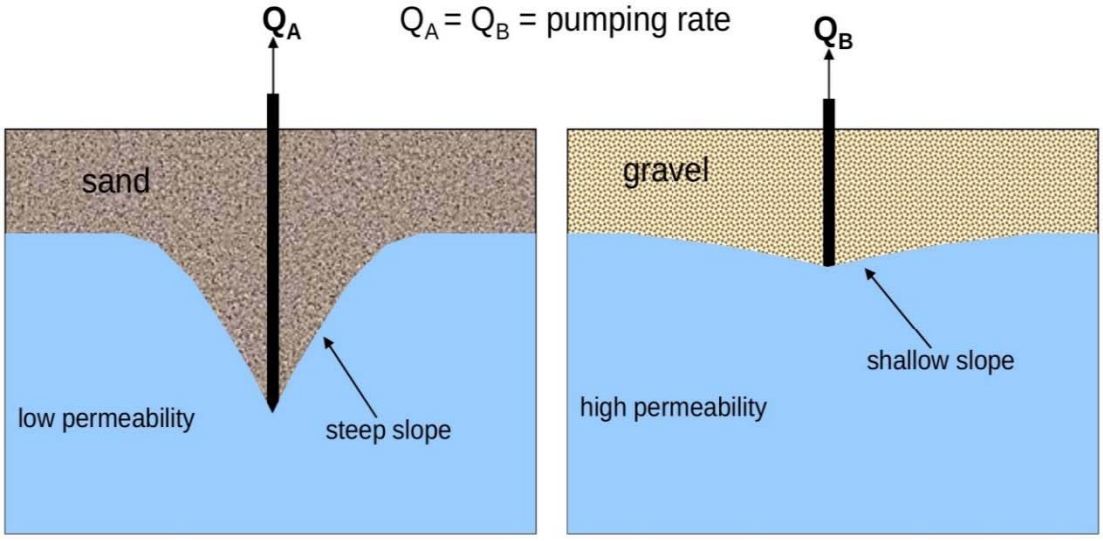

Figure 2.6. Illustration of the slope of the cone of depression. Slope is dependent upon the permeability of the stationary media, from R. J. Mitchell, used with permission.

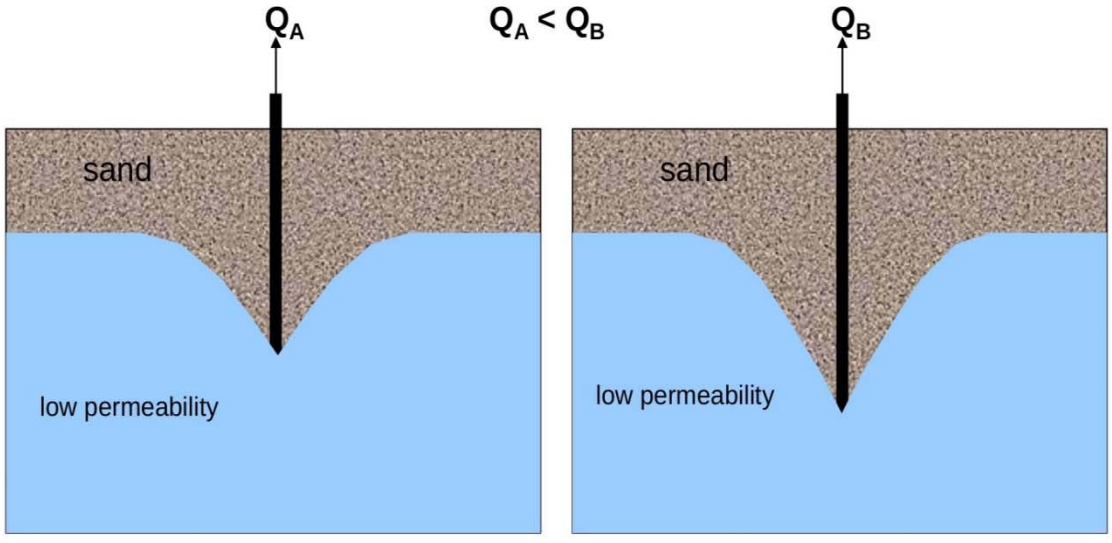

Figure 2.7. Cone of depression depth is attributed to pumping rate, from R. J. Mitchell, used with permission.

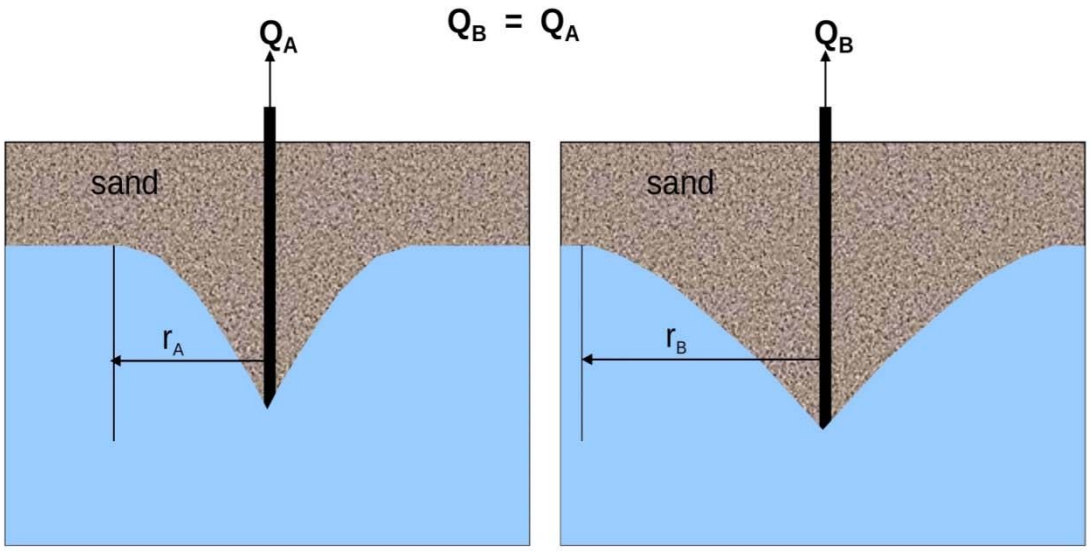

Figure 2.8. The radius of the cone is dependent upon the duration of pumping, from R. J. Mitchell, used with permission. Q_B illustrates the effect of longer pumping periods on the cone of depression.

Figure 2.4 illustrates two wells completed in similar fashion but in two different types of stationary media. Water will not move through different media at the same rate. This is seen in Figure 2.5. The output of both pumps is the same, but the water moves through the gravel media easier than the sand media. The slope of the cone will also be influenced by the permeability of the stationary media as shown in Figure 2.6. The higher the permeability, the easier it is for water to move to the pumping well. Figure 2.7 illustrates the depth of the cone, based on differences in pump output. Not all wells completed within the saturated zone will produce the same level of output. The effect of pumping time is shown in Figure 2.8. Assuming the stationary media is homogeneous, the longer a pump is allowed to withdraw water, the larger the cone will be.

As shown in the previous illustrations, the shapes of the cones of depression can change from well to well. Using the WMA to determine remaining water in the saturated thickness, the cone is not allowed to fully rebound prior to the water elevations being measured. The measurement of the wells generally occurs in January and February when wells are traditionally not pumped for irrigation. Depending on how deep the cone of depression develops and how far from the radius of the well it may extend, rebound may take years to reach a new equilibrium. This is one reason to explore the possibility of the presence of the mounded water between wells. The second reason is that current beliefs are that there is more water in the aquifer than currently projected.

It is important to note the slope of the ground surface across the model area. Figure 1.8, modified from Dutton (2004), illustrates the substantial elevation drop from west to east across the model area. Elevations approaching 4000 feet exist on the western side of the Texas Panhandle and approach 2000 feet on the eastern side of the Panhandle. This slope does present a small but naturally occurring flow from west to eat across the entire northern portion of the Ogallala aquifer. A geometric mean of the natural hydraulic conductivity of 14.8 feet per day was provided by Dutton (2004). Gutentag, et al. (1984) reported a hydraulic conductivity range of 25-300 feet per day with an average of 60 feet per day. The wide range in conductivity can be attributed to different sediment types which vary horizontally and vertically. The variability of sediment types violates assumptions 2 and 6 proposed by Fetter. Figure 2.9 shows that the base of the aquifer follows a similar west-east slope from about 4000 feet in the west to about 2000 feet in the east.

As described by Dutton (2004), the flow of groundwater is derived from a water balance equation as proposed by Domenico and Schwartz (1990). The proposed equation is:

$$inflow - outflow = -div\,\boldsymbol{q} - R^* = S_s \frac{\delta h}{\delta t} \qquad 2.8$$

where:

div **q** is a vector which is the difference between mass inflow rate and the mass outflow rate for the unit volume. It has the physical meaning of net outflow rate per unit volume of aquifer (1/time);

q is the specific discharge or velocity of water moving into and out of a unit volume of an aquifer (length/time);

R* represents various sources and sinks of water as a volumetric rate per unit volume of an aquifer (1/time);

S_s is specific storage (1/length);

$\frac{\delta h}{\delta t}$ expresses the time rate of change of hydraulic head (h) or water level.

The R* term in Equation 2.8 uses boundary conditions and aquifer stresses to account for the sources and sinks within the model. The stresses include the specific storage, storativity, permeability, transmissibility and transmissivity of the aquifer (Dutton 2001) which are defined below.

Specific storage is the volume of water that an aquifer can absorb or expel from a unit volume when the pressure head changes by a unit amount (Fetter 2001). In an

unconfined aquifer like the Ogallala, storage changes are primarily attributed to the filling and draining of pore spaces (Dutton 2001). Storativity is the volume of water released from a vertical column of the aquifer per unit surface area of the aquifer and unit decline in water level (Dutton 2001):

$$S = Ss * b \qquad 2.9$$

where:

S is the storativity of an aquifer (dimensionless);

Ss is the specific storage (1/L);

b is the saturated thickness of the aquifer (L).

The intrinsic permeability is a function of the size of the openings in the stationary medium of the aquifer. Permeability measures the capacity of the stationary medium to allow fluids to pass through it (Fetter 2001) and is shown by:

$$K_i = C d^2 \qquad 2.10$$

where:

Ki is the permeability (L^2);

C is a proportionality constant called the shape factor (dimensionless);

d^2 is the square of the diameter of the soil particles (L^2).

Transmissivity is a measure of the rate at which water is transmitted through a unit width of an aquifer under a unit hydraulic gradient. It is a function of the properties of the liquid, the stationary medium and the thickness of the stationary media (Fetter 2001):

$$T = bK \qquad 2.11$$

where:

T is the transmissivity of the aquifer (L^2/T);

b is the saturated thickness of the aquifer (L);

K is the hydraulic conductivity of the aquifer (L/T).

Recharge rates across the northern Texas GAM have been proposed to range from 0.01 to 6 inches per year (Mullican and others, 1997). As noted by Dutton (2001), the recharge distribution is poorly known but seems to be focused through playa basins (see Nativ and Smith, 1987; Osterkamp and Wood, 1987; Nativ and Riggio, 1989; Mullican and others, 1997 for more detail). Figure 2.10 illustrates the saturated soil hydraulic conductivity using the soil textural triangles. Based upon the saturated conductivity rates provided in

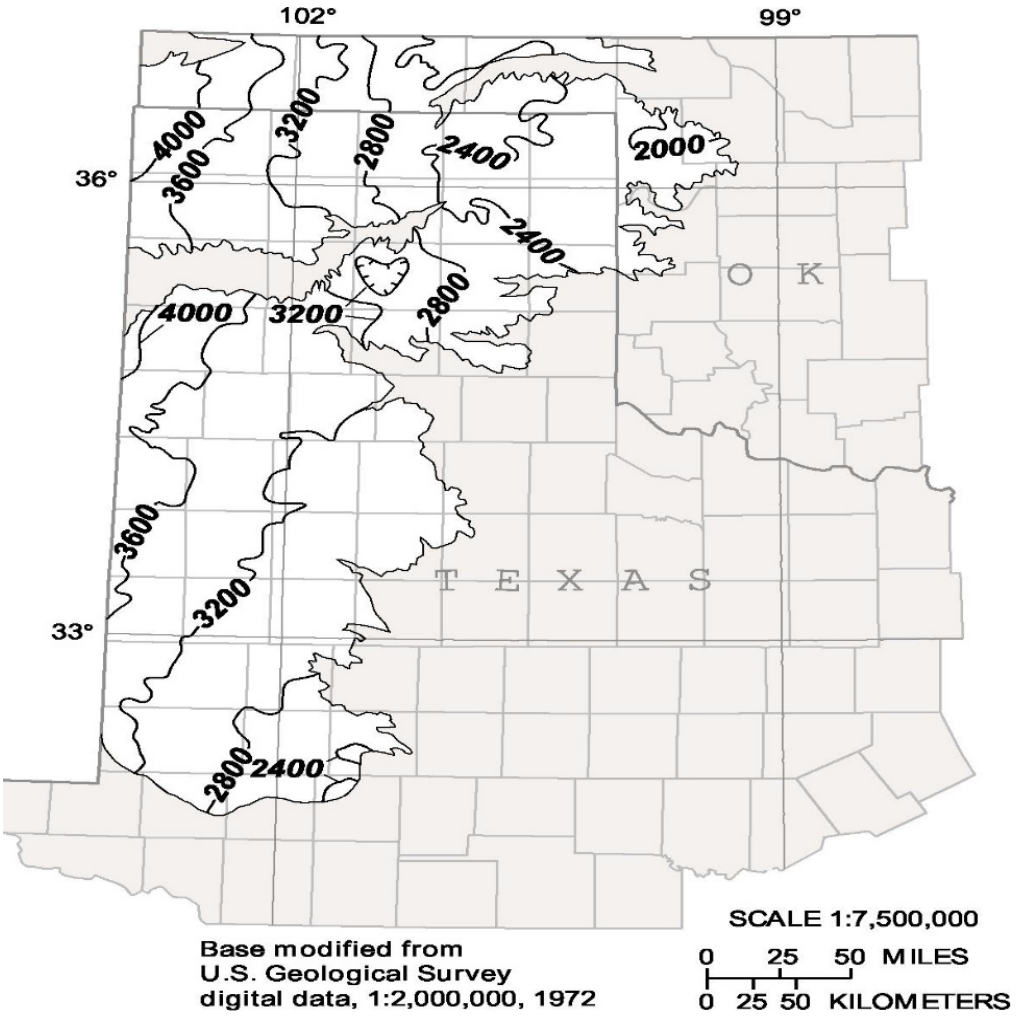

Figure 2.9. Ogallala base contour map (modified from Weeks 1981). Used with permission

Figure 2.10 for low, medium and high density soils, recharge rates in excess of fractions of an inch would appear to be unattainable.

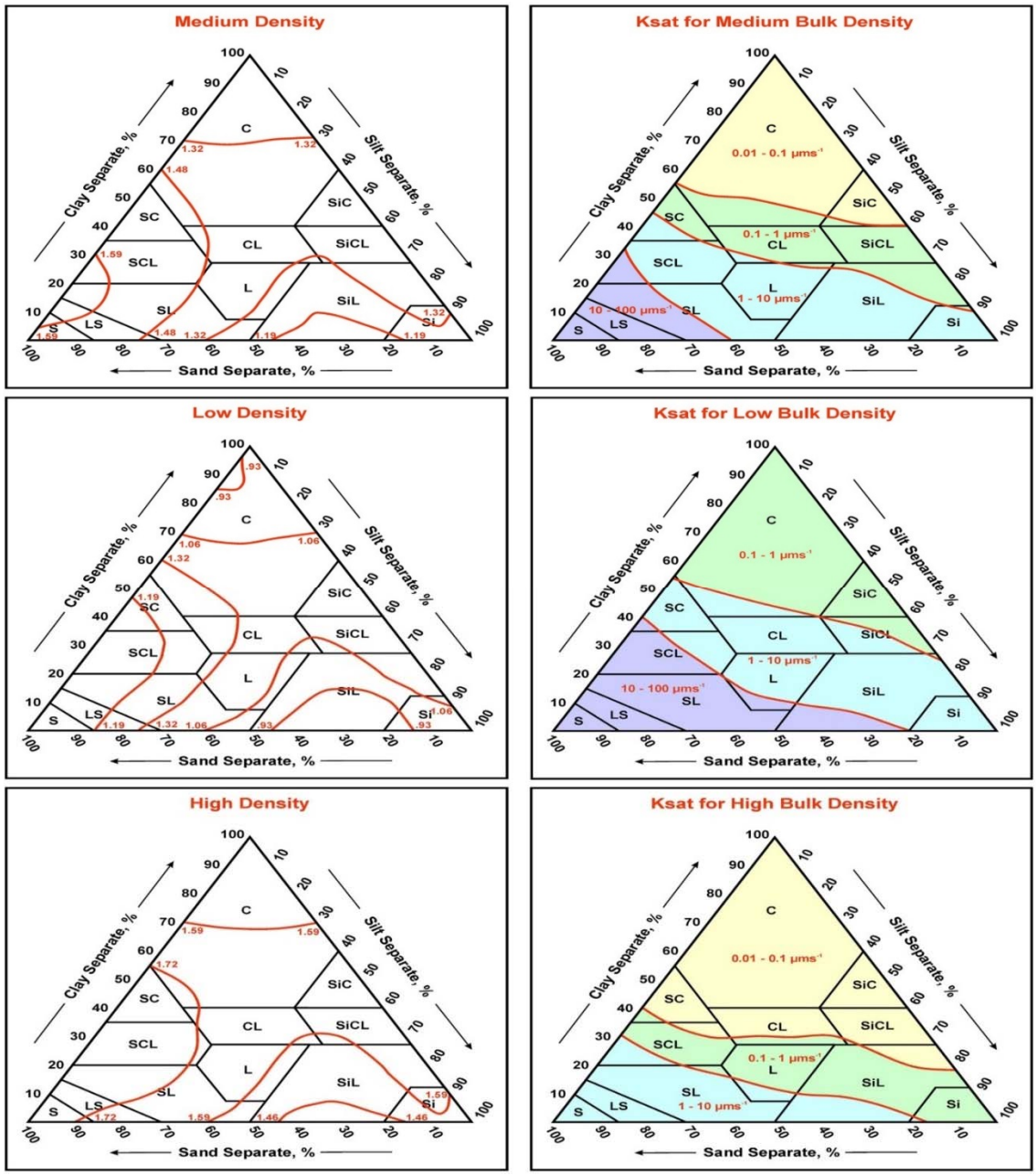

Figure 2.10. USDA NRCS National Soil Survey Handbook guide for estimating saturated soil hydraulic conductivity from soil properties (USDA NRCS NSSH, 2016). Used with permission.

Precipitation increases from west to east across the Panhandle as shown by Narasimham in Figure 2.11.

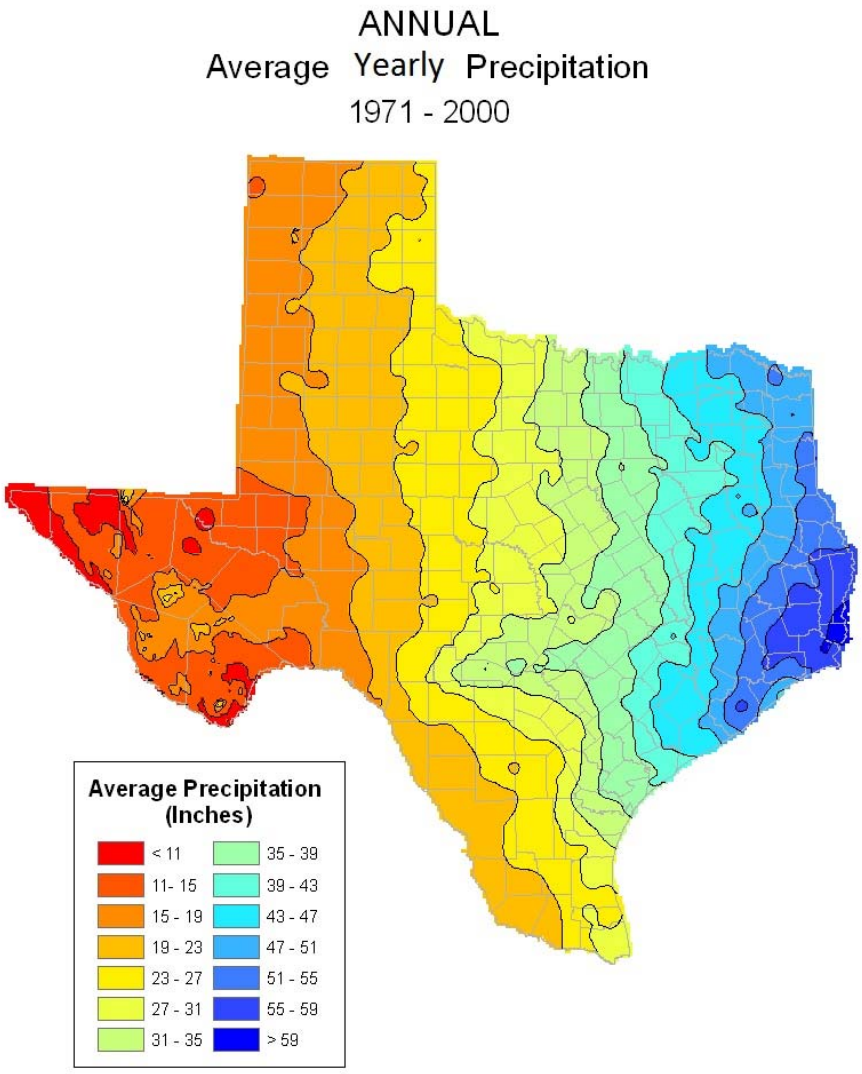

Figure 2.11. Annual average precipitation in Texas 1971-2000 (Narasirham 2008)

As noted in Figure 2.11, the annual precipitation in the vicinity of the northern Texas GAM ranges from less than 11 inches in a small region of the western Panhandle to a maximum of 27 inches annually in the eastern Panhandle. The northern modeled area is located on the Dallam-Hartley county line so it falls in the region of 11-15 inches of annual rainfall. The southern modeled area is in northeastern Lamb County where the average annual rainfall is also 11-15 inches. The majority of the annual precipitation occurs from May to August, Figure 2.12, coinciding with the most active agriculture production period. Given the amount of plant growth, either in agricultural production, grassland, or other, it is assumed the majority of the precipitation during most events will be used well before much of the water could percolate below the root zone and ultimately reach the water table.

The average amount of surface evaporation from 1971-2000 is shown in Figure 2.13. The range in the region of the northern Texas GAM is from 48-72 inches per year from the extreme northwestern part of the GAM to the central Texas Panhandle area. This further supports the exclusion of recharge in the model.

Finally, Figure 2.14 below shows the annual average potential evapotranspiration (PET) rate in Amarillo is 55.51 inches (http://texasnet.tamu.edu/pet.php). This is the closest location to the modeled area so the assumption was made that the PET would be approximately the same rate.

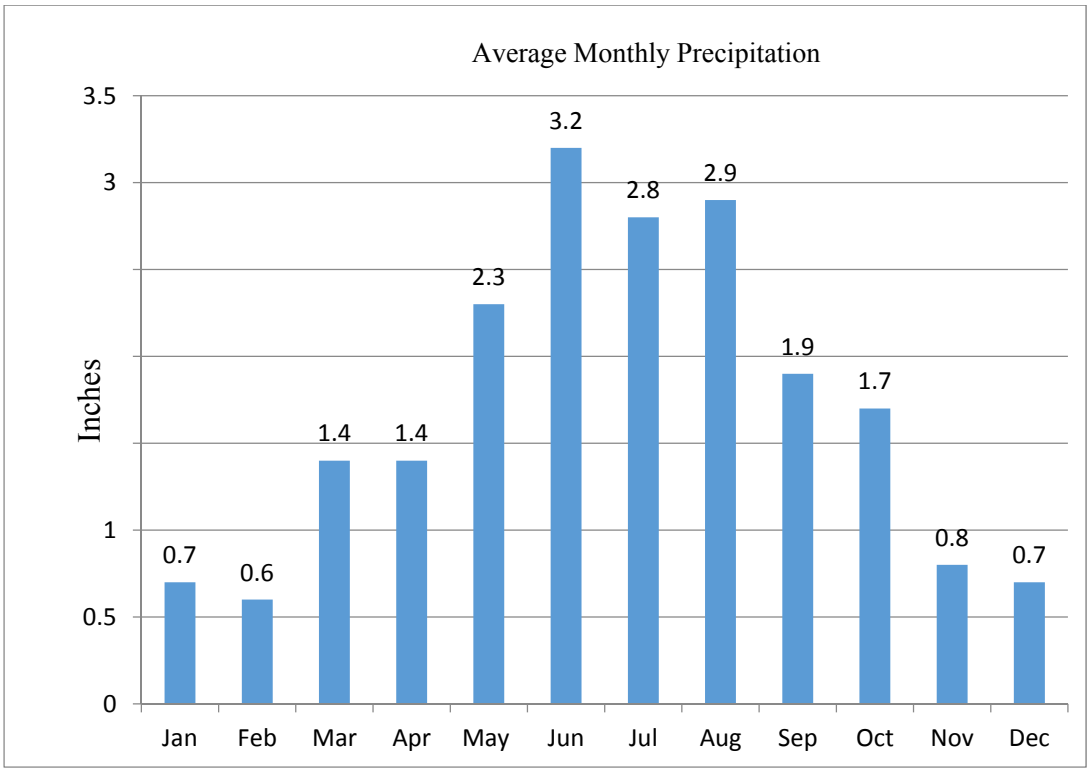

Figure 2.12. Average monthly precipitation in Amarillo, Texas (https://weather.com/weather/monthly/l/79109)

Due to the permeability of the soils, the average precipitation rates, evapotranspirtation and monthly distribution of rainfall it is assumed no significant recharge will occur in the modeled area and it was consequently excluded from this modeling effort.

Groundwater withdrawal in the northern portion of the GAM is substantial. Irrigation is the primary user of the groundwater withdrawn. Table 2.3 provides data on the amount withdrawn from 2008-2013 as reported by the North Plains Groundwater Conservation District. As can be seen from the data, the western group of counties withdraws substantially more groundwater than the eastern group of counties. This increased withdrawal rate is primarily attributed to the amount of irrigable land as compared to eastern counties. Other factors that contribute to differing pumping rates are reduced

rainfall in the western counties versus the east and to different cropping regimes in the western as opposed to eastern counties.

Table 2.4 provides the area of each county and the area of each county within the North Plains Groundwater Conservation District. If the total withdrawal within a given area is divided by the respective area associated with that withdrawal, there would be a starting point for aquifer decline. This withdrawal is shown in Table 2.5.

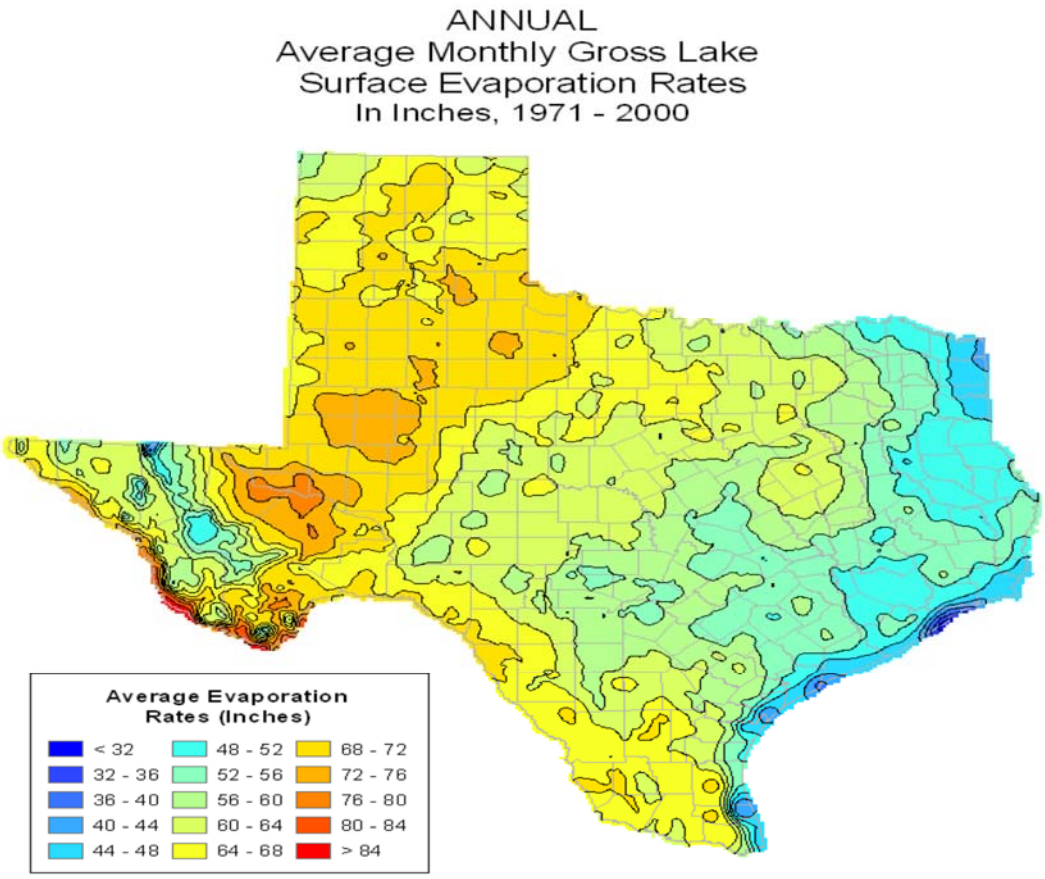

Figure 2.13. Annual average surface evaporation in Texas 1971-2000 (from Narasirham, 2008)

Average Monthly ETo (PET) (inches/month)													
City	Jan	Feb	Mar	Apr	May	Jun	Jul	Aug	Sep	Oct	Nov	Dec	Total
Amarillo	1.84	2.27	3.73	5.06	5.89	7.51	8.08	7.29	5.61	4.05	2.4	1.78	**55.51**

Figure 2.14. Average Monthly ETo for Amarillo, Texas over 52 years (http://texasnet.tamu.edu/pet.php)

Table 2.3. Reported Production for 2008-2013 (Hallmark, 2014)

County	2008 ac-ft	2009 ac-ft	2010 ac-ft	2011 ac-ft	2012 ac-ft	2013 ac-ft
Dallam	313,451	317,441	302,561	374,733	371,965	399,272
Hartley	364,560	387,305	401,506	519,684	458,696	458,998
Sherman	275,128	285,571	261,608	407,265	348,012	346,685
Moore	191,409	200,220	178,336	271,684	234,688	228,297
GMA-1 West	1,144,548	1,190,537	1,144,011	1,573,366	1,413,361	1,433,252
Hansford	142,694	152,686	129,984	234,903	218,793	201,914
Hutchinson	52,846	53,869	42,023	73,747	72,230	69,716
Ochiltree	75,527	65,840	62,269	114,392	109,213	98,280
Lipscomb	30,832	30,242	33,826	52,003	55,572	42,519
GMA-1 East	301,899	302,637	268,102	47,5045	455,808	412,429
Total	1,446,447	1,493,174	1,412,113	2,048,411	4,869,169	1,845,681

Table 2.4 County Area and Current Percent in District (Hallmark 2014)

County	County Area (Sq. Mi.)	Area in District (Sq. Mi)	Area in District (acres)	Percent of County in District
Dallam	1494	1494	956,160	100
Hansford	907	907	580,480	100
Hartley	1489	1267	810,880	85
Hutchinson	911	266	170,240	29
Lipscomb	934	934	597,760	100
Moore	914	633	405,120	69
Ochiltree	907	907	580,480	100
Sherman	916	916	275,128	100
Totals	8472	7324	4,687,360	

Numerous efforts have been conducted to model the valuable underground water resource known as the Ogallala. Efforts to include the entire aquifer area may be beyond the current capabilities of modeling. Natural boundaries where rivers cross the aquifer and bisect the north-south flow of groundwater seem to be justifiable locations to divide models. This will also coincide reasonably well with regional variations of temperature, evapotranspiration, rainfall, and potential recharge to the aquifer. However, variations in the hydrologic properties within regions will contribute further challenges for modeling. For purposes of this work, only small portions of the Northern and Southern aquifer will be used for analysis. These models are expected to provide sufficient data for the analysis of mounded water between pumped wells.

Table 2.5. Calculated aquifer decline (Hallmark 2014).

County	2008 ac-ft	2008 Aquifer Decline (feet)	2008 Decline 16% Yield (Feet)	2009 ac-ft	2009 Aquifer Decline (feet)	2009 Decline 16% Yield (Feet)	2010 ac-ft	2010 Aquifer Decline (feet)	2010 Decline 16% Yield (Feet)	2011 ac-ft	2011 Aquifer Decline (feet)	2011 Decline 16% Yield (Feet)	2012 ac-ft	2012 Aquifer Decline (feet)	2012 Decline 16% Yield (Feet)	2013 ac-ft	2013 Aquifer Decline (feet)	2013 Decline 16% Yield (Feet)
Dallam	313,451	0.33	2.05	317,441	0.33	2.07	302,561	0.32	1.98	374,733	0.39	2.45	371,965	0.39	2.43	399,272	0.42	2.61
Hansford	142,694	0.25	1.54	152,686	0.26	1.64	129,984	0.22	1.40	234,903	0.40	2.53	218,793	0.38	2.36	201,914	0.35	2.17
Hartley	364,560	0.45	2.81	687,305	0.85	5.30	401,506	0.50	3.09	519,684	0.64	4.01	458,696	0.57	3.54	458,998	0.57	3.54
Hutchinson	52,846	0.31	1.94	53,869	0.32	1.98	42,023	0.25	1.54	73,747	0.43	2.71	72,230	0.42	2.65	69,716	0.41	2.56
Lipscomb	30,899	0.05	0.32	30,242	0.05	0.32	33,826	0.06	0.35	52,003	0.09	0.54	55,572	0.09	0.58	42,519	0.07	0.44
Moore	191,409	0.47	2.95	200,220	0.49	3.09	178,336	0.44	2.75	271,684	0.67	4.19	234,688	0.58	3.62	228,297	0.56	3.52
Ochiltree	75,527	0.13	0.81	65,840	0.11	0.71	62,269	0.11	0.67	114,392	0.20	1.23	109,213	0.19	1.18	98,280	0.17	1.06
Sherman	275,128	0.47	2.94	285,871	0.49	3.05	261,608	0.45	2.79	407,265	0.69	4.34	348,012	0.59	3.71	346,685	0.59	3.70

Chapter III

MODEL DEVELOPMENT

Several options were considered prior to the model construction for this project. The first effort was to construct a simple conceptual model using accepted aquifer characteristics. The option of a multilayer model was considered. Harvesting a portion of the accepted GAM was considered and determined to be the best option upon which to base the working models in this work. The GAM was loaded into the software and a small region was selected and used for all modeling efforts related to this work. A very small conceptual model was also constructed to evaluate how the results could be viewed within the software.

The purpose of the model proposed in this project is not to contradict the decline in aquifer levels. The primary goal expands upon the work of Ouapo, et al. (2014) whose study suggested that the amount of water remaining within the aquifer may be underestimated. A modified conceptual representation of drawdown as proposed by Ouapo, et al. is incorporated here as Figure 3.1. The abstract model suggests that significant amounts of water may remain between pumped wells. This water is not taken into account when using the Well Measurement Approach (WMA) to determine

remaining water-surface levels within the aquifer. The mounds of water between wells are the result of the development of cones of depression between the wells, as illustrated in Figure 1.5. As more wells are drilled and pumped, it is hypothesized that additional mounds will develop between the wells or existing mounds will be mined from between older wells. This can be illustrated by considering two different views of an aquifer. Using an example from Beattie (1981), the first illustration considers an aquifer like a bathtub. When water is withdrawn from the tub, the overall water level of the entire tub will decline with no subsequent cone of depression being formed. This concept assumes there is no hindrance of the lateral flow of water. The second example would be to view the bathtub filled with sand and then water placed into the bathtub. If water were to be withdrawn by a well in the center of the tub the water levels near the edges of the tub will not be affected, at least not immediately. The sand limits the lateral movement of water towards the well and causes the cone of depression to form. If a second well were placed in the tub, the water-surface at the second location will be slightly depressed. When this second well is pumped, the water closest to the well will be pumped first, resulting in a second cone of depression and subsequent mound between the wells. This effect is illustrated in Figure 3.2. Here the effect of four wells withdrawing water from the aquifer results in mounds between the pumping wells. The cones and mounds illustrated in Figure 3.2 are from one pumping cycle that lasted 120 days. The water within the cells containing the wells will supply the stored water first. Since the model is a single layer the water stored in the four cells adjacent to the four faces of the well cell will then provide stored water to the well cell. Ignoring the cells i,j,k-1 and i,j,k+1, Figure 3.3 illustrates the four adjacent cells. Since there are four cells comprising the second level

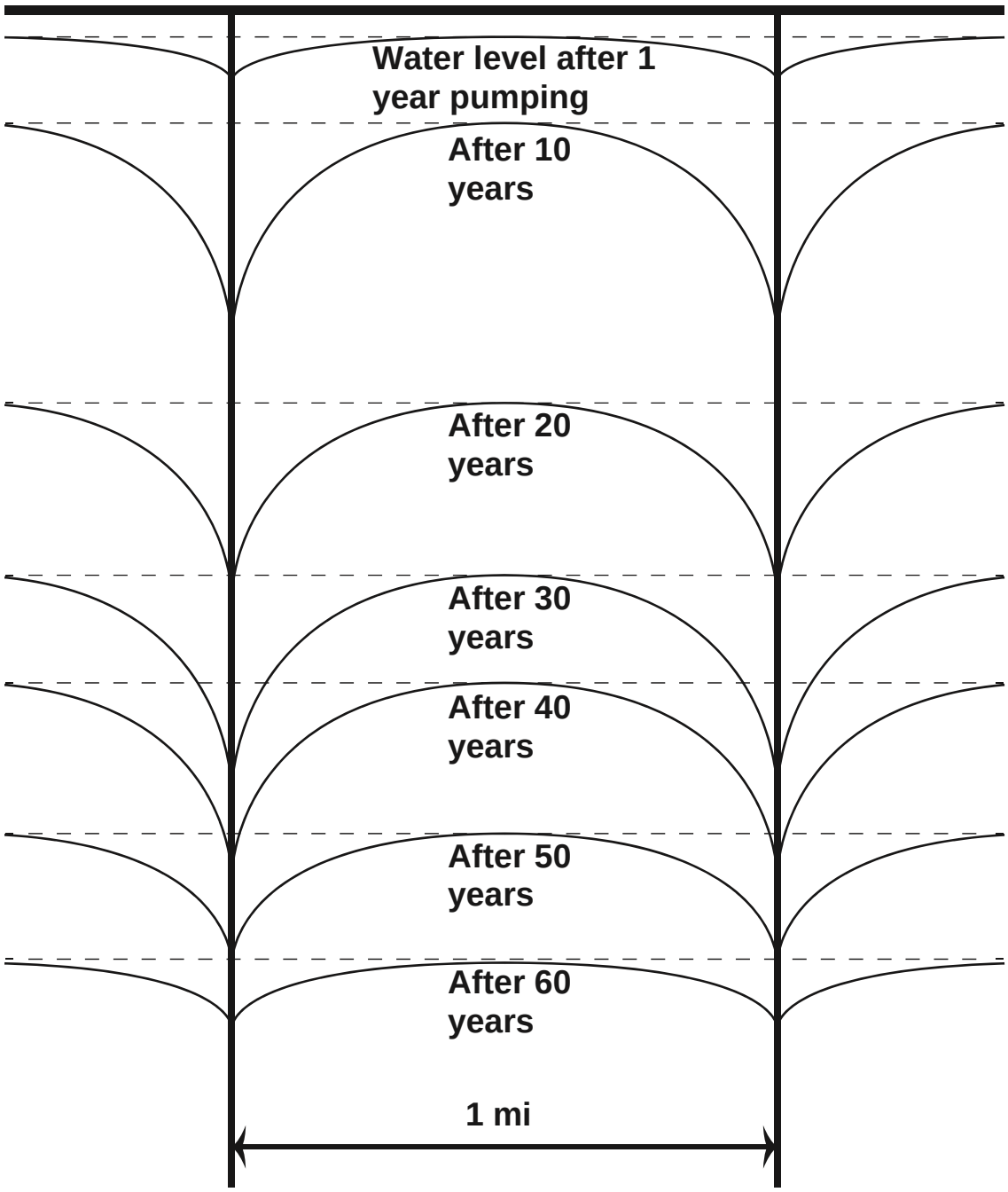

Figure 3.1. Modified conceptual model, proposed by Ouapo, et al., of the development and decline of a water mound between irrigation wells with succeeding years (Ouapo, et al. 2014).

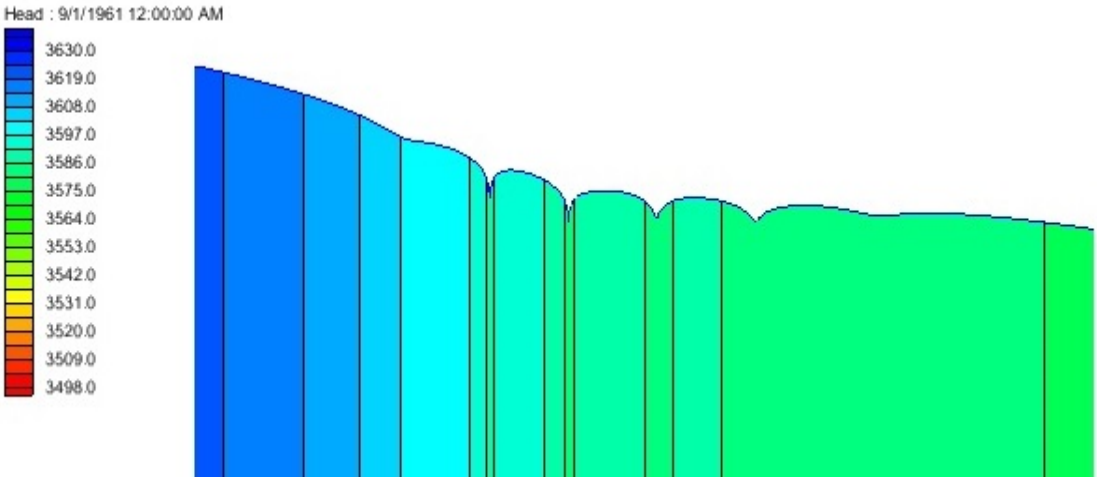

Figure 3.2. Residual mounds of water between pumping wells in the northern model. The wells are pumped for 120 days simulating the irrigation cycle for corn irrigation. Note the depression in the cells containing the wells and the overall depression towards the center where the four wells are located.

of cell, less water is required from storage to supply a constant amount of water. The third layer of cells would be comprised of twelve cells. The third layer would provide even less water to the well cell in order to maintain the output of the well. Each subsequent layer would be composed of more cells, each required to supply smaller volumes of water to maintain a flow rate of water to the well cell.

The modeling effort presented in this work is done using MODFLOW-2000 (Harbaugh, et al., 2000). MODFLOW is a widely accepted program used to perform simulations of groundwater movement and to estimate water remaining in storage. The program is used to solve the three dimensional flow equation (3.1) for porous media (McDonald and Harbaugh 1988, Harbaugh, et al., 2000). The following mathematical development is primarily taken from Harbaugh, et al., and McDonald and Harbaugh (2000, 1988) with specifics to this modeling effort added.

$$S_s \frac{\delta h}{\delta t} = W + \frac{\delta}{\delta x}\left\{K_{xx} \frac{\delta h}{\delta x}\right\} + \frac{\delta}{\delta y}\left\{K_{yy} \frac{\delta h}{\delta y}\right\} + \frac{\delta}{\delta z}\left\{K_{zz} \frac{\delta h}{\delta z}\right\} \quad (3.1)$$

where:

K_{xx}, K_{yy}, K_{zz} are hydraulic conductivity values along the x, y, and z coordinate axes, which are assumed to be parallel to the major axes of hydraulic conductivity and have the units (L/T) or Length/Time;

h is the potentiometric head (L);

W is volumetric flux per unit volume representing sources and/or sinks of water, with $W < 0.0$ for efflux from the ground water system, and $W > 0.0$ for influx (T^{-1});

S_s is the specific storage of the porous material (L^{-1});

t is time (T);

$\frac{\delta h}{\delta t}$ expresses the time rate of change of hydraulic head (h) or water level; and

$\left\{\frac{\delta h}{\delta x}\right\}\left\{\frac{\delta h}{\delta y}\right\}\left\{\frac{\delta h}{\delta z}\right\}$ are the changes in saturated thickness with respect to direction.

Specific storage is the volume of groundwater that an aquifer absorbs or expels from a unit volume when the pressure head decreases or increases (Fetter 2001)

Equation 3.1 describes transient three-dimensional groundwater flow in a heterogeneous and anisotropic medium. All flows into and out of a given cell are equated to the rate of change in storage, with respect to time, within a cell. In other words, MODFLOW evaluates the change in head, ∂h, over a given length of time, ∂t. Time is determined using a backward-difference approach where t^{m-1} is a time interval preceding t^m shown in equation 3.2.

The process of describing ground water flow requires the solution of equation 3.1 using a finite-difference method. The use of this method requires the flow system to be divided into a grid of cells. Central to each cell is a node, the point at which the head is calculated. The finite difference equation for a cell is (McDonald and Harbaugh, 1988):

$$CR_{i,j-\frac{1}{2},k}\left(h^m_{i,j-1,k} - h^m_{i,j,k}\right) + CR_{i,j+\frac{1}{2},k}\left(h^m_{i,j+1,k} - h^m_{i,j,k}\right) \quad (3.2)$$

$$+ CC_{i-\frac{1}{2},j,k}\left(h^m_{i-1,j,k} - h^m_{i,j,k}\right) + CC_{i+\frac{1}{2},j,k}\left(h^m_{i+1,j,k} - h^m_{i,j,k}\right)$$

$$+ CV_{i,j,k-\frac{1}{2}}\left(h^m_{i,j,k-1} - h^m_{i,j,k}\right) + CV_{i,j,k+\frac{1}{2}}\left(h^m_{i,j,k+1} - h^m_{i,j,k}\right) + P_{i,j,k}h_{i,j,k}$$

$$+ Q_{i,j,k} = SS_{i,j,k}(DELR_j * DELC_i * THICK_{i,j,k})\frac{h^m_{i,j,k} - h^{m-1}_{ij,k}}{t^m - t^{m-1}}$$

where:

$h^m_{i,j,k}$ is head at cell i, j, k at time step m (L);

CV, *CR*, and *CC* are hydraulic conductances between node i, j, k and a neighboring node (dimensions L^2/T);

$P_{i,j,k}$ is the sum of coefficients of head from source and sink terms (L^2/T);

$Q_{i,j,k}$ is the sum of constants from source and sink terms, with $Q_{i,j,k}$ <0.0 for flow out of the ground water system, and $Q_{i,j,k}$ >0.0 for flow in (L^3/T);

$SS_{i,j,k}$ is the specific storage (L^{-1});

$DELR_j$ is the cell width of column j in all rows (L);

$DELC_i$ is the cell width of row i in all columns (L);

$THICK_{i,j,k}$ is the vertical thickness of cell i, j, k (L); and

t^m is the time at time step m (T).

Figure 3.3 illustrates the location of cell i,j,k and the indices for the six adjacent cells and Figure 3.4 illustrates the flow into cell i,j,k from an adjacent cell. Equation 3.2 performs the influx and efflux flow calculations for each cell at each time step specified in the model.

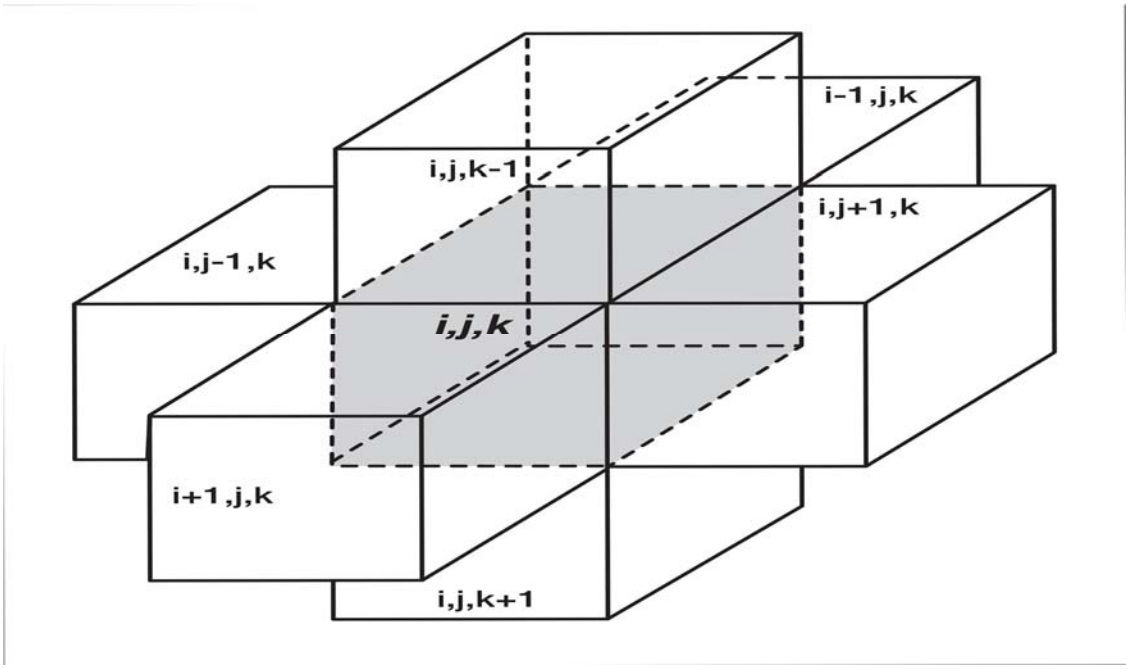

Figure 3.3. Cell i,j,k and the indices for the six adjacent cells (McDonald and Harbaugh 1988). Used with permission.

Conductance is the flow of water through a medium and is defined as the product of the hydraulic conductivity and cross sectional area perpendicular to flow divided by the length of the prism or cell parallel to the flow path. This is shown equation 3.5 below.

In order to designate hydraulic conductance between nodes and not hydraulic conductance within a cell, the notation "1/2" is employed. This designation is to show

that model calculations are carried out between the nodes which are centrally located within the cells as illustrated in Figure 3.4.

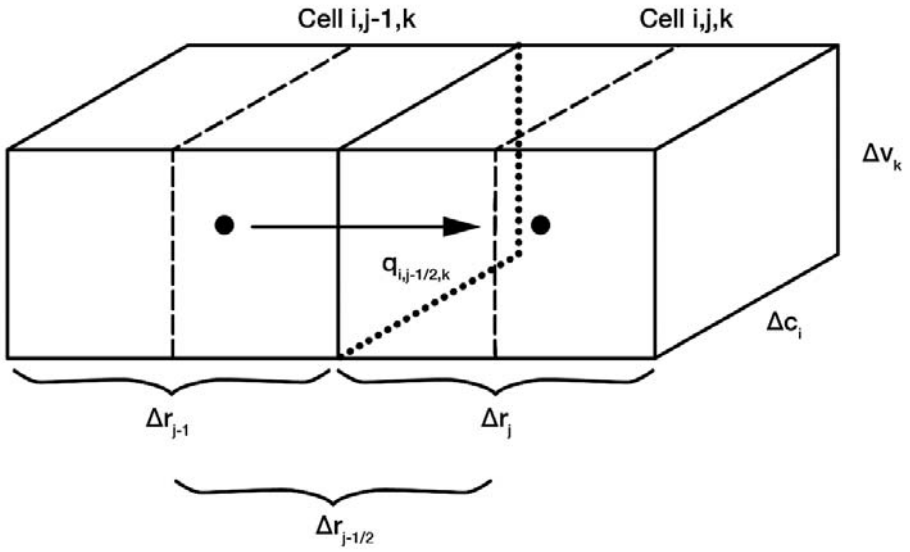

Figure 3.4. Flow into cell i,j,k from cell i,j-1,k (McDonald and Harbaugh 1988). Used with permission.

Equation 3.2 is applied to all cells which will define a set of simultaneous equations which are solved for head at each node. McDonald and Harbaugh modified equation 3.2 for computer simulations into the form:

$$CV_{i,j,k-\frac{1}{2}}h_{i,j,k-1} + CC_{i-\frac{1}{2},j,k}h_{i-1,j,k} + CR_{i,j-\frac{1}{2},k}h_{i,j-1,k} \quad (3.3)$$

$$+ (-CV_{i,j,k-\frac{1}{2}} - CC_{i-\frac{1}{2},j,k} - CR_{i,j-\frac{1}{2},k} - CR_{i,j+\frac{1}{2},k} - CC_{i+\frac{1}{2},j,k} - CV_{i,j,k+\frac{1}{2}}$$

$$+ HCOF_{i,j,k})h_{i,j,k} + CR_{i,j+\frac{1}{2},k}h_{i,j+1,k} + CC_{i+\frac{1}{2},j,k}h_{i+1,j,k}$$

$$+ CV_{i,j,k+\frac{1}{2}}h_{i,j,k+1} = RHS_{i,j,k}$$

where:

$$HCOF_{i,j,k} = P_{i,j,k} - \frac{SC1_{i,j,k}}{(t_m - t_{m-1})} \tag{3.4}$$

$$RHS_{i,j,k} = -Q_{i,j,k} - \frac{SC1_{i.j.k}h_{i,j,k}^{m-1}}{(t_m - t_{m-1)}} \tag{3.5}$$

$$SC1_{i,j,k} = SS_{i,j,k}\Delta r_{,j}\Delta c_{,i}\Delta v_k \tag{3.6}$$

Equation 3.2 applies to time step *m* but the superscript is removed. The term $HCOF_{i,j,k}$, Eq. (3.4), contains the term $P_{i,j,k}$ and the negative part of the storage term that includes the head. The *S* term, Eq. (3.5), includes –*Q* and the part of the storage term that is multiplied by the head at time step *m-1*.

The *CV*, *CR*, and *CC* conductance values and the storage portions of *HCOF* and *RHS* are calculated by a single package called an "internal flow package." Flow packages contribute different source term combinations that in turn generate different sources and sinks. Sinks are defined as negative sources in the package. Source term packages are either head dependent or head independent. Head dependent packages include riverbed, drain, and boundary conductances as well as maximum evapotranspiration flux. Head independent packages include well recovery rates (rebound) and aquifer recharge flux. The model in this work was designed using the Layer-Property Flow (LPF) package. Specific storage values for each cell are required input for the LPF if there are more than one transient stress periods. Specific storage is read layer by layer and multiplied by cell area and layer thickness to create storage capacity values. The LPF package assumes a

node is present at the center of each model cell. In this package, the input data that defines hydraulic properties are independent of cell dimensions. When incorporated, the LPF package uses only hydraulic conductivities during a model run and uses the conductivity to calculate other parameters such as transmissivity.

Hydraulic conductance is the principle force driving groundwater flow whether it be flow through an aquifer or flow to a well. Conductance can be derived from Darcy's law which defines one dimensional flow in a prism as shown in Figure 3.5:

$$Q = -KA\left(\frac{h_A - h_B}{L}\right) \tag{3.7}$$

where:

Q is the volumetric flow (L^3T^{-1});

K is the hydraulic conductivity of the material is the direction of flow (LT^{-1});

A is the cross sectional area perpendicular to the flow (L^2);

h_A - h_B is the head difference across the prism parallel to flow (L); and

L is the length of the prism parallel to the flow path (L).

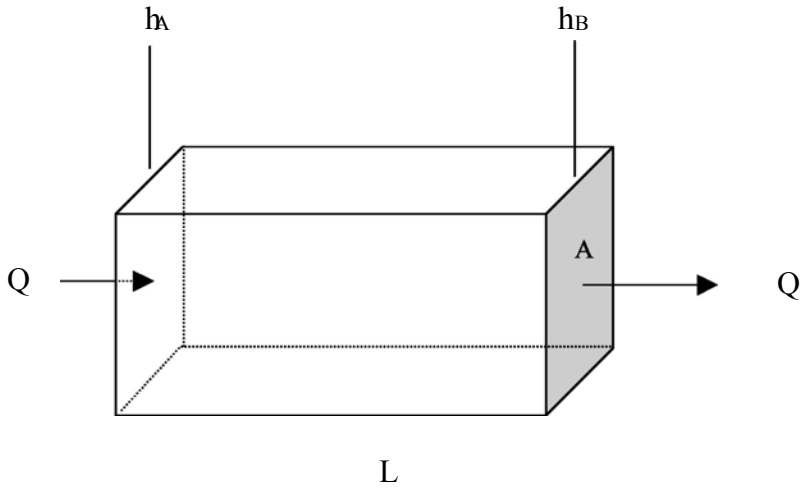

Figure 3.5. Prism of porous material illustrating Darcy's law (from Harbaugh, 2000). Used with permission.

The conductance (*C*) of a system is defined as:

$$C = \frac{KA}{L} \tag{3.8}$$

Substituting into equation 3.8 into equation 3.7 results in

$$Q = C(h_A - h_B) \tag{3.9}$$

Upon rearrangement, equation 3.9 defines Darcy's Law in terms of conductance across the entire prism. If several prisms are aligned in a series, Figure 3.6, and the conductance of each is known, the conductance for the combined prism series can be calculated.

$$C = \frac{Q}{h_A - h_B} \tag{3.10}$$

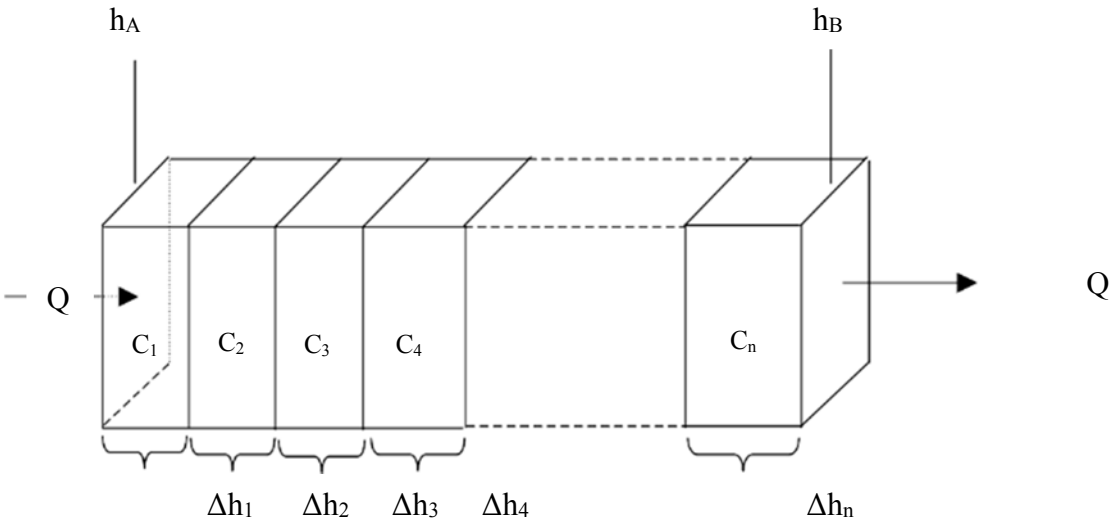

Figure 3.6. Calculation of conductances through several prisms in series. (Harbaugh 2000). Used with permission.

Harbaugh (2000) shows that if we assume the continuity of head across each section in a prism the result is the following identity:

$$\sum_{i=1}^{n} \Delta h_i = h_A - h_B \tag{3.11}$$

By substituting for head change across each section using Darcy's law equation 3.9 gives:

$$\sum_{i=1}^{n} \frac{q_i}{C_i} = h_A - h_B \tag{3.12}$$

Flow is one dimensional and the assumption is that there is no accumulation or depletion in storage, so all q_i are equal to total flow Q:

$$Q \sum_{i=1}^{n} \frac{1}{C_i} = h_A - h_B \qquad \text{and} \qquad \frac{h_A - h_B}{Q} = \sum_{i=1}^{n} \frac{1}{C_i} \tag{3.13}$$

By substitution equation 3.10 into equation 3.13 it can be shown that

$$\frac{1}{C} = \sum_{i=1}^{n} \frac{1}{C_i} \tag{3.14}$$

So for a set of conductances arranged in a series, the inverse of the equivalent conductance equals the sum of the individual conductances.

$$C = \frac{C_1 C_2}{C_1 + C_2} \tag{3.15}$$

If an assumption was made that an aquifer was a single layer, isotropic in all directions, the previous example would hold true. This means that the transmissivity of the aquifer would be calculated for each cell using the entire thickness of the aquifer since transmissivity is the product of the hydraulic conductivity of the aquifer and the thickness of the layer. However, using the entire thickness of the aquifer to determine

transmissivity does not adequately reveal the details of drawdown in the vicinity of the wells where the cones of depression will form.

MODFLOW uses equivalent conductances, called "branch conductances" between nodes of adjacent cells. *CR* and *CC* from equation 3.2 above are horizontal conductances within the grid of the model. These conductivity terms are calculated between adjacent horizontal nodes. *CR* terms are conductances between nodes along a row and *CC* are conductances between nodes in the same column. The Layer Property Flow package reads the horizontal conductivity data for individual cells and calculates conductance between nodes (Harbaugh, 2000).

The LPF package settings used in this model assume that transmissivity, the product of the hydraulic conductivity multiplied by the thickness, equation 3.16, is constant within cells. Coupled with the assumption that the nodes are at the center of the cells, the conductance is equal to the conductance of two half cells in series as shown in Figure 3.7.

$$T = Kb \tag{3.16}$$

where:

T is the transmissivity of the aquifer (L^2/T);

K is the hydraulic conductivity in the direction of flow (L/T);

b is the saturated thickness of the aquifer (L).

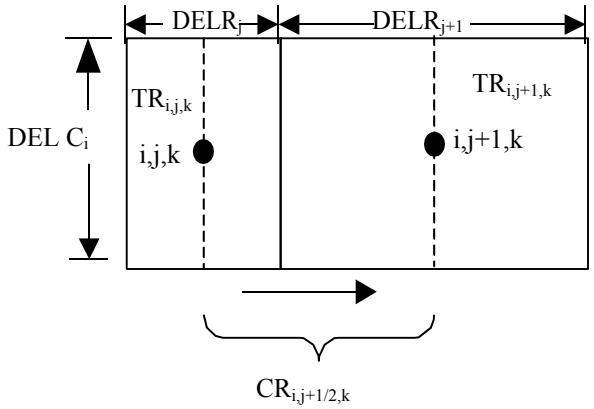

Figure 3.7. Calculation of conductances between nodes using transmissivities and dimensions of cells (Harbaugh, 2000). Used with permission.

Conductance can also be written for horizontal flow through a prism as shown in equation 3.17:

$$C = \frac{TW}{L} \tag{3.17}$$

where:

T is transmissivity (K times thickness of the prism) in the direction of flow (L^2T^{-1});

W is the width of the prism (L).

Substituting equation 3.17 into equation 3.15 and using Figure 3.7 above, the conductance between two half cells can be determined:

$$CR_{i,+\frac{1}{2},j,k} = \frac{\frac{TR_{i,j,k}DELC_i}{\left(\frac{1}{2}\right)DELR_j} \quad \frac{TR_{i,j+1,k}DELC_i}{\left(\frac{1}{2}\right)DELR_{j+1}}}{\frac{TR_{i,j,k}DELC_i}{\left(\frac{1}{2}\right)DELR_j} + \frac{TR_{i,j+1,k}DELC_i}{\left(\frac{1}{2}\right)DELR_{j+1}}} \tag{3.18}$$

where:

$TR_{i,j,k}$ is transmissivity in the row direction at cell i,j,k (L^2T^{-1});

$DELR_j$ is the grid width of the column j (L);

$DELC_i$ is the grid width of row i (L).

Simplifying equation 3.18 results in the final equation:

$$CR_{i,j+\frac{1}{2},k} = 2DELC_i \frac{TR_{i,j,k}TR_{i,j+1,k}}{TR_{i,j,k}DELR_{j+1} + TR_{i,j+1,k}DELR_j} \quad (3.19)$$

Following the same process the calculation of $CC_{i+1/2,j,k}$ can be derived:

$$CC_{i+\frac{1}{2},j,k} = 2DELR_i \frac{TC_{i,j,k}TC_{i+1,j,k}}{TC_{i,j,k}DELC_{i+1} + TC_{i+1,j,k}DELC_i} \quad (3.20)$$

where:

$TC_{i,j,k}$ is the transmissivity in the column direction at cell i,j,k (L^2T^{-1});

The transmissivity of the model is calculated with the following equations:

$$TR_{i,j,k} = THICK_{i,j,k}\, HK_{i,j,k} \quad (3.21)$$

$$TC_{i,j,k} = THICK_{i,j,k}\, HK_{i,j,k}\, HANI_{i,j,k} \quad (3.22)$$

where:

$HK_{i,j,k}$ is the hydraulic conductivity of cell i,j,k in the row direction (LT^{-1});

$HANI_{i,j,k}$ is the ratio of hydraulic conductivity along columns to the hydraulic conductivity along rows (dimensionless); and

$THICK_{i,j,k}$ is the saturated thickness of cell i,j,k (L).

$HK_{i,j,k}$ and $HANI_{i,j,k}$ are input data and were extracted from the original Groundwater Availability Model (GAM) by Dutton (2001). $THICK_{i,j,k}$ is calculated from cell elevations within the model. Both top and bottom elevations were replicated from the original GAM.

In this work, efforts were made to separate the existing GAM into three layers. This made it necessary to designate them as "confined" or "convertible." If a model is defined as confined, then the thickness is considered the entire cell thickness. If a layer is convertible, then a cell or layer is representative of a water table and new head values can be determined. This model designates the layers as convertible layers. Harbaugh (2000), demonstrates that if the layer is designated as convertible the saturated thickness is calculated throughout the simulation based upon the head ($HNEW_{i,j,k}$):

$$\text{if } HNEW_{i,j,k} \geq TOP_{i,j,k}, \quad \text{then } THICK_{i,j,k} = \left(TOP_{i,j,k} - BOT_{i,j,k}\right); \tag{3.23A}$$

$$\text{if } TOP_{i,j,k} > HNEW_{i,j,k} > BOT_{i,j,k}, \text{then } THICK_{i,j,k} = \left(HNEW_{i,j,k} - BOT_{i,j,k}\right); \tag{3.23B}$$

$$\text{if } HNEW_{i,j,k} \leq BOT_{i,j,k}, \quad \text{then } THICK_{i,j,k} = 0; \tag{3.23C}$$

When MODFLOW begins solving the flow equation at the start of an iteration, the cell transmissivity values are recalculated using equation 3.18. Conductance is then calculated using equations 3.19 and 3.20.

The model is set up to calculate the interblock conductance using the "harmonic mean" method. This method is used when there are outliers in the population that are much greater than the rest of the data within the population. This reduces the bias of the outliers on the mean. Harbaugh (2000) shows that the transmissivity is a distance-weighted harmonic mean of and can be seen as the equivalent transmissivity between nodes i,j,k and i,j+1,k in equation 24.

$$CR_{i,j+\frac{1}{2},k} = \left(\frac{\left(\frac{1}{2}\right) DELR_j + \left(\frac{1}{2}\right) DELR_{j+1}}{\frac{\left(\frac{1}{2}\right) DELR_j}{T_{i,j,k}} + \frac{\left(\frac{1}{2}\right) DELR_{j+1}}{T_{i,j+1,k}}} \right) \frac{DELC_i}{\left(\frac{1}{2}\right) DELR_j + \left(\frac{1}{2}\right) DELR_{j+1}} \qquad (3.24)$$

Vertical conductance is another parameter that must be considered for a multi-layer model. This is illustrated in Figure 3.8. The LPF package has an option to determine vertical hydraulic conductivity in terms of anisotropy. The vertical anisotropy is the ratio of the horizontal hydraulic conductivity to the vertical hydraulic conductivity. The model uses this method to manage vertical hydraulic conductivity values.

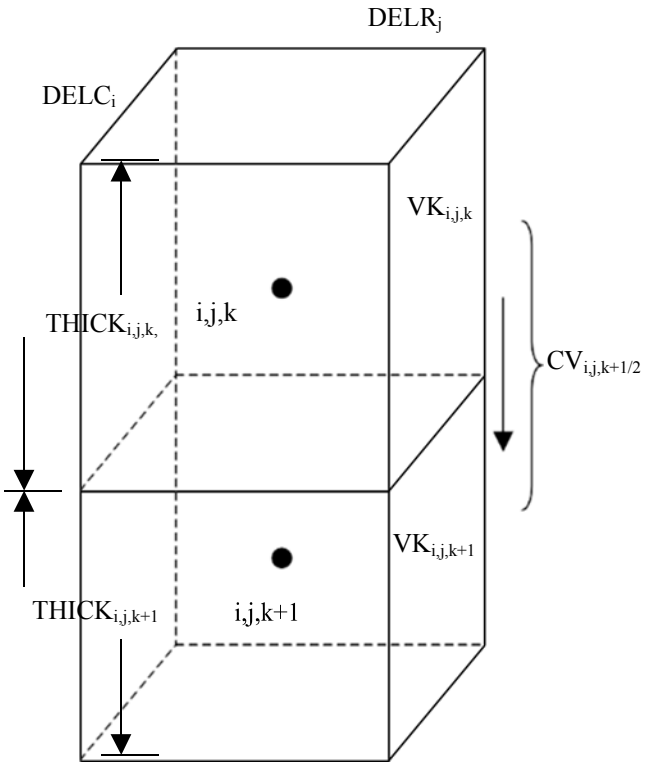

Figure 3.8. Calculation of vertical conductances between two nodes (Harbaugh 2000). Used with permission.

For a model with multiple layers there will be periods when the cells are not saturated. When a cell is saturated in the vertical direction, the head value is above the top elevation of the cell and complete vertical conductance is expected. As the aquifer declines there are times when MODFLOW iterations must run with cells less than full in the vertical direction. The cells have a head value below the top elevation of the cell as shown in Figure 3.9. The LPF package, will formulate storage terms for transient stress periods (Harbaugh, 2000).

When a cell is not saturated the following storage formulation applies:

$$\frac{\Delta V}{\Delta t} = SY\left(DELR_j DELC_i\right) \frac{h_{i,j,k}^{m} - h_{i,j,k}^{m-1}}{t^{m} - t^{m-1}} \tag{3.25}$$

where:

SY is the specific yield (dimensionless, usually represented as percent).

Specific yield is the ratio of the volume of water which a rock or soil will yield by gravity drainage to the volume of the rock or soil (Fetter 2001).

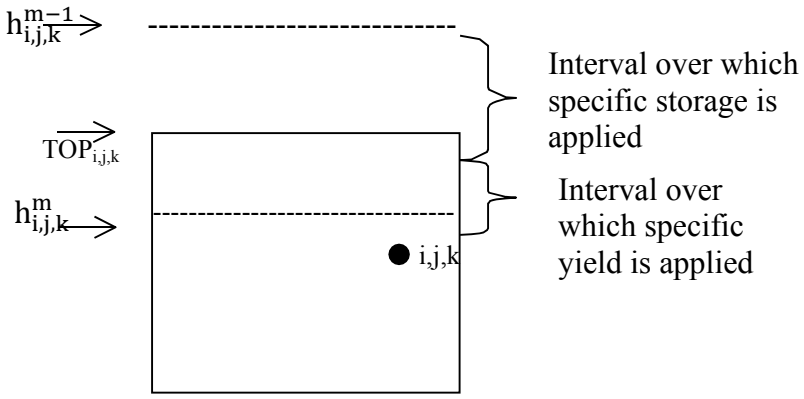

Figure 3.9. A model cell for which two storage factors are used during one time step (Harbaugh 2000). Used with permission.

Equation 3.25 can be rewritten to include a secondary storage capacity, $SC2_{i,j,k}$ to represent specific yield multiplied by cell area.

$$\frac{\Delta V}{\Delta t} = SC2_{i,j,k} \frac{h_{i,j,k}^{m} - h_{i,j,k}^{m-1}}{t^{m} - t^{m-1}} \tag{3.26}$$

According to Harbaugh (2000), there are four possible storage conditions for each cell:

- The cell is confined for the entire time step:
- The cell is unconfined for the entire time step:
- The cell converts from confined to unconfined: and
- The cell converts from unconfined to confined.

Confined cells are considered cells that remain saturated during a model run, while unconfined cells exhibit top elevation below the top elevation of the cell.

Since many cells during a model run may experience any of these conditions, Harbaugh and McDonald derived the following expression:

$$\frac{\Delta V}{\Delta t} = \frac{SCB\left(h_{i,j,k}^{m} - TOP_{i,j,k}\right) + SCA(TOP_{i,j,k} - h_{i,j,k}^{m-1})}{t^{m} - t^{m-1}} \qquad (3.27)$$

Equation 3.27 would apply under the four conditions anticipated to exist in this model run. The LPF package will determine the head at the beginning of a time step. Rearrangement of equation 3.27 yields:

$$\frac{\Delta V}{\Delta t} = \frac{SCB * h_{i,j,k}^{m}}{t^{m} - t^{m-1}} + \frac{SCA\left(TOP_{i,j,k} - h_{i,j,k}^{m-1}\right) - SCB * TOP_{i,j,k}}{t^{m} - t^{m-1}} \qquad (3.28)$$

Depending upon the condition of the cell, substitutions for *SCB* and *SCA* will be made in equation 3.27, according to the following:

$\frac{SC1_{i,j,k}(TOP_{i,j,k} - h_{i,j,k}^{m-1})}{t^{m} - t^{m-1}}$ is the rate of release from confined or compressive storage

$\frac{SC2_{i,j,k}(h_{i,j,k}^{m-1} - TOP_{i,j,k})}{t^m - t^{m-1}}$ is the rate of release from water table storage

Following an iteration, cell conditions are dependent upon subsequent substitutions of *SBC*, and *SCA* will be made with $SC1_{i,j,k}$ and $SC2_{i,j,k}$. The LPF package progressively evaluates the head status of each cell, following each iteration, and makes the appropriate substitution as long as the model is set to use the convertible option.

The Preconditioned Conjugate-Gradient 2 (PCG2) was the solver package selected for model calculations. Solver packages provide simultaneous solutions for the matrix of linear equations generated with the application of the finite difference method. These equations discretize the groundwater flow equation as it is applied to 3D representations of aquifers. Discretization of the flow equation is accomplished by dividing the aquifer geometry into finite segments to approximate a solution. The PCG2 uses an iterative method for solving the set of liner equations (Hill 1990). An iterative method is a mathematical process of using successive approximations to obtain more accurate solutions to linear systems at each step (Dongarra 1995).

Groundwater Modeling System (GMS) is a pre- and post-model run program designed by Aquaveo which is used to build groundwater models. As shown in the flowchart below, the models are initially built in GMS and MODFLOW is used for processing and simulation. GMS reads the MODFLOW output and creates 2D and 3D models. GMS version 10.0.1 was used for model development and to view output files. All modeling

work was performed on a Hewlett Packard Probook laptop computer using Windows 7 with an Intel® Core 2 Duo CPU P8700 at 2.53 GHz and 4.00 GB of RAM.

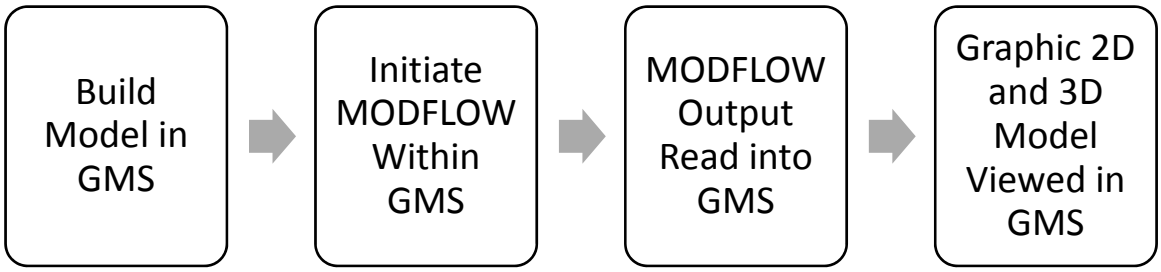

The model parameters used in this effort are based on the current GAM (Dutton, 2000).

Portions of the Ogallala in both the northern and southern GAM will be evaluated in this work.

Models are mapped geographically using the Albers equal area conic projection which is a means of projecting a grid upon the surface of the Earth for mapping purposes and is exclusively used by the United States Geological Society (USGS). As summarized by Snyder (1987) and shown in figure 3.10, the projection:

- Is Conic
- Has equal parallels
- Has parallels that are unequally spaced arcs of concentric circles, more closely spaced at the north and south edges of the map.
- Has meridians that are equally spaced radii of the same circles, cutting parallels at right angles.
- Has no distortion in scale or shape along two standard parallels, normally, or along just one.
- Has the poles as arcs of circles.
- Is used for equal-area maps or regions with predominant east-west expanse, especially the conterminous United States.

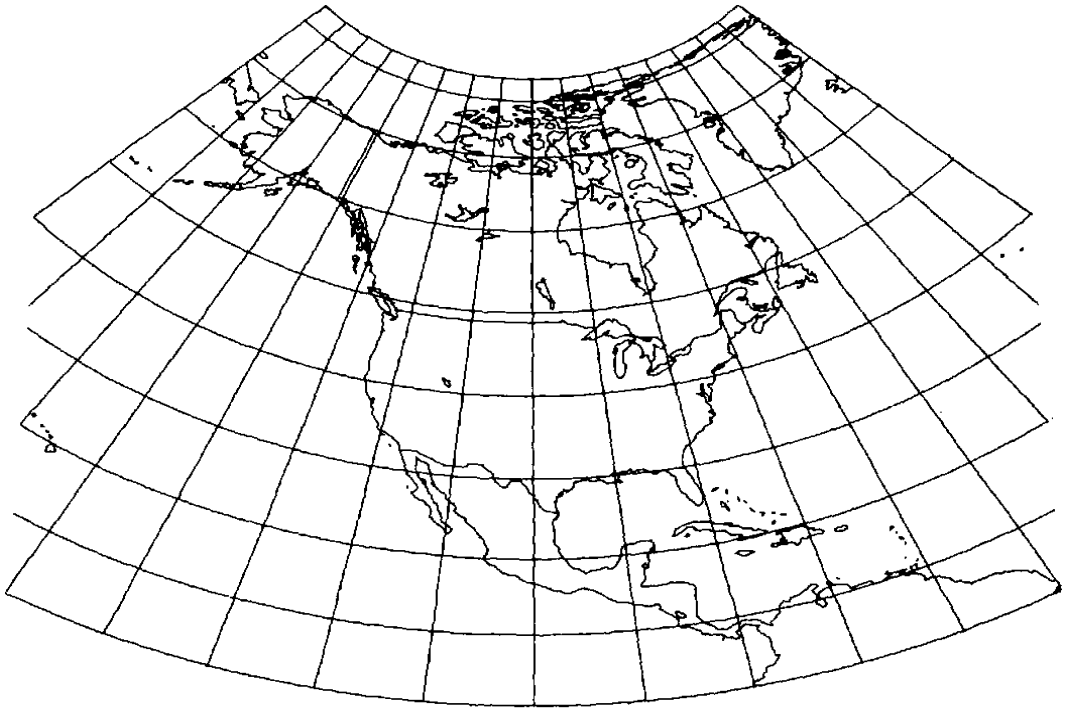

Figure 3.10. Albers Equal-Area Conic projection (Snyder 1987). Used with permission.

The North American Datum 1983 (NAD 83) is based upon a horizontal control network maintained by the United States government to provide geodetic latitudes and longitudes for the North American Datum reference system. The control network is made up of points across the United States for developing precise surveys, maps and charts (Bossler 1984). NAD 83 is the result of adjustments completed in 1983 of the geodetic control networks in North America (Schwarz 1990).

Dutton (2001) suggested the Ogallala can be modeled as a one layer aquifer. This approach assumes that the aquifer is homogeneous in all directions. The issue with using a one-layer model is that it is not expected to provide a detailed enough output to allow for observation of the mounded water. The vertical heterogeneity of the aquifer is not

accounted for in a single layer. However, due to the lack of accurate data allowing for accurate construction of a layered saturated thickness, multiple layers may not be useful. The other concern is that the one-layer approach forces MODFLOW to perform the calculations from cell to cell using the entire saturated thickness of the aquifer. Again this assumes that all vertical layers have the same properties. This causes some loss of detail and masks the mounded water between wells. This report demonstrates that the wells do not rebound as quickly as current modeling efforts imply. As a result, the cones of depression will be present. Further, the wells have been drilled over decades. For these reasons the development of the mounds will vary. If the vertical heterogeneity can be accurately established, multi-layer modeling may provide a more accurate representation of the water-surface where wells are present.

In this modeling effort, attempts will be made to convert the single layer model proposed by Dutton to a multi-layer model to improve resolution and to better demonstrate the cone of depression and subsequent mounding effect of water between pumping wells. By adding additional layers the movement of water will not be assumed to be isotropic through the full saturated thickness. Given the heterogeneous nature of the aquifer, the flows cannot be assumed to be the same. Although the horizontal flow through the aquifer is the primary direction of flow, there could be some vertical components that would improve the accuracy of the model output. This would be most obvious near a pumped well. As a cone of depression is formed, the curvature of the water-surface becomes distorted. The Dupuit-Forchheimer assumption states that groundwater flows horizontally in an unconfined aquifer provided the slope of the aquifer is small and the

depth of the aquifer is shallow (Freeze and Cherry 1979). Assessment of the flows when cones are present in a single layer model could result in large calculation errors in the cells where the cone is present. This would influence the results of the mass-flow and could misrepresent the overall mass-flow of water through the aquifer. The addition of multiple layers would not eliminate the problem but should result in decreased flow related errors.

All models were developed with transient head boundary conditions. Head values change with time so they are time dependent or unsteady. By setting the boundary cells to allow for the head change over time the model accounts for water influx and efflux. This helps to maintain the overall water mass conservation of the portion of the model being studied. Further, it allows water to move into the model to prevent cells from being pumped dry prematurely. The model incorporated the Time Variant Specified Head Package to set the head levels at the transient head boundaries. This head package incorporates the maximum number of constant-head cells that can be specified for a stress period. The package then reads the number of boundary cells at which head will be specified for each stress period. Head values are read for each boundary cell at the beginning and end of each stress period. For time steps occurring between stress periods, the specified head is linearly interpolated from the starting and ending head values. Head values are assigned proportionally to the about of time that has elapsed within the stress period (Leake 1991).

The grid was refined around the wells in order to observe more detail of the drawdown and recovery at the well. Contours of the model were drawn from the original GAM to match anticipated groundwater flow from northwest to southeast across the area. The modeled area is shown in Figure 3.11 with the starting heads as the upper layer. The east and west sides have transient head boundaries set to allow for water to flow into the modeled area but to also allow the boundaries to decline as the saturated thickness of the area declines.

The internal model parameters are listed in Table 3.1. Generally, the parameters were not modified from the original GAM except to test the sensitivity of the model to changes in two of the parameters.

Table 2.1. Internal Model Parameters

	Conductivity	Specific Yield	Specific Storage
Northern Model	24-55 ft/day	0.2	0.0001 ft^{-1}
Southern Model	2-67 ft/day	0.2	0.0001 ft^{-1}

Two Well Conceptual Model

A conceptual model using a two well system was designed to gain a better understanding of the model design process and to view a simple model output. Of particular interest in this model was whether or not the model would show the cone of depression about the

well and whether a mound of water could be observed between the wells after pumping ceased.

Model of Northern Region

A 4.7 mile by 3.5 mile portion of the aquifer was taken from the original GAM for an area located on the Dallam-Hartley county lines. This area was selected due to the apparent lack of topographical geologic features which were expected to cause subsurface issues with the modeling effort. These would include streambeds, lakes or other apparent problematic feature. The coordinates for the four corners of the model are provided in Table 3.1

Table 3.1. Location of mapped area in Northern study area.

Corner	Latitude	Longitude
Northwest	36º 4’ 38.5657” N	102º 19’ 41.4208” W
Northeast	36º 4’ 41.7553” N	102º 14’ 36.9148” W
Southwest	36º 1’ 36.9379” N	102º 19’ 34.0062” W
Southeast	36º 1’ 40.6223” N	102º 14’ 32.4067” W

The model consists of 251 columns and 208 rows and the grid was projected in GMS using Albers equal-area projection and NAD83 to define the geodetic network.

The modeled area contains 21 wells. The wells are located geographically by utilizing a well map provided by the North Plains Groundwater Conservation District (NPGCD). The wells are not evenly spaced and the actual pumping rates of each well are not known.

However, for demonstration purposes, the well spacing and pumping rates are not considered critical. Figure 3.12 shows the active wells and their proximity to each other. The boundary of the model was placed far enough away to avoid influences of water crossing the boundaries of the model. The hydraulic conductivity of the aquifer was the same as in the original GAM. Values noted in the transferred data indicate a range from approximately 23 feet per day in the northeastern corner of the area to 54.5 feet per day in various regions within the model. Generally, the trend indicated shows that the hydraulic conductivity decreased from west to east. Figure 3.13 shows the contour image of the hydraulic conductivity of the model.

Since the accepted GAM has been calibrated, it was assumed for the current modeling effort that it would be acceptable to consider it calibrated. After several discussions with NPGCD personnel, it was determined no suitable areas exist which contained pumping wells and observation wells with which to recalibrate this model.

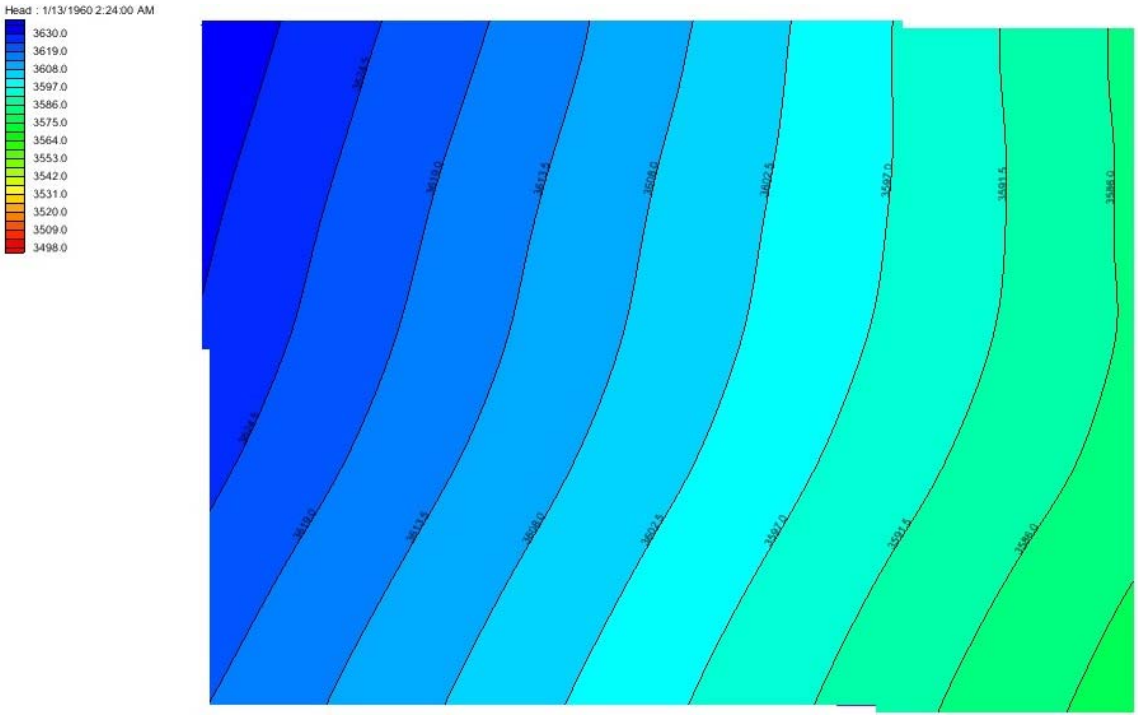

Figure 3.11. Surface contour of the northern model prior to the initiation of drawdown showing starting heads in the northern model.

The specific yield for the model area is set at 0.2. This is consistent with data provided by Dutton (2001, p. 105). The specific storage for the area is set at 0.2 ft^{-1}. The wells were set to pump at a rate of 800 gallons per minute and pumped for a 120 day cycle to coincide with the approximate irrigation period for corn production. This cycle started in 1960 and ran through 2015. The rebound of the aquifer was observed for the periods between pumping. Model initiation prior to 1960 was not expected to add much to the drawdown. Most of the drawdown is attributed to the widespread adoption of irrigation in the area which here-to-for were dryland. The output of all wells was set at the same rate to eliminate any influences in the simulation which would be attributed to varying pump output.

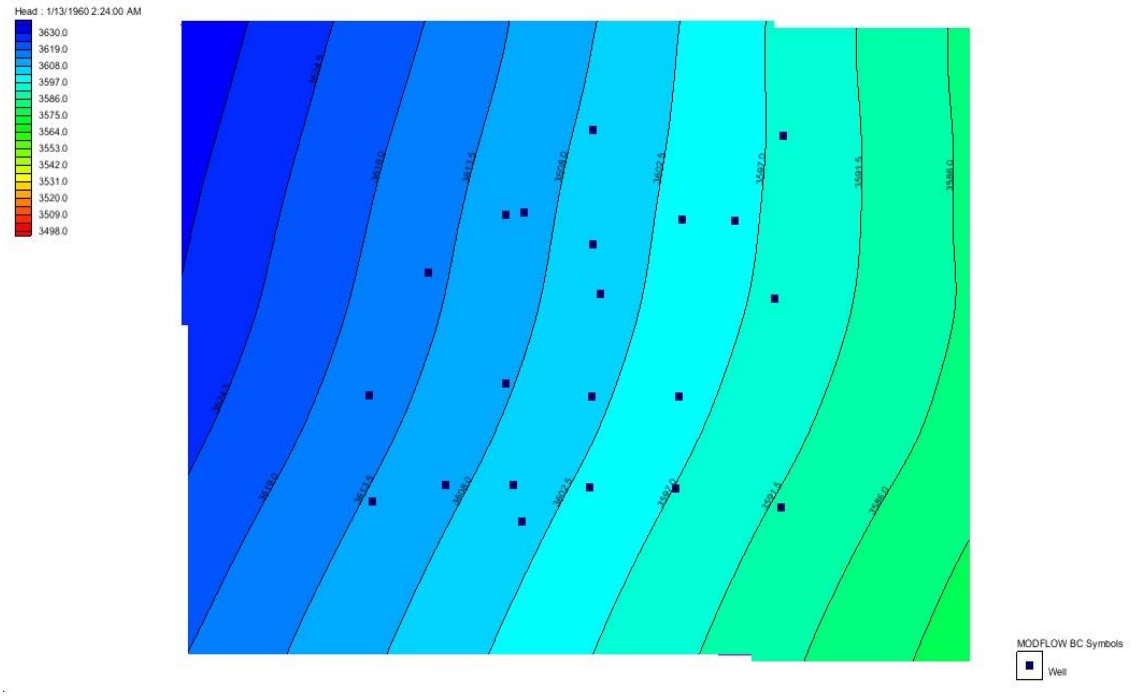

Figure 3.12. Locations of pumping wells and the relative proximity to each other in the northern model.

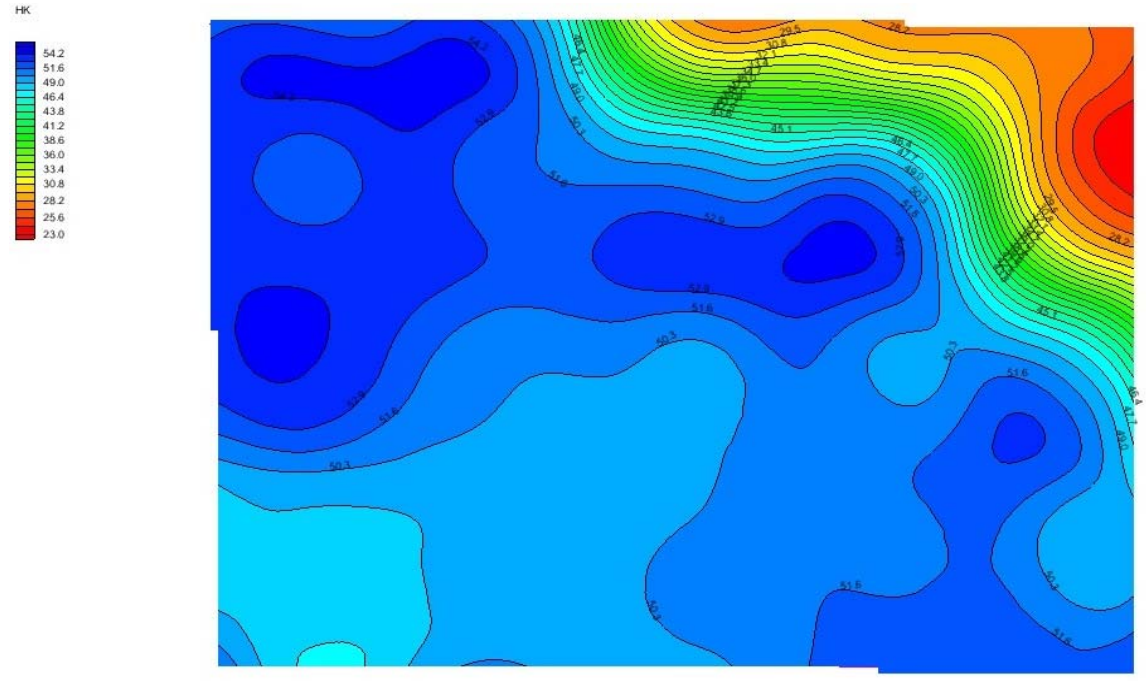

Figure 3.13. Contour map of the hydraulic conductivity in the northern model.

A second version of the northern model was prepared using the same conditions as above; however, the cycle was from 1960 to 1980 and pumping ceased from 1980 to 2015. The wells were pumped at 800 gallons per minute for 120 days per year. The purpose of this model was to observe the rebound of the pumped region as it approaches a new equilibrium. Refer to Figures 3.11-3.13 show the initial model conditions prior to initiating the pumping. The second model is identical to the first model with the exception of the pumping period. Shown in Figures 3.14 and 3.15 are the final head of the modeled field in 1980 and the rebound of the well field in 2015.

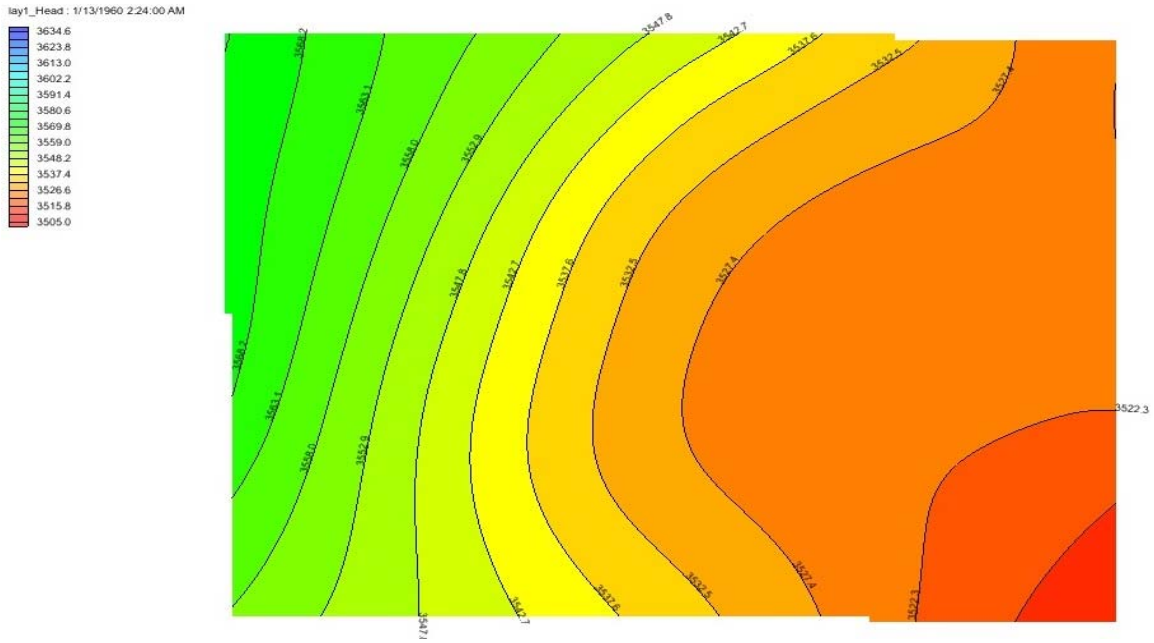

Figure 3.14. Top layer of northern model post pumping in 1980. The water-surface elevations represented by 20 years of pumping within the northern modeled area. The annual pumping cycles were 120 days in each year. Note decline in head as compared to the image in Figure 3.11.

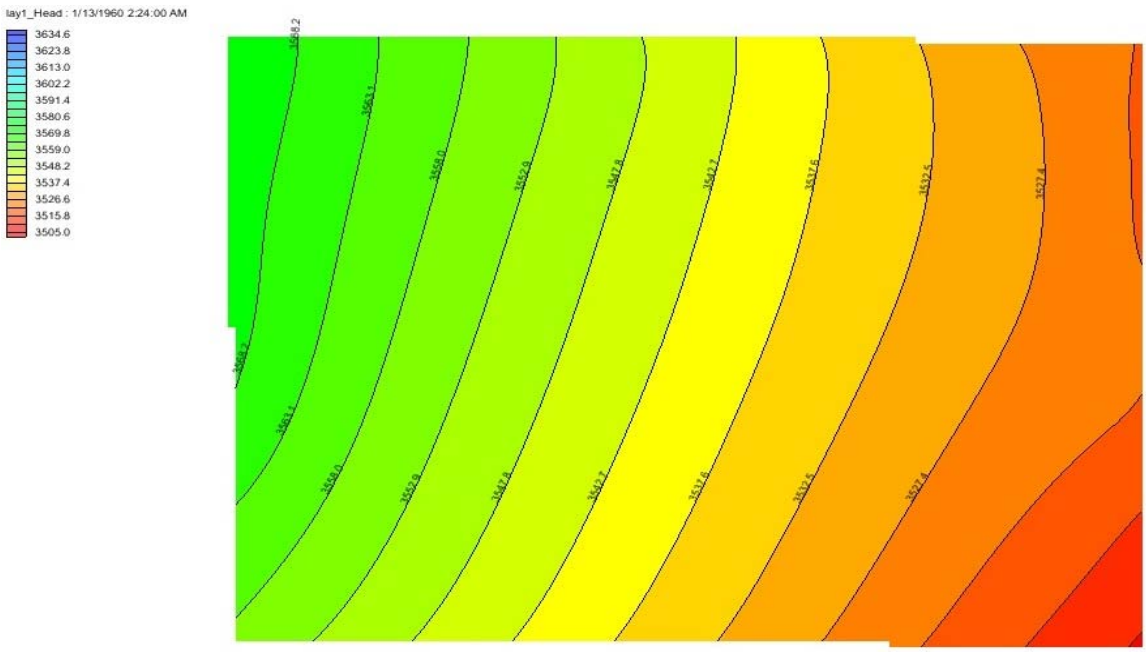

Figure 3.15. Top layer of northern model. The model was pumped for 120 days from 1960-1980 at which time the pumps were stopped. The water-surface elevations slowly approach a new static equilibrium at reduced water-surface elevations when compared to Figure 3.14 above.

Model of Southern Region

As with the Northern model area, a portion of the Southern GAM was taken for use in this work. The area was also selected based on topographic evidence that there would be minimal interference from geologic sources such as rivers, streams or lakes. The model parameters used in the Southern model are based on the current GAM. A 5.0 mile by 3.0 mile portion of the aquifer located in Lamb County was taken from the original GAM. Table 3.2 provides coordinates for the four corners of the model.

Table 3.2. Location of mapped area in Southern study area.

Corner	Latitude	Longitude
Northwest	34° 15’ 53.4084” N	102° 12’ 6.21658” W
Northeast	34° 15’ 5.4823” N	102° 6’ 51.244” W
Southwest	34° 13’ 16.179” N	102° 12’ 8.76248” W
Southeast	34° 13’ 12.9758” N	102° 6’ 52.8248” W

The model consists of 131 columns and 182 rows. The model grid was projected in GMS using Albers equal-area projection and NAD83 to define the geodetic network

The grid was refined around the wells in order to observe more detail of the drawdown and recovery at the well. Contours of the model were drawn from the original GAM to match anticipated groundwater flow across the area from northwest to southeast. The modeled area is shown in Figure 3.16 with the starting heads as the upper layer. The east and west sides have transient head boundaries set to allow for water to flow into the modeled area but also to allow the boundaries to decline as the saturated thickness of the area declines.

The modeled area contains 6 wells. The wells are located geographically by utilizing a well map provided by the High Plains Groundwater Conservation District (HPGCD). The wells are not evenly spaced and the actual pumping rates of each well are not known. As was assumed for the Northern Region, for demonstration purposes the well spacing and pumping rates are not considered critical. Figure 3.16 also shows the active wells and their proximity to each other. The boundary of the model was placed far enough away to avoid influences of water crossing the boundaries of the model.

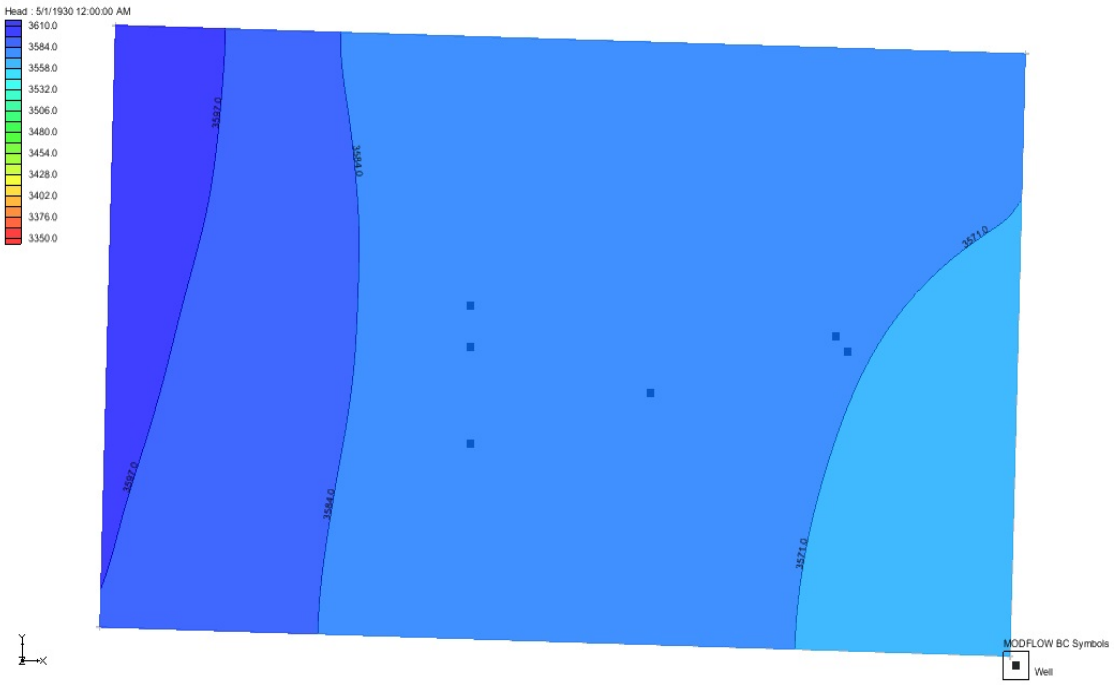

Figure 3.16. Surface contours for the southern model in 1930 prior to the initiation of irrigation cycles. Image shows well locations and water surface elevations of the model.

The hydraulic conductivity of the aquifer was the same as in the original GAM. Values noted in the transferred data indicate a range from approximately 4 feet per day in the western portion of the area to 67 feet per day in the northeastern portion within the model. Generally the trend indicated shows that the hydraulic conductivity increased from west to east. Figure 3.17 shows the contour image of the hydraulic conductivity of the model. The specific yield for the model area is set at 0.2. The specific storage for the area is set at 0.0001 ft^{-1}. Blanford et al., report a range of hydraulic conductivity from 0.01 ftd^{-1} to 2,600 ftd^{-1} with a geometric mean of 6.8 ftd^{-1}.

Since the accepted GAM has been calibrated, it was assumed that using the same values for the current modeling effort would be acceptable.

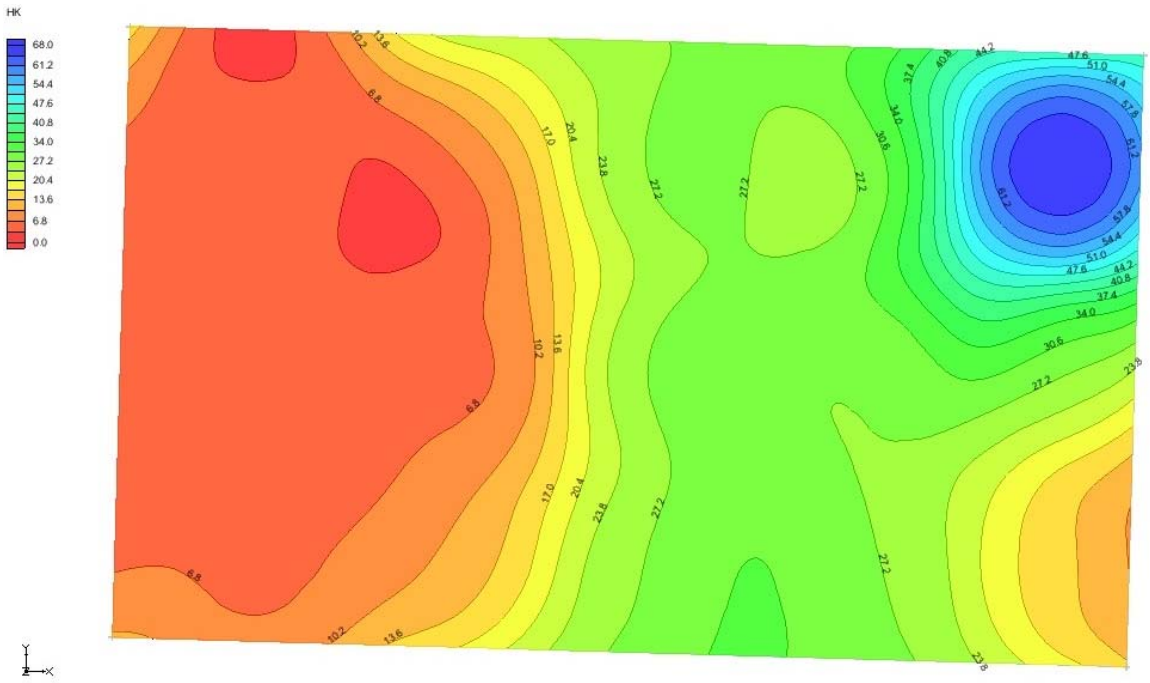

Figure 3.17. Contour map of hydraulic conductivity in southern model.

Three models will be developed to observe whether or not mounds of water could exist between pumping wells. The first conceptual model will primarily be used to learn how the software will present the cone of depression about wells and to observe what the model shows in the cells between the wells. The northern and southern models will be efforts to use actual GAM data to investigate whether or not residual mounds will be present after pumping periods. The time required for wells to recover after several pumping cycles will also be examined.

Chapter IV

RESULTS

Three models were evaluated to investigate whether or not cones of depression would persist about pumped wells and if residual mounds of water could be observed between the wells. The goal with all models was to determine if cones of depression persist about wells after a pumping season and remained until the next pumping season begins. Provided the cones remained after the wells rebounded, the study then investigated whether or not mounds of water existed between wells as suggested by the Agronomic Water Mass Balance Approach (AWMBA). If mounds were shown to be present, efforts to quantify the water within the mounds would be made. The investigation began with a simple conceptual two well model and moved to more complex multi-well models.

The initial goal of this research project was to develop a conceptual model of the aquifer to determine whether residual mounds of water would persist between wells after pumping cycles. More specifically, the goal was to determine whether there would be decreased head in the cells containing the wells as compared to the cells immediately adjacent to them prior to the initiation of the next pumping cycle.

Currently accepted values for the required aquifer parameters would be used. Discussions with the software developer revealed the possibility of cropping a portion of the currently accepted GAM and using it for this modeling effort, a step which provided an accepted model as a basis for this project and also allowed for the assumption the model was calibrated. Cropping from the accepted GAM also allowed for the use of the established aquifer parameters.

Models representing portions of both the northern and southern GAM were developed using the model accepted by the Texas Water Development Board and developed by Dutton (2000). The northern GAM portion was taken from an area along the Dallam-Hartley County line and the southern GAM portion was taken from the northeastern portion of Lamb County. These areas were selected based upon the topography. No topographical features such as canyons, lakes, rivers or streams which could influence the simulations were noted in these areas.

Initially the values for specific storage and specific yield for both models remained the same as those used by Dutton (2000). Also, the water surface elevations and the lower boundary (redbed) were left unchanged from the original GAMs. Any recharge sources in the GAMs were omitted from this model. Recharge of the aquifer for the purposes of this research were considered negligible and assumed not to occur. As previously discussed, sufficient rainfall does not occur across the Texas Panhandle to meet evapotranspiration in the area. Recharge, if any could occur, would be such a small amount that it would not be expected to influence the outcome of the simulations. This

modeling effort did not incorporate drains which are geologic features (streams, rivers, seeps) that allow the water in storage to flow freely out of the aquifer. These features were not incorporated since these features were not present within the modeled areas.

Two Well Conceptual Model

To verify that a computational model would support the hypothesis that cones of depression and mounds between wells could be delineated, a simple model with only two wells was conceived. The two wells were placed approximately 500 feet apart in a single layer model consisting of 23 columns and 13 rows and one layer. The columns, rows and layer represented the grid cells of the model in the horizontal plane while the layer is in the vertical dimension. The grid in the vicinity of the wells was subdivided further providing additional resolution. Wells were allowed to pump for one cycle. A flooded contour surface view of this model in Figure 4.1 showed that the MODFLOW program and GMS software provided an output showing the decreased head in the vicinity of the well, indicating the development of a cone of depression. The model further indicated a diminished head between the wells but a definite indication that mounded water was present in the space between the wells.

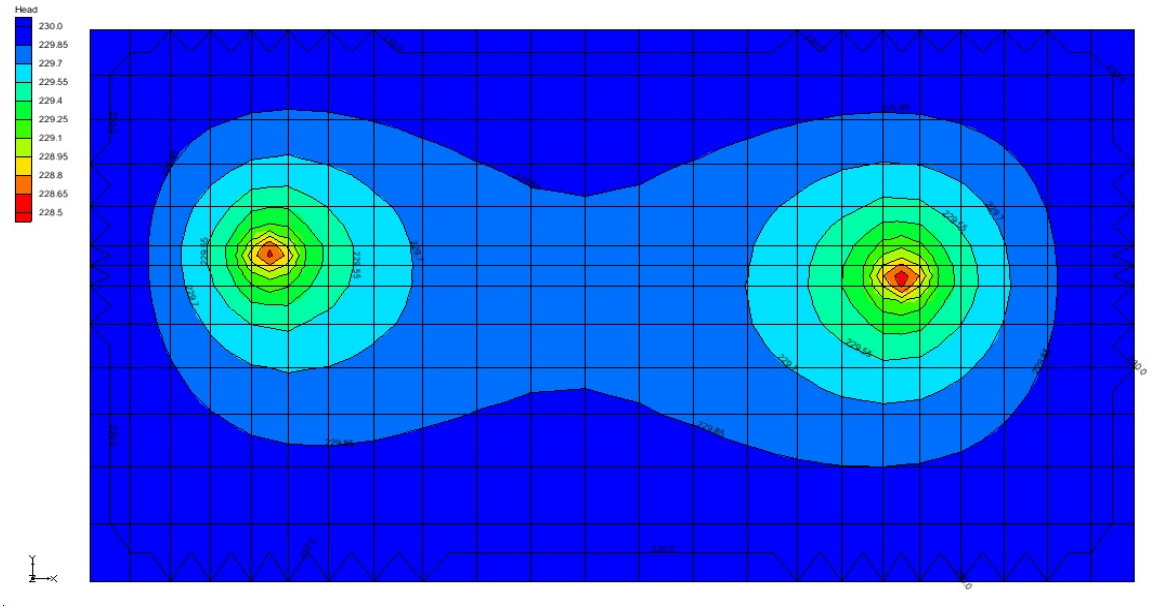

Figure 4.1. Two well system illustrating cone of depression and mound between wells. Cells containing the wells will show the largest decrease in water-surface elevation and are denoted by the red color. Progressively increasing water-surface elevations are seen through the green coloration into the blue.

Figure 4.2a is the profile view of the two well system. Using a one-layer model, the drawdown was shown by the subsequent cone of depression surrounding the well cells. The mound of water existing between the wells is clearly shown in this view as well. Under the Well Measurement Approach (WMA) currently used to determine remaining saturated thickness, the wells would be measured to the water-surface elevation in the well. As illustrated in Figure 4.2b, the water table would then be assumed to be level between the two wells. From this image it is evident the mounded water between the wells is not captured using the WMA method, indicating the water remaining is being underestimated and more water remains in the aquifer than currently reported.

Assuming both wells recovered to the head indicated of 228 feet, a mound of 1.7-2.0 feet exists between them. Although the distance between wells is only 500 feet, this indicated

an amount of water remaining between the wells. Figure 4.3 illustrated area between two wells. Assuming an average saturated thickness mound of 1.85 feet between the wells, and by taking a swath 100 feet wide between the wells, an estimated volume of water remaining between the two wells was determined as follows:

$$V = L * W * H$$

where:

V is the volume of the area (L^3);

L is the length of the area (L);

W is the width of the area (L);

H is the height of the area (L).

So the volume of saturated thickness contained within the mound was determined to be:

$$V = 500\ ft * 100\ ft * 1.85\ ft$$

$$V = 92,500\ ft^3$$

From this, the volume of water released can be estimated using the specific yield of the aquifer. In this model a specific yield of 20 percent was assumed, so:

$$V_{Water} = S_y * V_{Total}$$

where:

V_{Water} is the volume of water released from the aquifer (L^3);

S_y is the specific yield of the aquifer (dimensionless);

V_{Total} is the total volume being evaluated (L^3).

So the actual volume of water that could be removed from within the mounded area was determined to be:

$$V_{Water} = 0.20 * 92{,}500 ft^3$$

$$V_{Water} = 18{,}500 ft^3$$

This volume represented about 138,380 gallons (0.43 ac-ft) of extractable water and represents in the mounded water between the two wells spaced only 500 ft apart as predicted by the conceptual model.

This will be expanded to look at the cumulative effect of multiple pumping cycles in subsequent models.

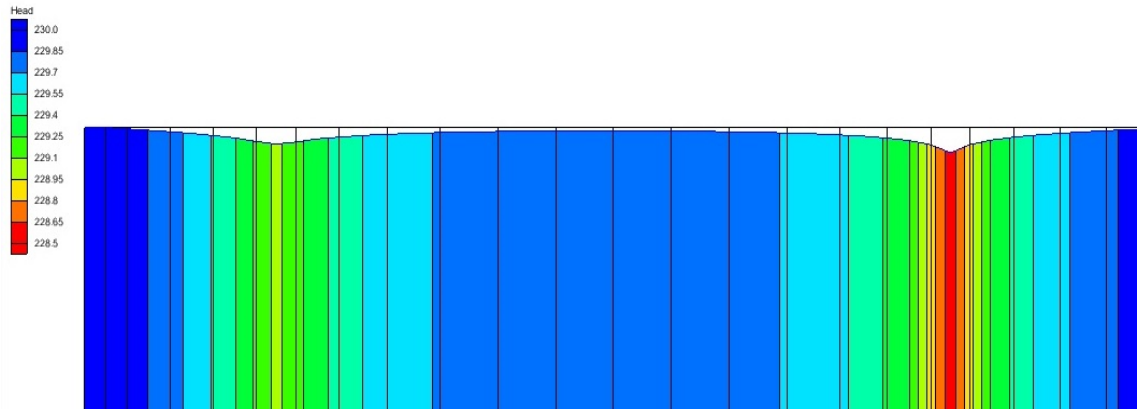

Figure 4.2a. Side view of two well system illustrating drawdown about the wells and mounded water between the wells. Wells are not in the same plain therefore the cones appear to be different.

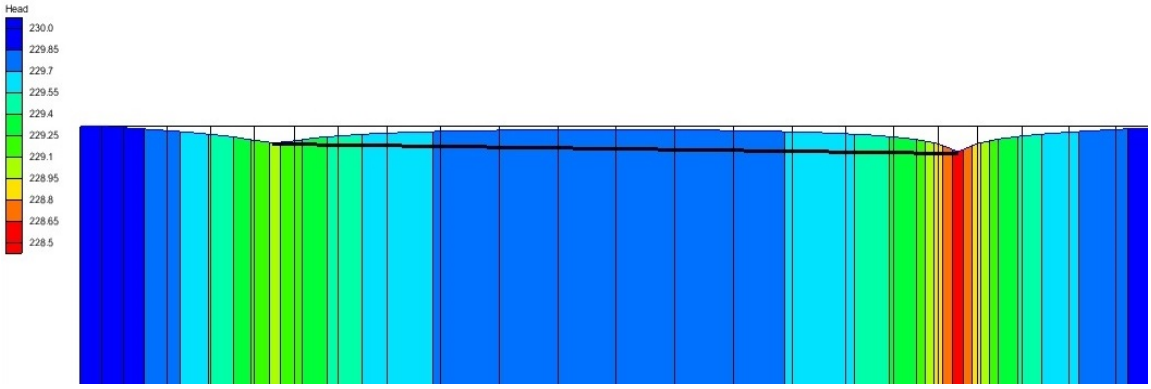

Figure 4.2b. Side view of two well system illustrating drawdown about the wells and mounded water between the wells highlighting the mound existing between wells. Wells are not in the same plane therefore the cones appear to be different. The water surface elevation as determined by the WMA is illustrated by the dark line connecting the wells.

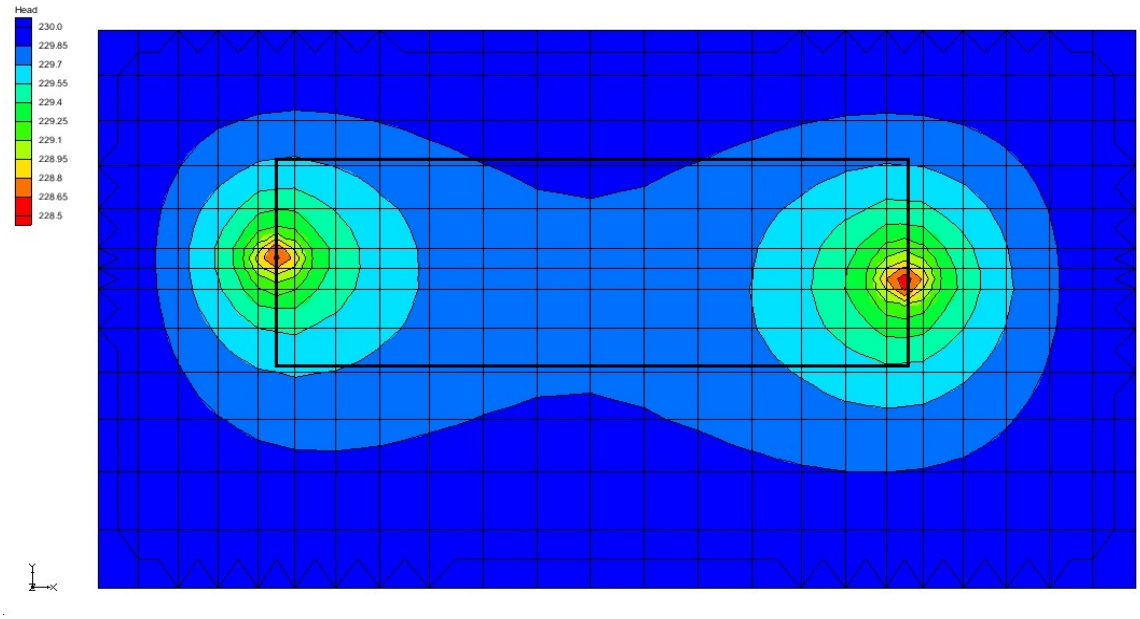

Figure 4.3. Area in the vicinity of two wells where estimated water remains between wells. Drawdown is the result of one pumping cycle.

Model of Northern Region

Results from the two-well conceptual model indicated cones of depression and mounded water between wells could be seen in the model output. Figure 4.4 is a series of water-surface elevation plots from the northern model after two pumping cycles. The water-

surface data was taken from two wells 570 feet apart. Water-surface elevations were taken from the same cells for each set of data between the wells. Five curves of the water-surface elevation were generated in the plot for clarity. The wells were located at zero feet (Well 2) and the 570 feet (Well 3) points. The skew of the plots from left to right was consistent with the anticipated elevation decline from west to east across the aquifer. The curve on 4/30/1960 represented the water-surface elevation prior to initial pumping of the aquifer. A relatively smooth surface is noted. The second curve, 5/13/1960, presented the water-surface elevation after thirteen days of pumping. The curvature of the plot indicated the development and magnitude of the mounded water between these two wells. The plot for 1/24/1961 showed the water-surface elevation during January, approximately the time period when the water-surface elevation would be measured using the WMA approach. Under model conditions the mounded water filled the cones of depression created by the pumping cycle of the wells. The curve for the time period 4/6/1961 was lower than the curve in January which indicated that further water movement had occurred. This suggested that additional time was needed for the establishment of a new, flat water-surface. The minimal decline seen between the 4/6/1961 curve and the 1/24/1961 curve may be due to effects of other wells within the model area and a model-wide establishment of a water table. The plot on 5/13/1961indicates the development of the mound of water again between the wells once pumping is resumed.

Figure 4.5 is a water-surface contour map which showed the developed cones of depression surrounding the wells after the initial 120 day pumping period. This was the

anticipated outcome since the water nearest the wells would be the first removed due to the water's proximity to the wells and the water farther away will not replace that in the cone of depression rapidly enough to keep the water surface at equilibrium. Once the pump was stopped, the water in the cells adjacent to the well moved towards the well thereby establishing a new water surface at that geographic location. This process was repeated for each successive series of cells radiating out from the well and was illustrated in Figure 4.6. Each ring represents a series of cells about the well showing the wells' zone of influence. Because each successive ring represents an increasing area, less depth of water is required to establish a new equilibrium with adjacent rings as the water moved towards the central well ring. As pumping continues, the cone will continue to increase in depth and diameter. To maintain the output of the well during this time, the flow of water through the porous medium must equal the output of the well. As the depth of the cone increased through multiple pumping cycles, the rate at which the cone could rebound decreased. The delay in the rate was due to the distance the water had to travel in establishing a new equilibrium. This resulted in cones that persisted throughout the entire rebound period until the next pumping cycle began.

The plot in Figure 4.7 was similar to that shown in figure 4.4 but with a well spacing over 3300 feet. This graph demonstrated that, as the distance between the wells increased, the length of the mound between the wells also increased. Of particular interest in this plot were the curves illustrating the well rebound. The curve for 1/24/1961 showed that the wells have rebounded from the mound developed during the pumped period. The curve for 4/6/1961 illustrated further rebound. However, since the later plot actually surpassed

the rebound seen on the 1/24/1961 curve, this suggested that continued rebound occurred after the water-surface elevation data would be collected for the WMA. Similar data is presented in Figure 4.7 for the years 1973-1974. The curve for 4/30/1973 was just prior to the initiation of a pumping cycle. The mound was again seen in the curve of 5/13/1973. Two periods of rebound were shown. The first was the curve 1/24/1974 which would be approximately the time when water-surface elevation levels were taken for the WMA. Again, additional rebound was seen in the plot 4/30/1974. This plot of rebound occurring three months later suggested additional water was available allowing the rebound of the wells to continue well after the water-surface elevations would normally be taken. The continued rebound suggested the existence of a residual mound of water between the wells.

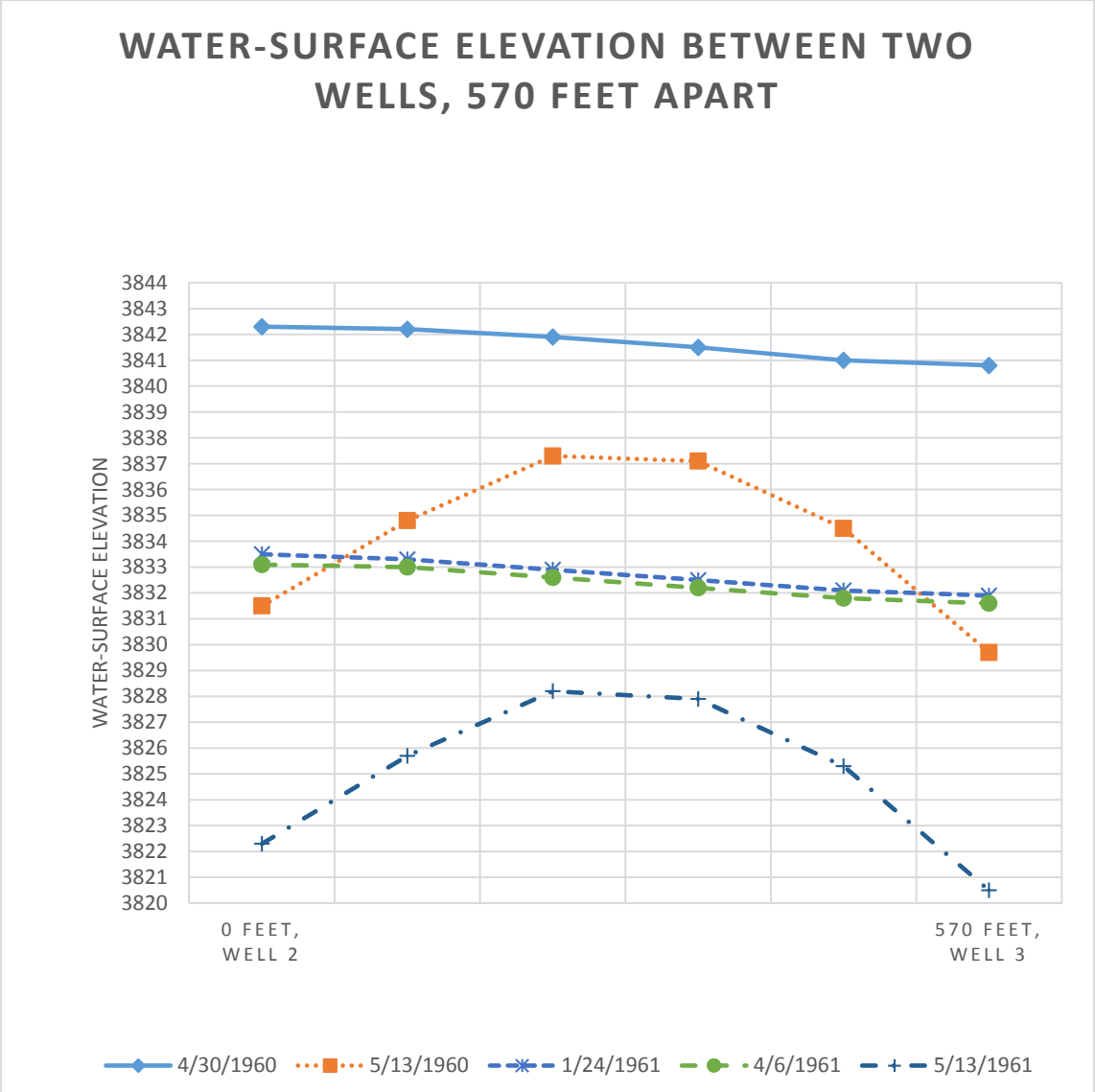

Figure 4.4. Plot of data from northern model run showing mounded water between wells and water table approaching equilibrium after a pumping period. Wells 570 feet apart. Pumping periods were 120 days and rebound periods were 245 days. 4/30/1960 shows water-surface elevation just prior to pumping. 5/13/1960 illustrates drawdown at the wells and mound of water between. 1/24/1961 and 4/6/1961 show recovery of aquifer since pumping stopped in September of previous year. 5/13/1961 shows the initiation of the second pump drawdown period.

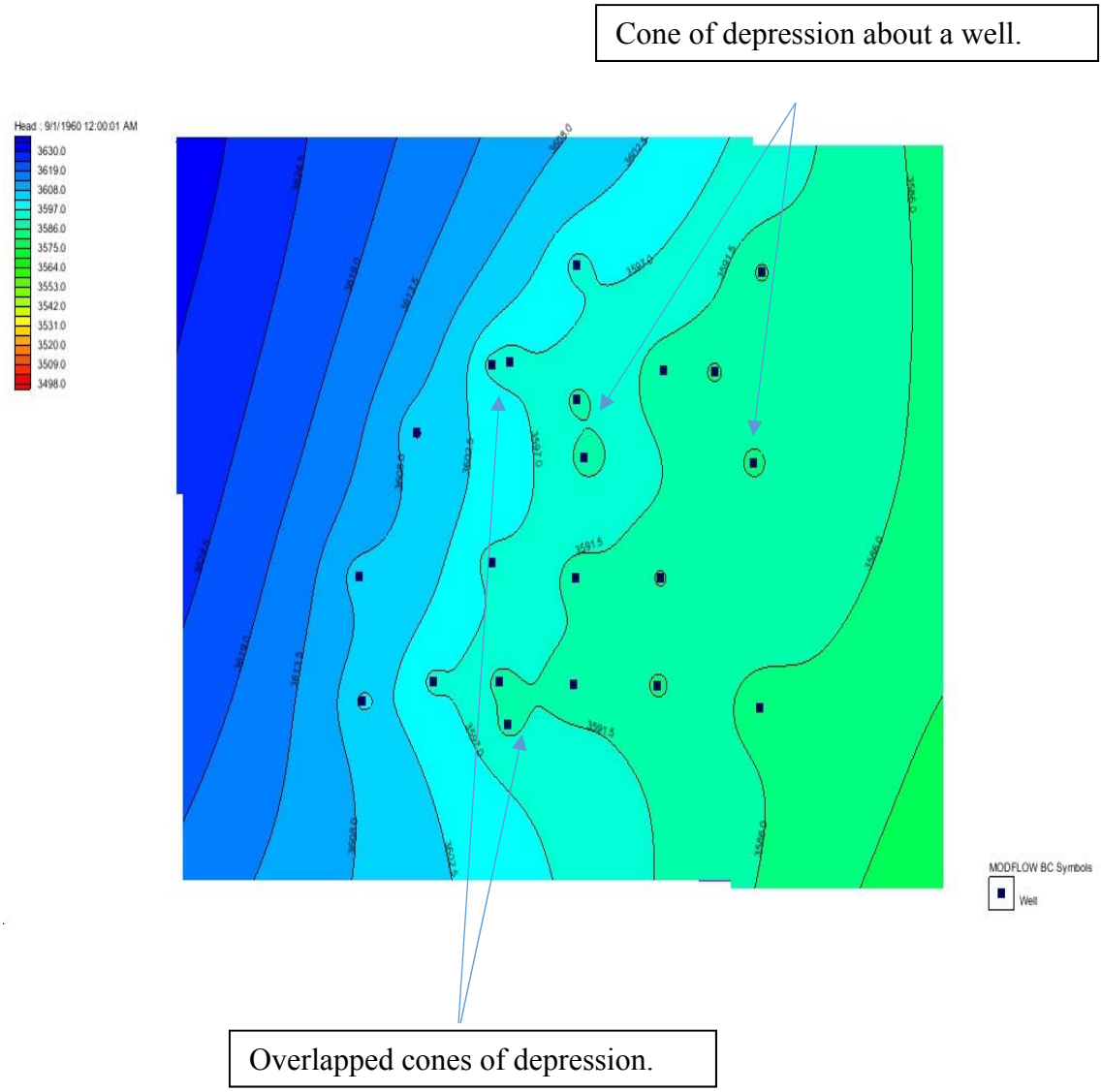

Figure 4.5. Contour of northern model output showing development of the cones of depression about the wells after a 120 day pumping cycle. Decreased water-surface elevations are apparent about the wells prior to the rebound period. Overlapping cones of depression are noted where wells are in close proximity of one another.

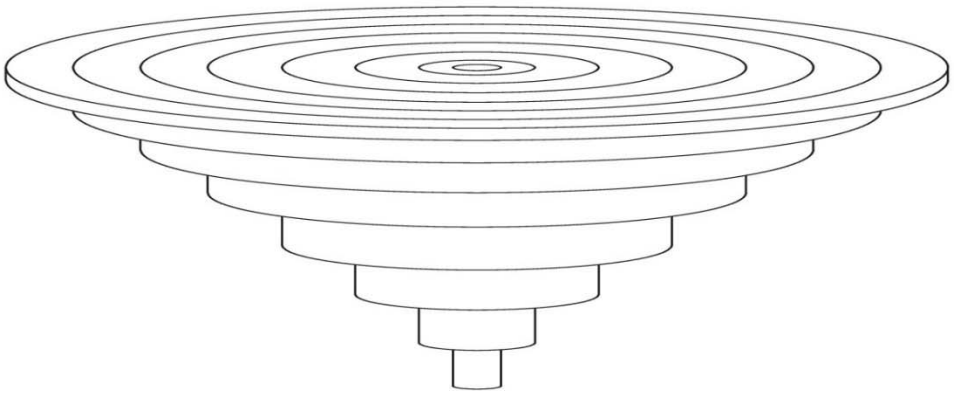

Figure 4.6. Well would be located in the center most cylinder. Depth of drawdown represented would decrease moving from the center outward.

In order to determine whether residual cones of depression would be observed, initial model runs were completed without altering the original GAM parameters. The northern model was located on the Dallam-Hartley county line. In the following images, four wells were observed; not all are contained in the same cross section. Figure 4.8 shows the impact of one pumping cycle on the aquifer. The withdrawal rate of all wells is 800 gallons per minute, and the wells were operated for a 120 day period. The cones of depression were apparent in the vicinity of the wells after only one pumping season. In this image, the initial head layer was shown on top, to provide a better perspective of the drawdown of the wells.

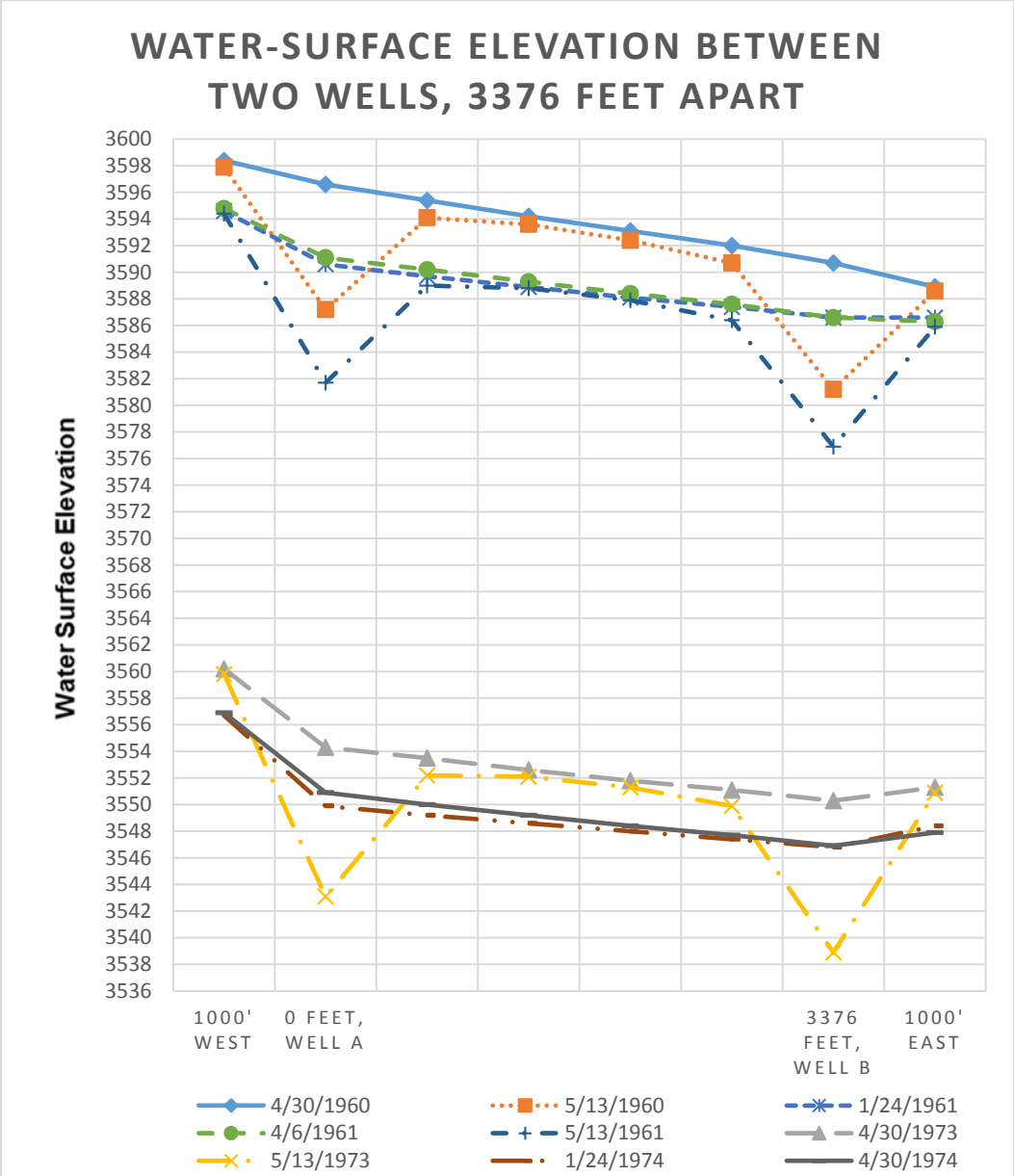

Figure 4.7. Plot of data from northern model run showing mounded water between wells and water table approaching equilibrium after several pumping periods. Wells are located 3376 feet apart and designated as Well A and Well B. Included are water-surface elevations 1000 feet west and 1000 feet east of the cells containing the wells.

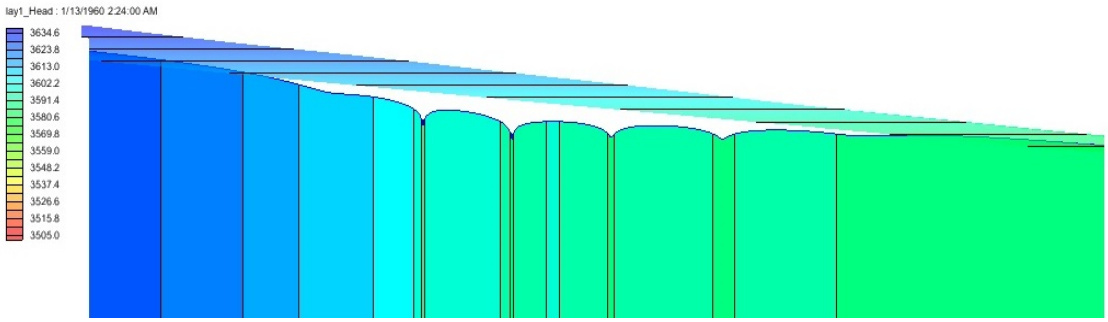

Figure 4.8. Cones of depression in the northern model used in the study. Original GAM parameters and pumped for 120 day cycle. Upper layer is initial starting head. Cones of depression are visible where wells are located. All wells are not in the same plane of the image.

Figure 4.9 shows the rebound of the aquifer after only 25 days subsequent to cessation of pumping and Figure 4.10 was a zoomed image more clearly illustrating the rebound. The aquifer had rebounded very quickly approaching the beginning head values, indicating that mounds of water between wells may not persist until the next pumping season. However, as illustrated by the difference between the new water-surface elevation and the initial head values, the aquifer had not yet fully recovered. Additionally, as seen in this image to the left and right sides (West and East respectively), there was an indication that the aquifer had not yet reached a new equilibrium head level. This was indicated by what appears to be mounded water on either side of the pumped region. This analysis was carried out to the assumed full rebound period of 245 days as shown in Figure 4.11. The aquifer appeared to have fully rebounded and approached the original equilibrium.

Figure 4.12 was the result of four pumping cycles and four rebound periods. Although not prominent, a slight depression of the aquifer existed towards the center of the image. This does not show individual cones of depression but it indicated an average value showing a zone of depression. Using the original model conditions; specific yield set at

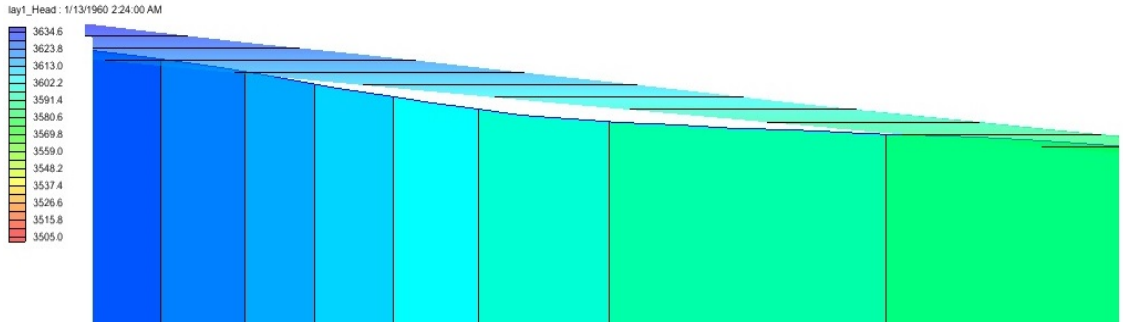

Figure 4.9. Rebound of the northern model after one pumping cycle and 25 days after pumping stopped. Upper layer is initial starting head. Mounds of water between wells have moved to fill cones of depression resulting in a more regional zone of depression. The decline in the water-surface elevation is indicated by the white region between the initial starting head and the lower layer.

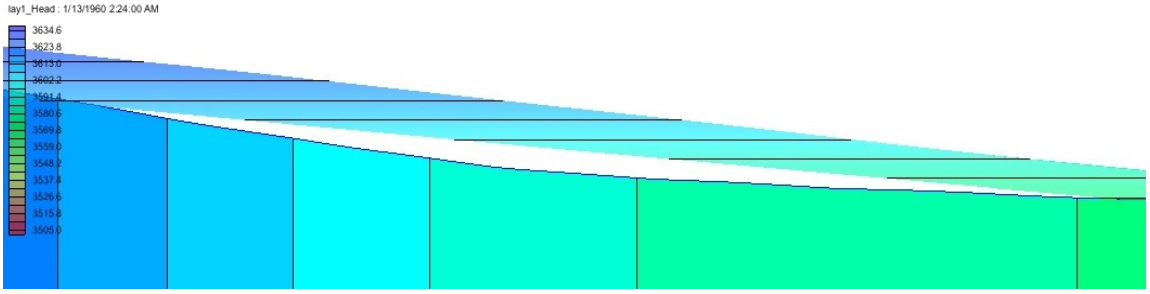

Figure 4.10. Rebound of northern model after one pumping cycle and 25 days after pumping stopped, zoomed image. Upper layer is initial starting head. Mounds of water between wells has moved to fill cones of depression resulting in a more regional zone of depression. No apparent mounding between wells is visible, however, there appears to be "mounds" of water on either side of the depressed region. The decline in the water-surface elevation is indicated by the white region between the initial starting head and the lower layer.

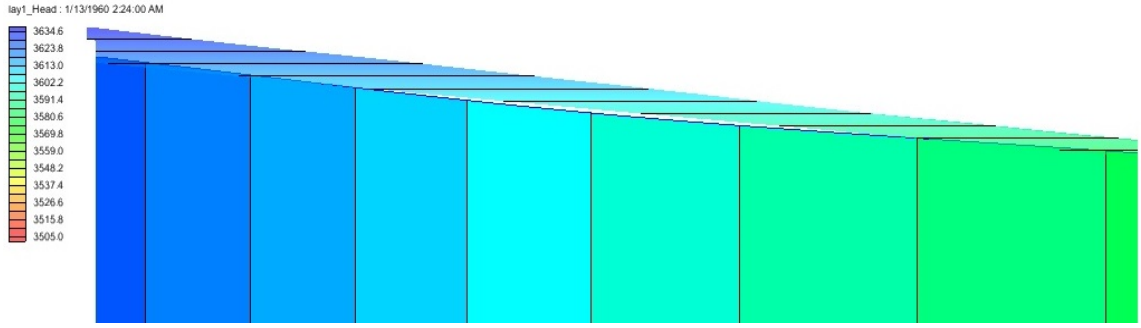

Figure 4.11. Rebound of northern model after one pumping cycle and 245 days after pumping stopped. Upper layer is initial starting head. This represents one complete pumping and rebound cycle. Essentially no aquifer decline is observed after one irrigation season.

0.2%, specific storage set at 0.2 ft^{-1}, and a hydraulic conductivity range from 23-54 $ft\text{-}day^{-1}$, the zone of depression was not clearly visible. There was a greater decrease in head near the center of the model than towards the outer edges indicating there was some water available to move and establish a new water table.

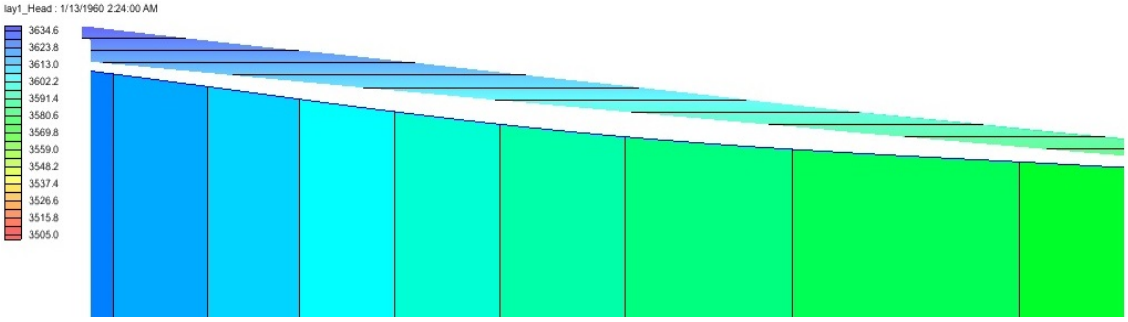

Figure 4.12 Northern model area after four pumping cycles (120 days each) and four rebound cycles (245 days each) with original specific yield value. Note depression towards center of model. There is less decline in the saturated thickness towards the outer edges of the model indicating water will still move towards the center to establish a new, flat water table. The decline in the water-surface elevation is indicated by the white region between the initial starting head and the lower layer.

Figure 4.13a represented a typical drawdown and recovery plot for each cell in the model. Observations here were that the water-surface elevation was declining overall and that the rebound of each cell attempted to achieve a new static equilibrium. The rebound curves indicated a rapid but rebound rate for each pumping cycle.

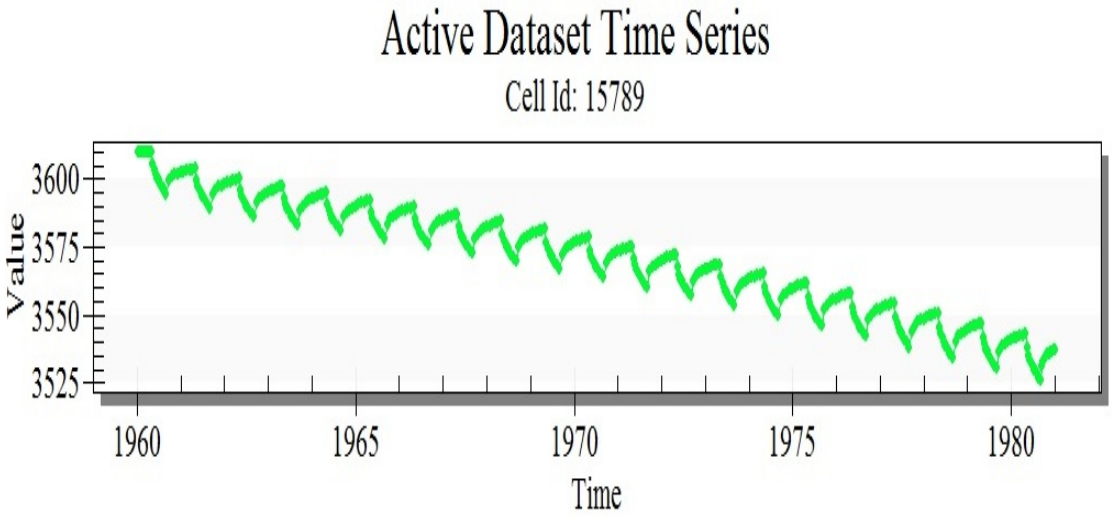

Figure 4.13a. Cyclic drawdown and rebound of individual well cell 1960-1980. The well cells appear to rebound rapidly but never reaches equilibrium prior to the initiation of the next pumping cycle. The water-surface elevation trend declining over time was apparent.

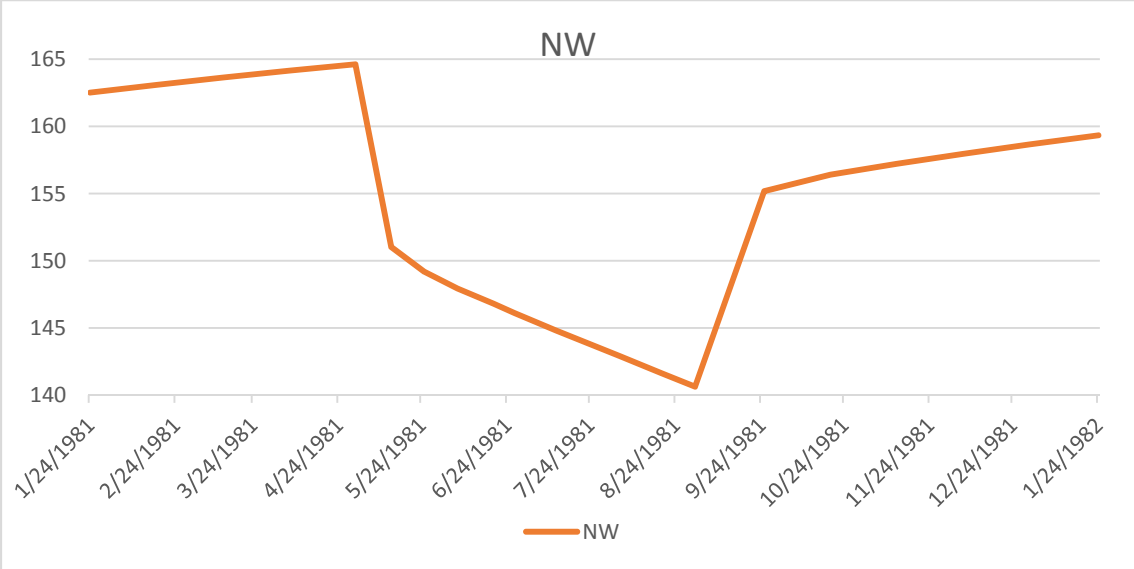

Figure 4.13b. Typical drawdown and rebound of individual well cell in 1981. The well cells show rapid decline in water-surface elevation when wells start on May 1. Wells are stopped on August 31. Most of the well rebound occurs within a few days of the pump being stopped. The gradual increasing curve to the right of the plot indicates slower but continued rebound of the well.

After the well pumping is stopped, most of the well rebound occurs. This would seem reasonable since flow to the well must be sufficient to maintain well output. Further, when the well was shut down after a pumping period, the maximum head difference in water-surface elevation between the well cell and the peak of the mound existed. This would represent the maximum rebound potential for movement of the water towards the well. As the rebound slows, the flattening areas of the curve indicate that the well rebound slows but never reaches a new static head elevation.

The long term rebound of a well was plotted and shown in Figure 4.14. The last pumping cycle was included prior to a cessation of pumping in 1981. The majority of the rebound occurred rapidly after the pump was stopped as seen in Figure 4.13b. A prolonged rebound of the well was noted after the well was no longer being pumped. As can be seen, a new static water-surface elevation was not achieved for several years.

Figure 4.15 is a recently published map of the specific yield of the Ogallala aquifer was developed by Deeds (2015) and shown in Figure 4.15. Deeds reported the geometric mean of the specific yield of the study area to be 0.17 which was consistent with specific yields dating back to Gutentag (1984). The variability of the specific yield across the Ogallala aquifer area which may range from <0.12-0.28 was noted from this image. The model developed near the Dallam-Hartley county line was located in an area where the specific yield reported by Deeds was higher than the specific yield in the GAM. For this reason a new model was prepared with a multiplier to increase the specific yield to 0.25 across the modeled area. Increasing the specific yield of the model allowed for

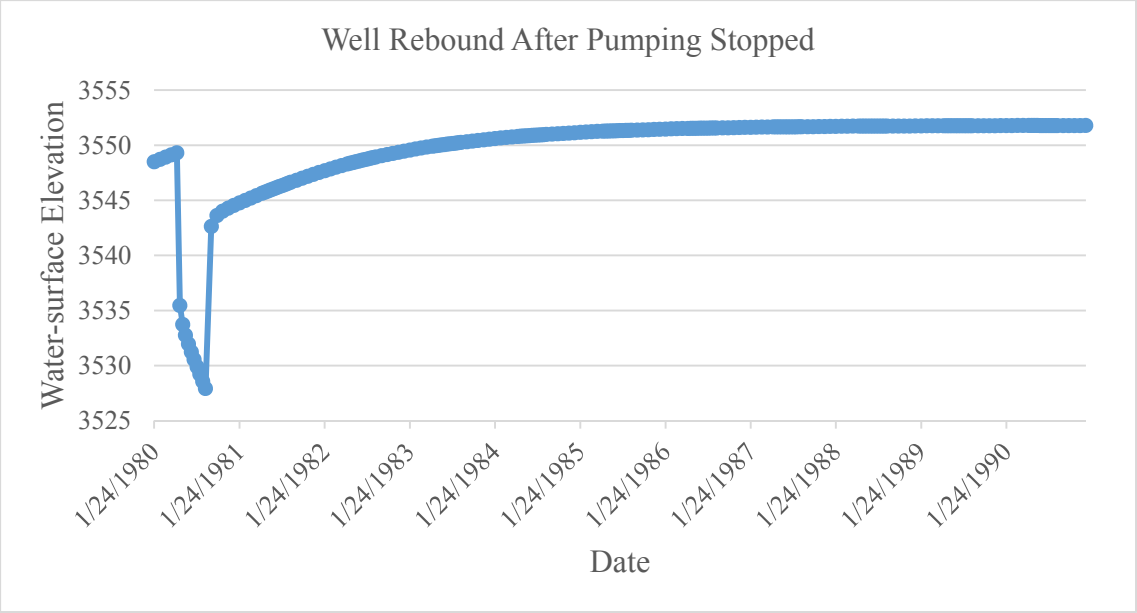

Figure 4.14. Prolonged well rebound of wells post 1980. The well was pumped from 1960-1980 for 120 days each year. The well was no longer pumped after 1980 but the model was allowed to continue to run through 2015. A new static water elevation was achieved after 8 years of rebound. No change was observed in well recovery after 1990 indicating a new static level was reached. The peak water surface in 1980 was the result of several cycles of pumping, none of which allowed for complete rebound. In about 1983 the water surface elevation has recovered to 1980 levels and the subsequent water-surface equilibrium elevation exceeds the water-surface in 1980 due to the progression of movement of mounded water over time.

more water to be taken from each cell during each MODFLOW iteration. Figure 4.16 shows the drawdown and subsequent cones of depression formed at the end of one pumping cycle, which was 120 days. Compared to the cells on either side of them, a significant decrease existed in the cells containing the wells. In all models the pumping rates for all wells were set at 800 gallons per minute.

Figure 4.17 shows the rebound of the aquifer after only 25 days with the higher specific yield. Increasing the aquifer yield allowed the cells to provide more water to be removed from them. This caused a reduction in the need for water to move from adjacent cells.

For this reason a more pronounced zone of depression, as compared to the original GAM where the specific yield was set to 0.2 (Dutton 2000), was seen.

Figures 4.18-4.20 show the results of pumping and rebound. The results from a full 245 day rebound period were shown in Figure 4.18. The rebound of the aquifer is evident but the original water-surface elevation was reduced due to the removal of water. As seen with the original GAM settings, a zone of depression resulted from the rebound of the wells. Figure 4.19 shows a zoom of the rebound period from Figure 4.18. There was a clear depression of the water-surface elevation noted. One pumping cycle did not result in the development of a substantial cone of depression or show a clearly evident mound of water.

Figure 4.20 shows the water-surface elevations after four pumping and rebound cycles. Although individual cones of depression are not evident a much more pronounced zone of depression was seen near the center of the image. Also noted was the decreased drawdown towards the edges of the image. This would indicate that the rates of decline at the boundaries of the modeled area are less than those in the pumped region.

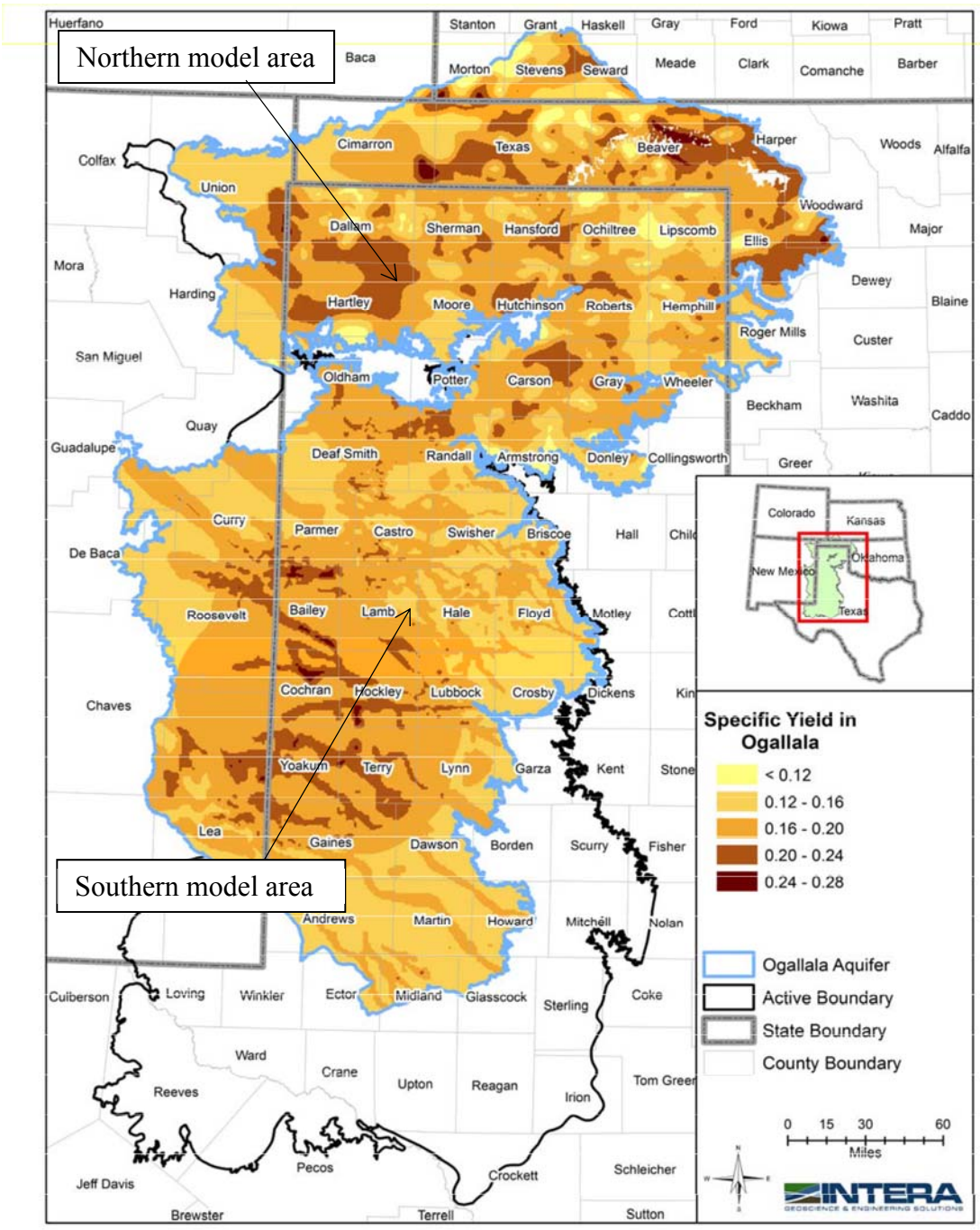

Figure 4.15. Calibrated specific yield in the Ogallala Aquifer (Deeds 2015).

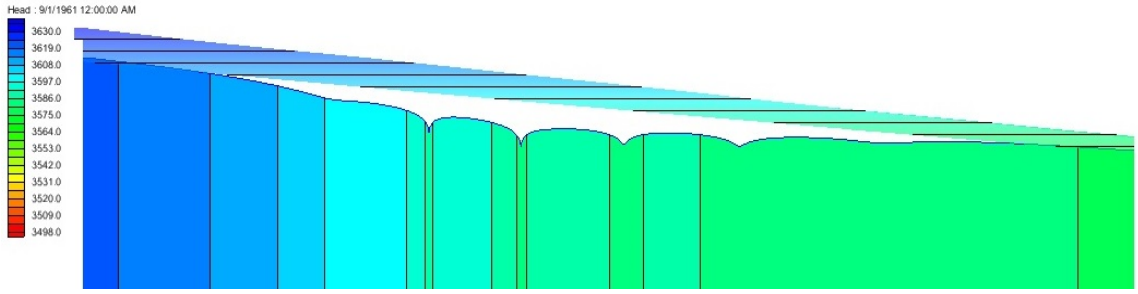

Figure 4.16. Northern model area. Specific yield adjusted to 0.25 and pumped for one 120 day cycle. Upper layer is initial starting head. Mounds between well cells are evident at this time.

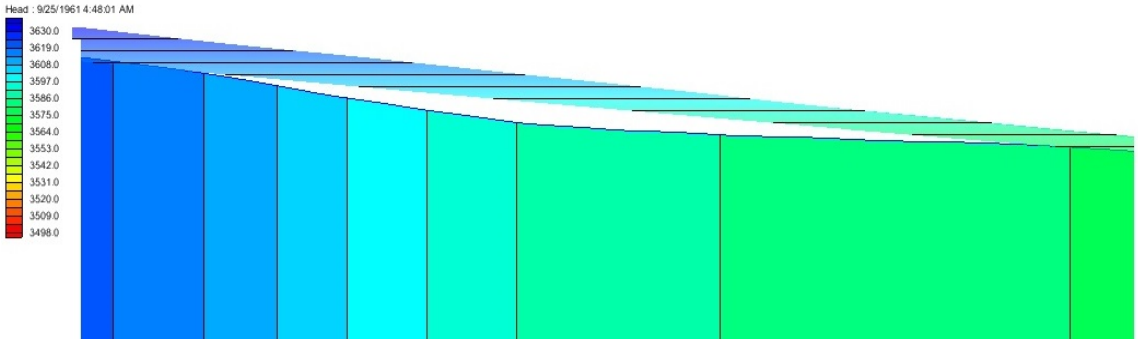

Figure 4.17. Northern model area. Rebound of aquifer after one pumping cycle and 25 days after pumping was stopped. Individual mounds between wells do not appear but there is indication a regional zone of depression. The upper layer is initial starting head. The decline in the water-surface elevation is indicated by the white region between the initial starting head and the lower layer.

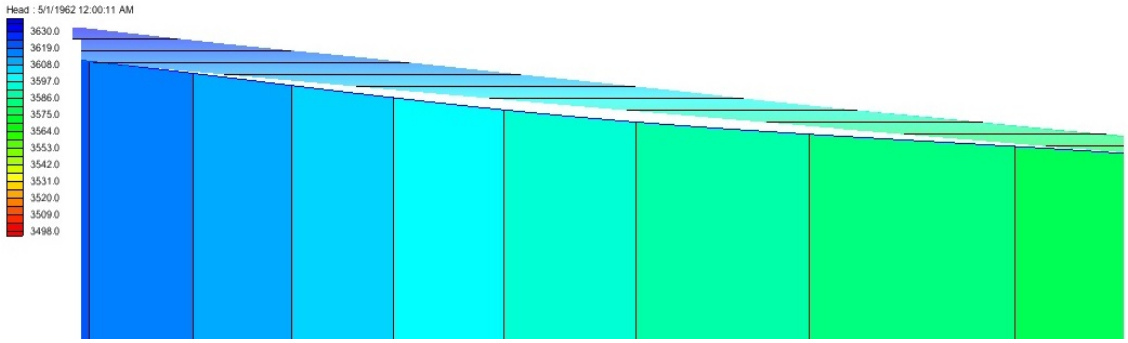

Figure 4.18. Northern model area. Rebound of aquifer after one pumping cycle and 245 days after pumping was stopped. Region of depression is noted and attributed to the cumulative effect of multiple cones of depression. Upper layer is initial starting head. The decline in the water-surface elevation is indicated by the white region between the initial starting head and the lower layer.

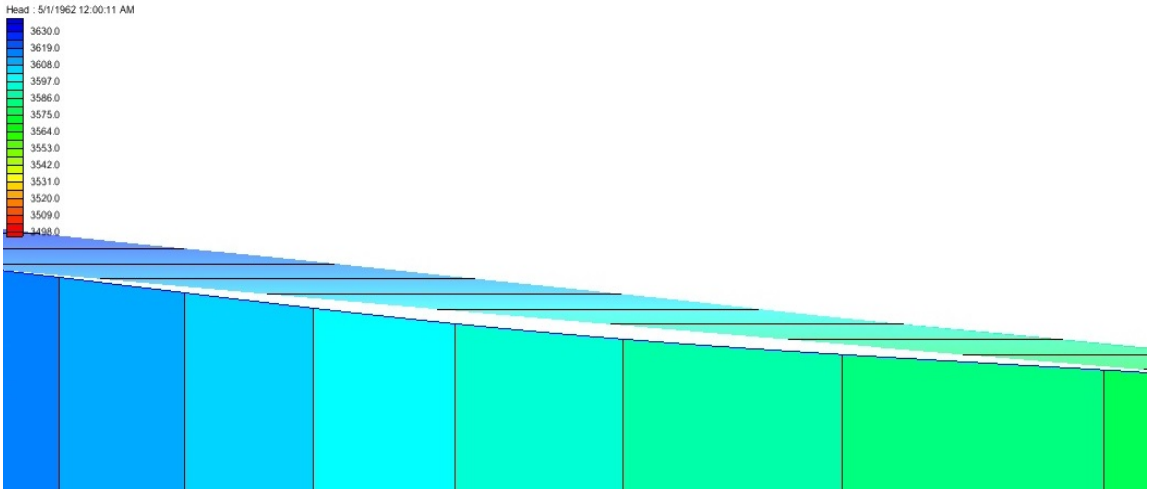

Figure 4.19. Northern model area. Zoomed image of the rebound of aquifer after one pumping cycle and 245 days after pumping was stopped. Region of depression is noted and attributed to the cumulative effect of multiple cones of depression. The upper layer is initial starting head. The decline in the water-surface elevation is indicated by the white region between the initial starting head and the lower layer.

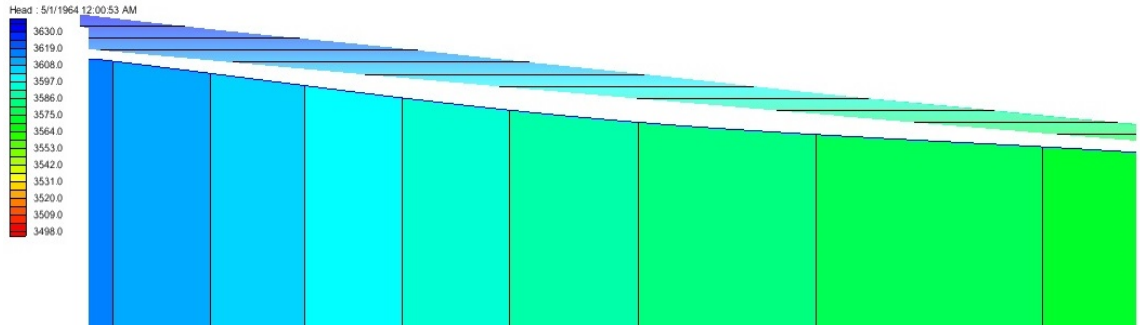

Figure 4.20. Northern model area after four pumping cycles and four rebound cycles. Note depression towards center of model. The rate of decline at the boundaries of the model are less than the area towards the center where the wells are located.

A model run was completed where the well output was decreased over time. Initial pumping values were set at 800 gpm from 1960-1979. The pumping rate was reduced to 600 gpm from 1970-1979, 400 gpm from 1980-1989 and 200 gpm from 1990-2015. Reduced pump rates are attributed to declining saturated thickness resulting in the aquifer having a reduced head. This would cause the flow rate from the porous media to the well

to decline which, in turn, would reduce the flow rate of the well. Observations of the saturated thickness in this model design were not conducive to this type of analysis. Although diminishing heads were observed, the wells did not go dry when the well outputs were maintained at 800 gpm from 1960-2015. This could be due to the number of wells relative to the size of the modeled area.

Reduced pump output over time is a well-known process and has been seen in wells owned by the author. Analysis of this model run shows no evidence of mounds between wells. This is likely due to the reduced pump output which reduces the rate of decline in the aquifer. As shown in Figure 2.7, reduced pump output reduces the well influence on the aquifer as well as the cone of depression. Aquifer properties coupled with a reduction in the rate of withdrawal likely accounts for the lack of mounds under the conditions of this simulation.

The northern model can be shown to exhibit small cones of depression which become even more apparent with a slight increase in specific yield. These results and the prolonged well recovery demonstrated indicate that mounds of water were present within the aquifer.

Model of Southern Region

The southern model area was evaluated in the same manner as that in the north. Eastern Lamb County was selected and a portion of the southern GAM was used for analysis. This area was selected since it lacked apparent topographical features, i.e., streams beds,

lakes, which could influence subsurface geology. The southern model was constructed with different time intervals than the northern model. This reduced the number of time steps required during each iteration of the model run and reduced the total amount of time required for the model to run to completion. This was accomplished by reducing the time steps during pumping from ten in the northern model to four in the southern model. The time steps were reduced during the rebound period from nine in the northern model to three in the southern model. Figure 4.14 from Deeds (2015), showed that the specific yield where this model was harvested from the original GAM was in the 0.16-0.20 range. Since the specific yield in the original GAM was set at the upper end of the range (0.2), no additional models were prepared with increased specific yield.

The model area contained six wells as shown in Figure 3.17 each representing an actual well location. The original specific yield was unchanged from the original GAM. Wells were set to pump at 800 gallons per minute, and the pumping cycles were 120 days. Rebound periods were 245 days. Figure 4.21 shows the result of one pumping cycle in the southern model. One well was visible in this view and the cone of depression was distinct. The cone of depression of a second well was visible but the well was not in the plane of view presented so only an edge of the cone appears.

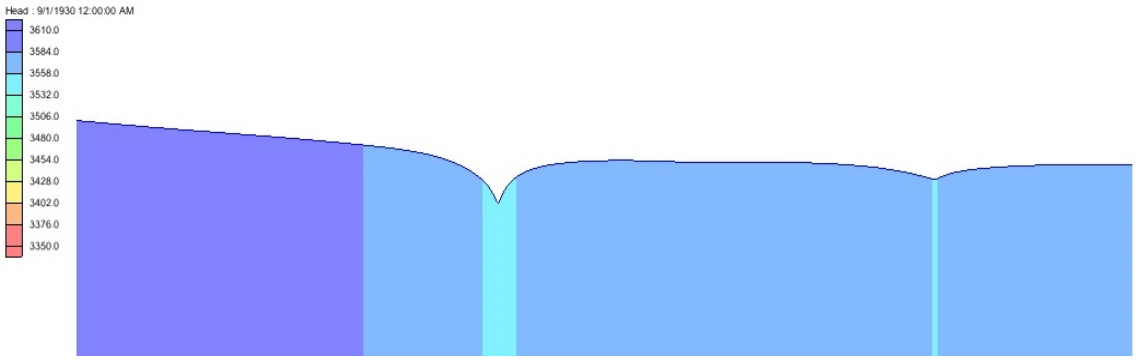

Figure 4.21. Southern model showing one well after one 120 day pumping cycle. The influence of a second well is visible on the right side of the image. The cone of depression is obvious.

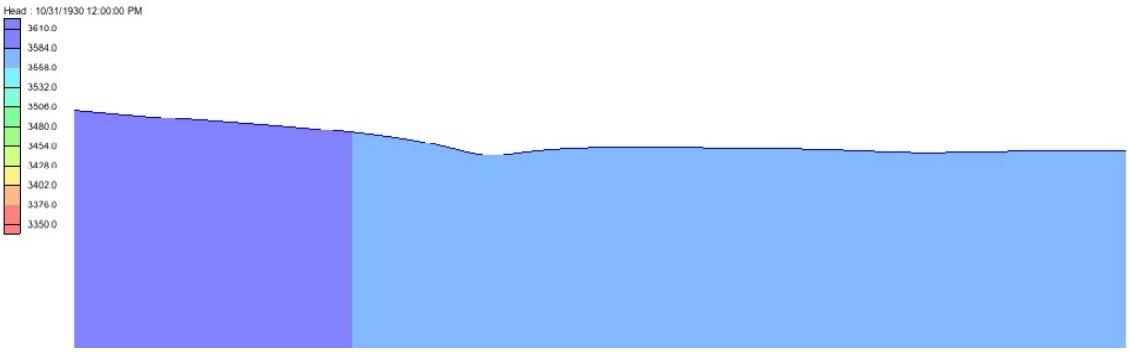

Figure 4.22 Southern model after one pumping cycle and one 60 day rebound period. The cone of depression remains visible.

Figure 4.22 shows the slight cone of depression after a 60 day rebound period after one pumping cycle. Elevated heads to either side of the cone indicated mounded water. Figure 4.23 is the rebound after 245 days. Note a slight cone of depression at the location of the well.

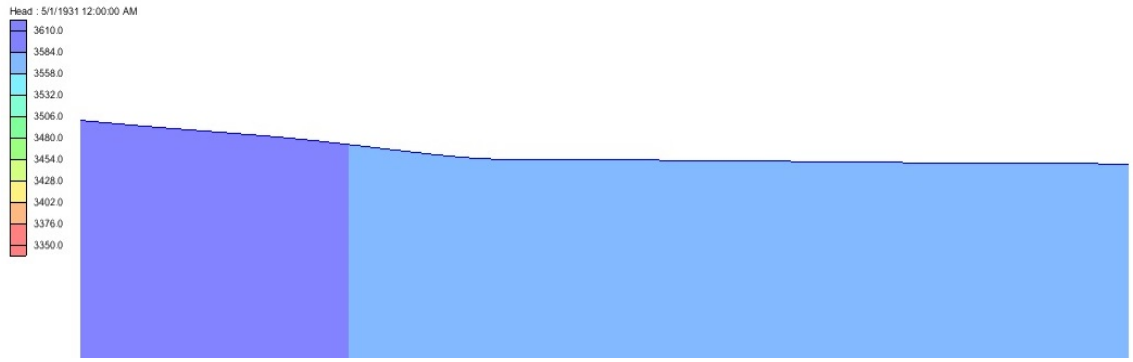

Figure 4.23. Southern model after one pumping cycle and a 245 day rebound period. Note slight dip in head where the well is located.

Figure 4.24 shows the state of the southern model after 10 pumping cycles and rebound periods. As seen in this image, little has apparently changed from the single pumping cycle of Figure 4.23. There is a more pronounced cone of depression at the location of the well, and there is a more visible mound of water to the west of the image. Close comparison of this image with Figure 4.23 shows that the dark blue band on the left decreased in size and the lighter blue region increased in size. This indicated the decreased head values from West to East across the model. Evidence of mounded water was apparent to both to the West and East of the well location, with the West side showing more mounding than to the East.

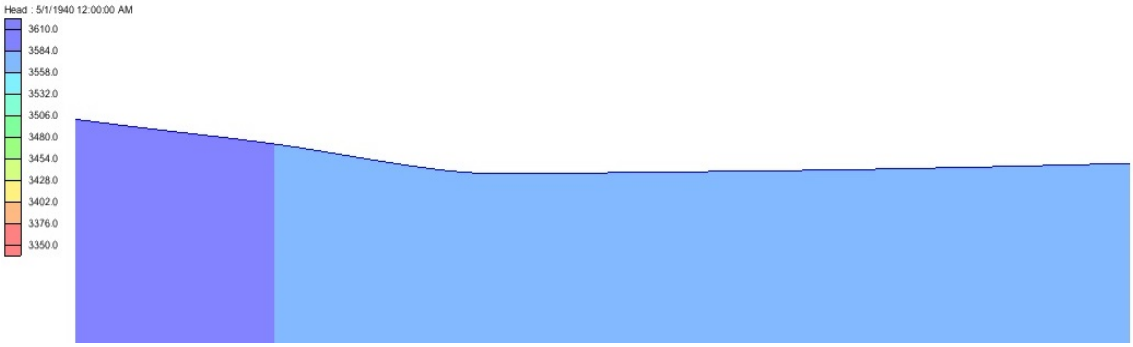

Figure 4.24. Southern model after 10 pumping cycles and rebound periods. Pumping cycles were 120 days and rebound periods were 245 days. Saturated thicknesses to the east and west indicate water is mounded outside of the zone of depression.

After the analysis of the northern and southern models was completed and the specific yield adjusted, the values for the hydraulic conductivity were evaluated.. The hydraulic conductivity of both modeled areas was taken directly out of the GAM. Initial model runs were completed without altering the original values in the GAMS. Figure 4.25 shows the range of hydraulic conductivity in the northern model. Hydraulic conductivity varies considerably across the Ogallala aquifer. Deeds (2015) reported an overall geometric mean for hydraulic conductivity of 19.6 feet/day, an increase from the initial values proposed by Gutentag (1984) who indicated a hydraulic conductivity of 10.7 feet/day. The range as reported by Deeds is from 0.422 feet/day to 550 feet/day and is shown in Figure 4.27. The hydraulic conductivities of the models were not altered from the original GAMs. Since the GAMs had been recognized as the accepted aquifer models, there is an implied acceptance of the parameters used to generate the model. Adhering to the accepted aquifer parameters was used to justify maintaining the same aquifer parameters for this modeling effort. The original hydraulic conductivity values for both the northern model and southern model can be seen in Figures 4.25 and 4.26. The range of the northern model is 23-54 feet/day and that of the southern model is 6-65 feet/day. The wide variance of conductivity could explain some of the differences noted between the northern and southern models.

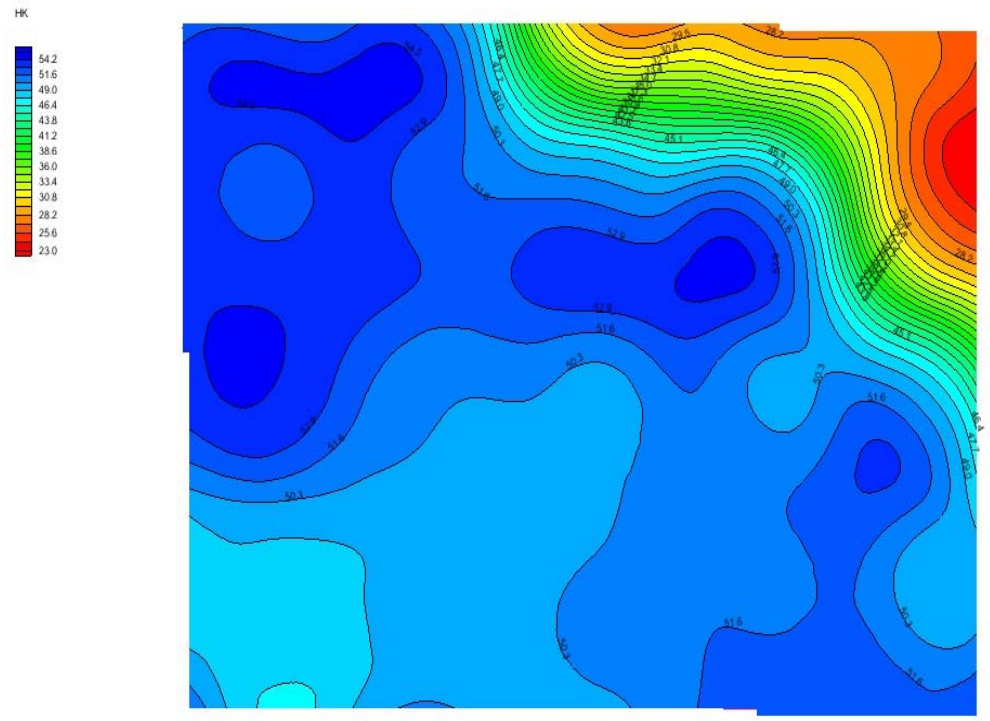

Figure 4.25. Range of original hydraulic conductivity across the northern modeled area in feet/day.

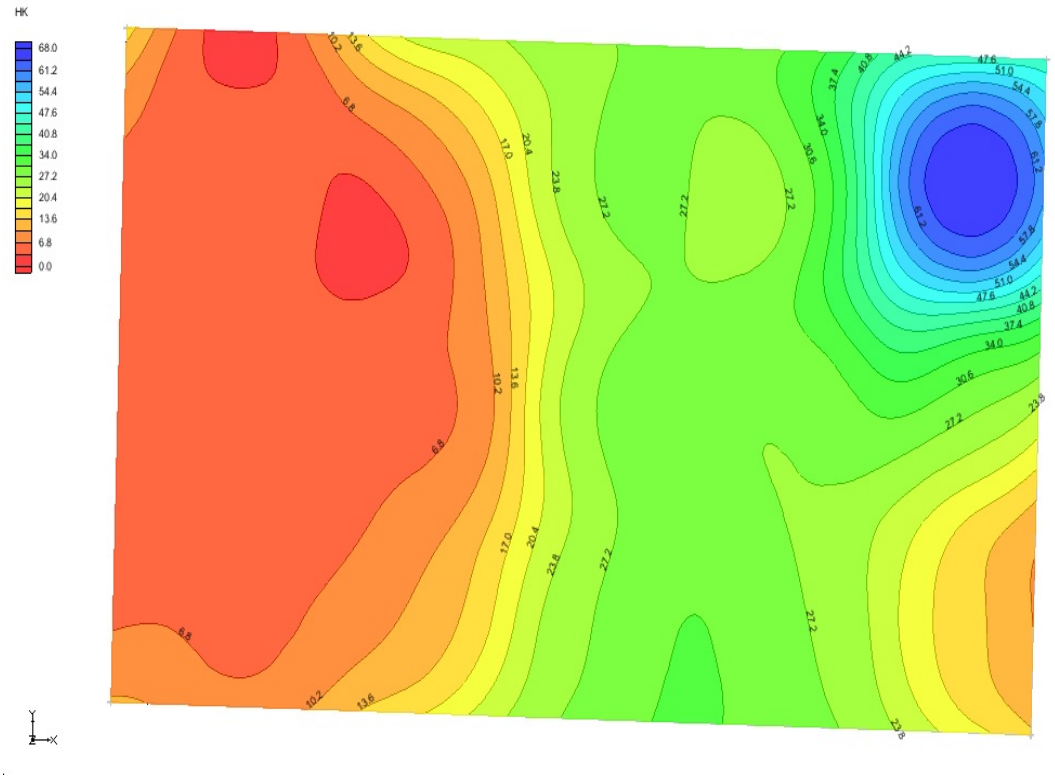

Figure 4.26. Range of original hydraulic conductivity across the southern modeled area in feet/day.

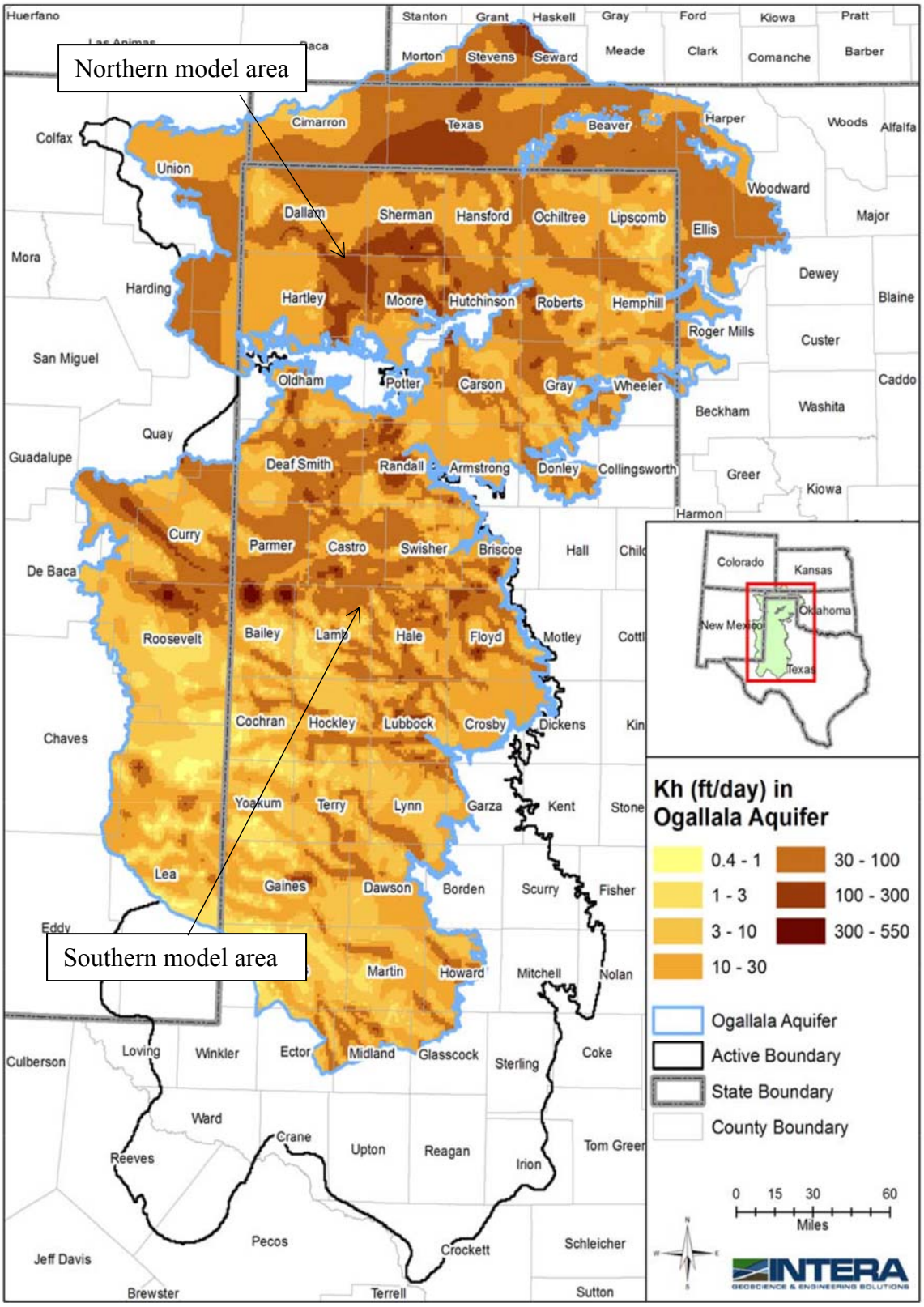

Figure 4.27. Calibrated horizontal hydraulic conductivity in the Ogallala Aquifer (Deeds 2015).

The model developed in this work for the northern portion of the Groundwater Availability Model (GAM) showed the presence of small mounds of water between the wells using water-surface elevations. Zones of depression were evident where wells were likely influencing each other. Also, the magnitude of the water mound between wells was unknown but not anticipated to be large. Since mounds were not clearly present after rebound periods, another approach was considered in order to observe variations in the water-surface elevations. By evaluating the water-surface elevation, a plot of the water-surface could be evaluated for the presence of mounded water. Results of a portion of the northern model run are shown in Figure 4.28. Using the water-surface elevation reveals the mound of water remaining after a pumping cycle.

The NW and NE curves shown in Figure 4.28 are cells containing pumping wells. The locations of the plotted cells are shown in Figure 4.29. The plot shows the drawdown over a 120 day pumping cycle and the 245 day rebound. The Center plot is a cell located between the wells and is also shown in Figure 4.28.

As anticipated, Figure 4.28 shows that the Center point was affected by the pumping. The entire aquifer indicated an overall drop. However, since the Center point had a slightly higher water-surface elevation over time and since the wells were located on the west and east sides of the Center point, the consistent trend of higher water-surface elevations indicated a mound between the wells.

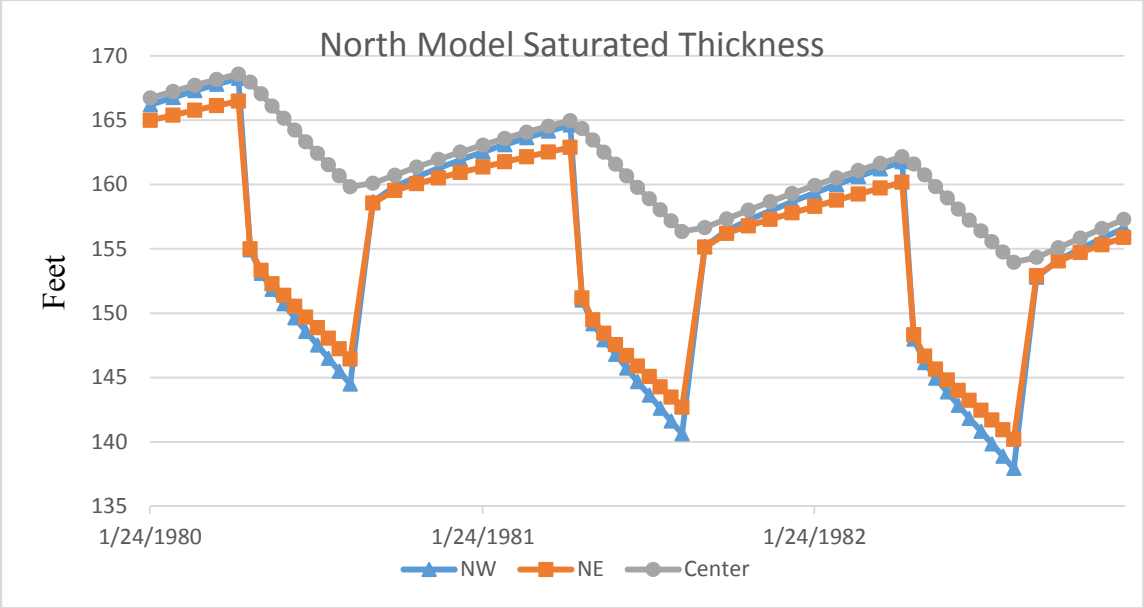

Figure 4.28. Plot of saturated thickness during the northern model run from 1980-1985. NW and NE are cells containing pumped wells. The Center plot represents a cell equidistant between the wells.

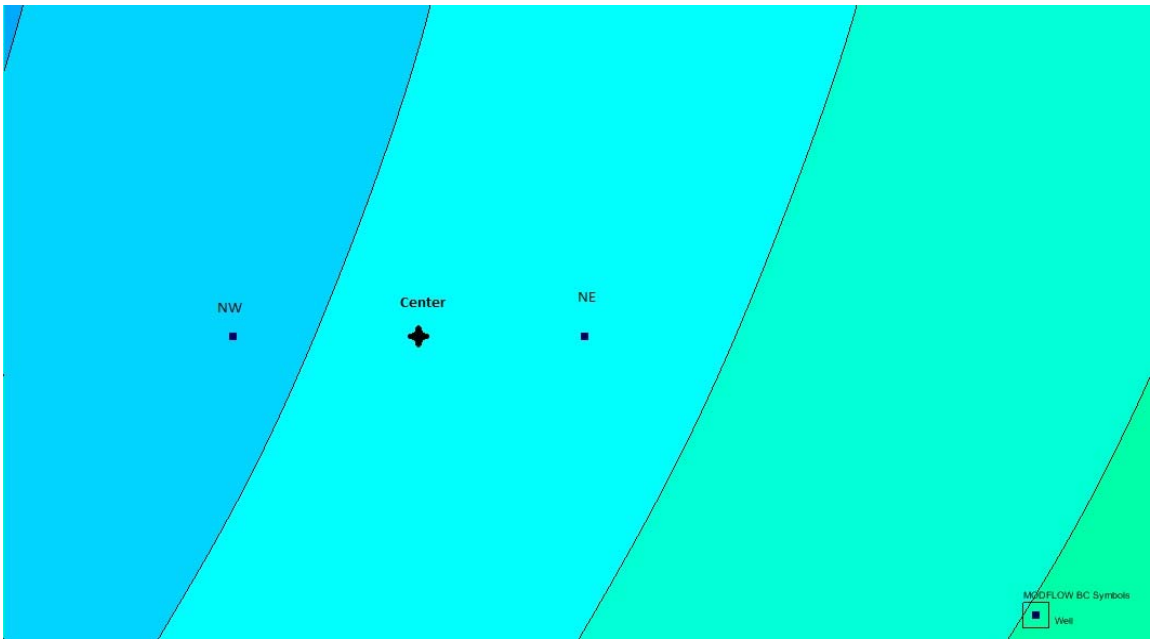

Figure 4.29. Wells and Center point used for water-surface elevation evaluation. Wells are located in the NW and NE cells. The Center point is roughly centrally located between the wells.

Two additional cells were selected between the NW well cell and the Center point and the NE well cell and the Center point. The water-surface elevation at a single point in time was selected for each of the five cells. The data points selected represent the maximum rebound time, 245 days, between pumping cycles. The plot is shown in Figure 4.30. There was not a clearly developed mound of water between the wells.

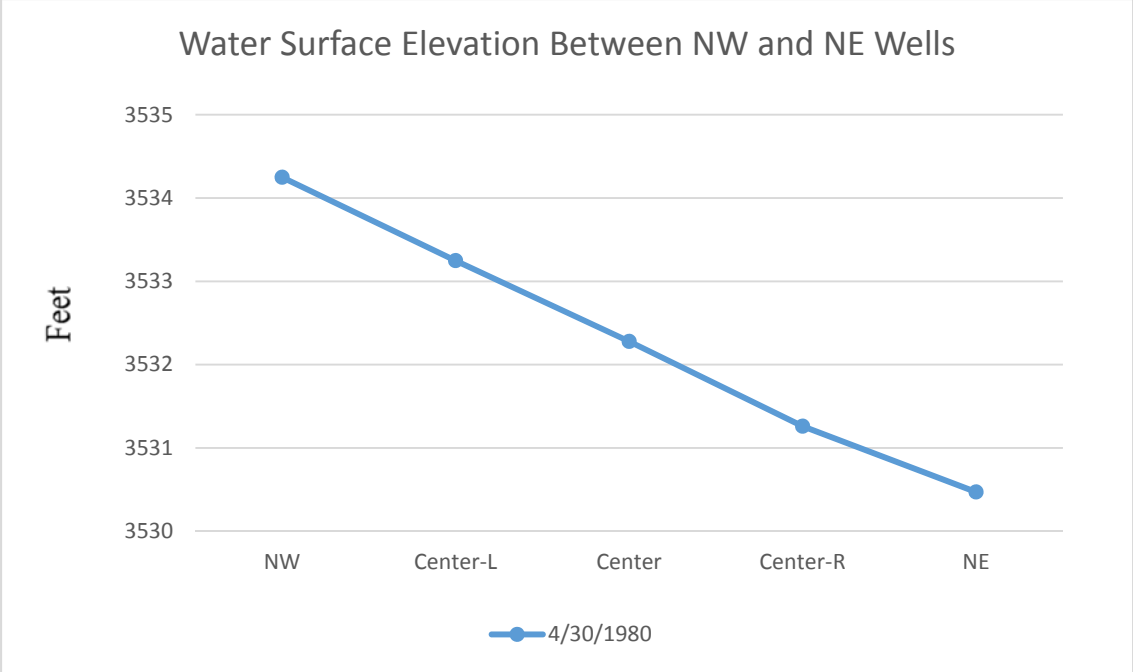

Figure 4.30. Plot of water-surface elevation in the northern model. NW and NE cells contain wells. The three points between were spaced evenly between the wells where water-surface elevation was measured.

The saturated thickness in the northern model was plotted in Figure 4.31. In this plot a mound of water between wells was evident. This approach was not considered the best approach to determine the presence of a mound due to the uncertainties in the elevations of the confining layer (redbed) of the aquifer. However, for estimating purposes, a semi-quantitative analysis of the mounds was offered.

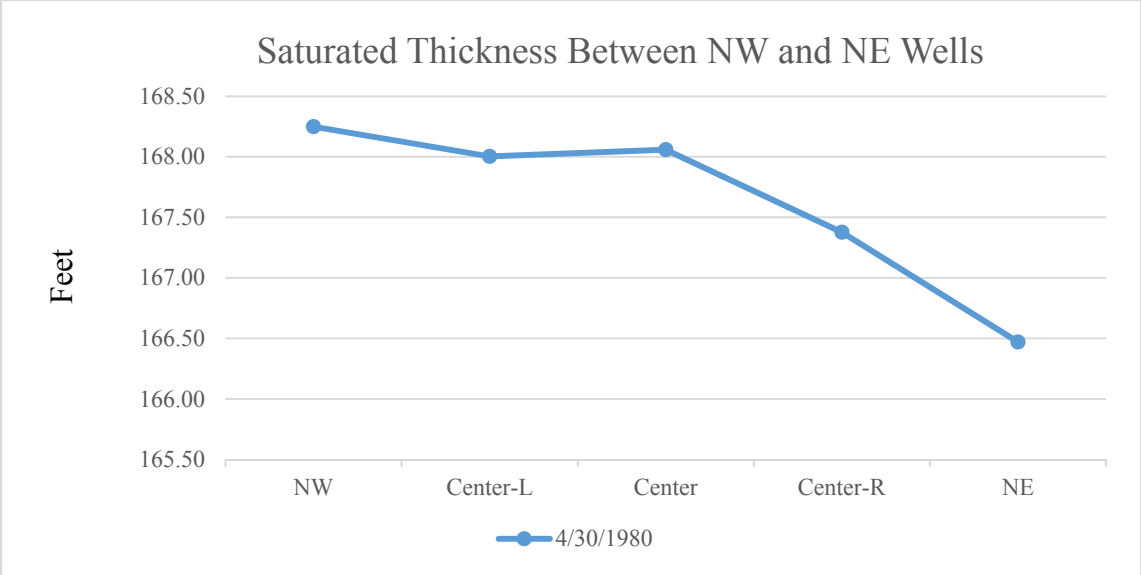

Figure 4.31. Plot of the saturated thickness of the northern model. NW and NE cells contain wells. The three points between were spaced evenly between the wells where saturated thickness was measured.

Using the Well Measurement Approach (WMA) and applying this to an area between wells, the amount of water unaccounted for can be estimated. Figure 4.32 included the wells from the northwest and northeast and adds wells in the southwest and southeast. The four wells provide a roughly square area which was used to calculate and estimate a volume of water remaining in storage assuming a similar mound from west to east between the four wells in the plot. The distance from west to east between the wells was approximately 2750 feet. The distance from north to south was approximately 2750 feet as well. Assuming the average mound height, between the four wells, from west to east across this highlighted area was 0.25 feet, the remaining additional water can be found as follows:

$$V = L * W * H$$

where:

V is the volume of the area (L^3);

L is the length of the area (L);

W is the width of the area (L);

H is the height of the area (L).

So the volume of saturated thickness contained within the mound was determined to be:

$$V = 2750\ ft * \ 2750\ ft * 0.25\ ft$$

$$V = 1{,}890{,}625\ ft^3$$

From this, the volume of water released can be estimated, using the specific yield of the aquifer. In this model a specific yield of 20 percent was assumed; therefore,

$$V_{Water} = \ S_y * \ V_{Total}$$

where:

V_{Water} is the volume of water released from the aquifer (L^3);

S_y is the specific yield of the aquifer (dimensionless);

V_{Total} is the total volume being evaluated (L^3).

So the actual volume of water that could be removed from within the mounded area was determined to be:

$$V_{Water} = 0.20 * 1{,}890{,}625 ft^3$$

$$V_{Water} = 3{,}778{,}125 ft^3$$

This volume represented about 2,828,375 gallons (8.7 ac-ft) of extractable water remaining in the mounded water between the two wells. This would be considered an inconsequential amount of water in the mound between the four wells in the northern model, so the north behaves hydraulically different than the south.

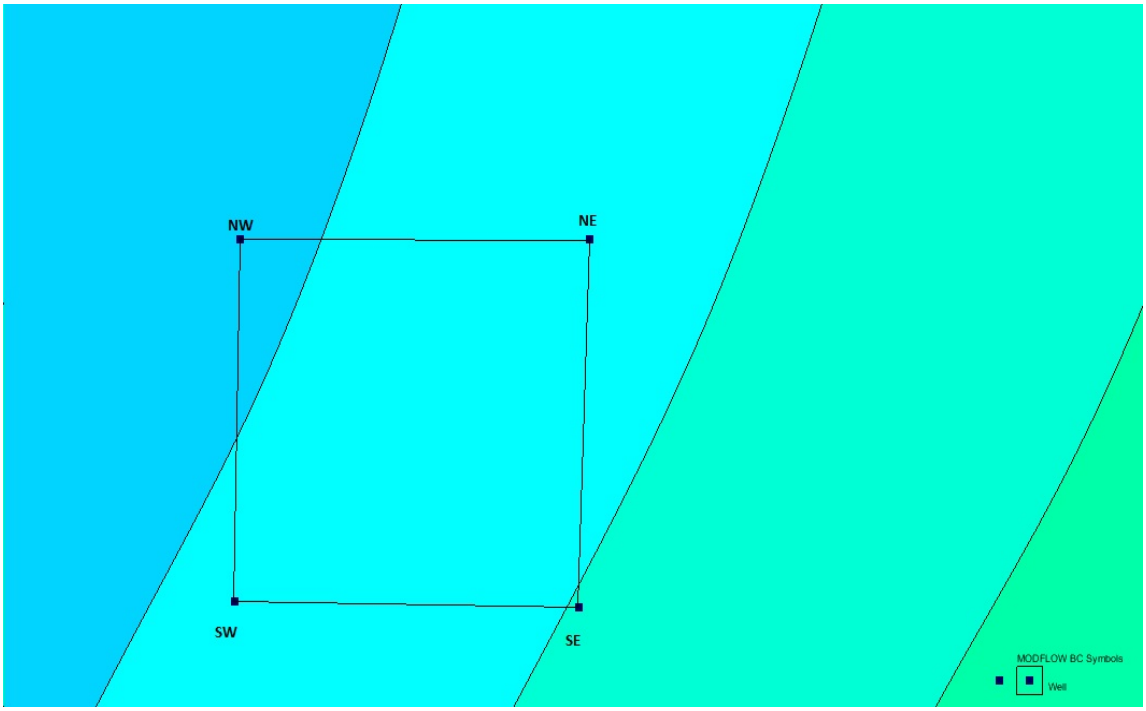

Figure 4.32. Four well plot for mound evaluation in the northern model. Wells are located in the four corners of the diagram.

Additional analysis was done on the southern model area. This model contained data beginning in 1930 and concluded in 2001. A manual scan through the model output was performed to monitor the development of the cones of depression. Figure 4.33 shows the presence of a cone of depression surrounding a well that does not completely rebound prior to the beginning of the next pumping cycle. Of particular interest in this image was

that the cone was offset to the east. This would imply that the cones were not symmetrical about the wells, an outcome which may be attributed to the slope of the aquifer from west to east. A comparison of Figures 4.32 and 4.33 revealed an increase in the cone of depression. The images were from exactly one year apart in the model output. Both images show the anticipated dip at the water-surface elevation and the mounding effect to the east and west of the cone.

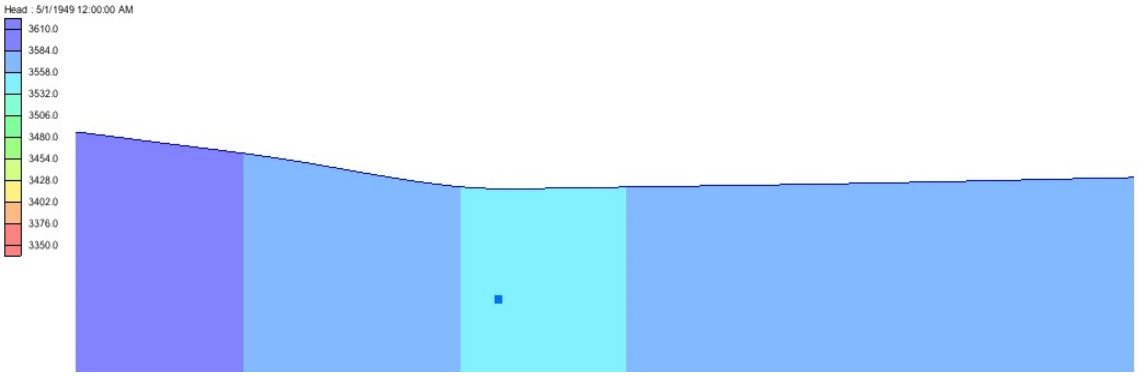

Figure 4.33. Presence of cone of depression after rebound period in southern model. The model output shows a decreased head about the well which was indicative of a cone of depression.

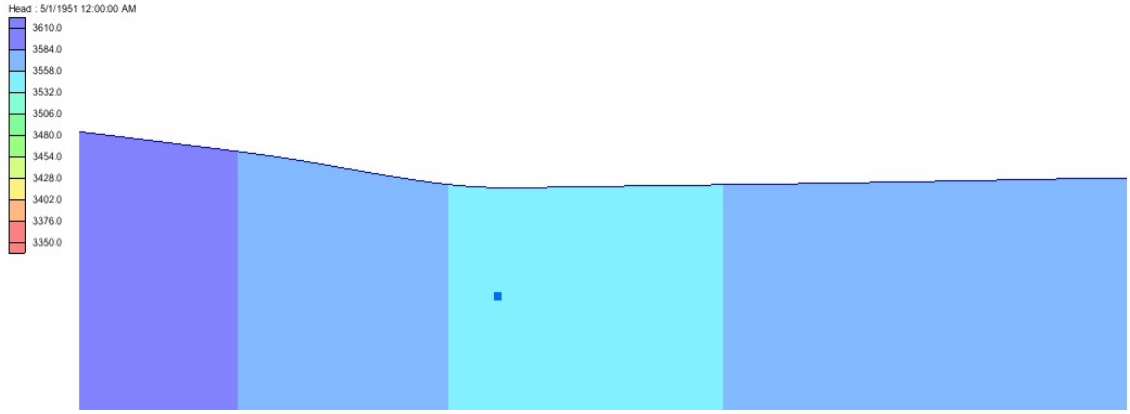

Figure 4.34. Increase cone of depression after rebound period in southern model.

As with the northern model, a plot was made of the water-surface elevations in the southern model. The plot is shown in Figure 4.35. The water-surface elevations were taken from 1930-1990. The locations of two wells and the cells from which the data was taken is shown in Figure 4.36.

Figure 4.35 clearly shows a mound of water to the west of the wells. The mound varies over time but generally shows about 20-25 feet of additional saturated thickness over the pumped area about the wells. At twenty percent yield, this would be approximately 5 feet of additional water available in this mound.

Based on the results seen in Figure 4.35, the model in the northern area was revisited. An additional model run was prepared in which only four wells were active. This model allowed observations of the water-surface elevations where well densities were reduced. In addition, this allowed for the analysis of water-surface elevations which would simulate those approaching undeveloped rangeland. Figure 4.37 shows the plots from the northern model from 1960-2011. One point was selected 5,000 feet northwest of the NW Well and one point was selected 5,000 feet southeast of the SE Well as shown in Figure 4.38

Figure 4.37 shows increased saturated thickness to the west of the wells. Approximately 12 feet of additional saturated thickness was available in a mound. At twenty percent yield, this would be approximately 2.4 feet of additional water available in this mound. This would only apply to rangeland and undeveloped areas in the model region.

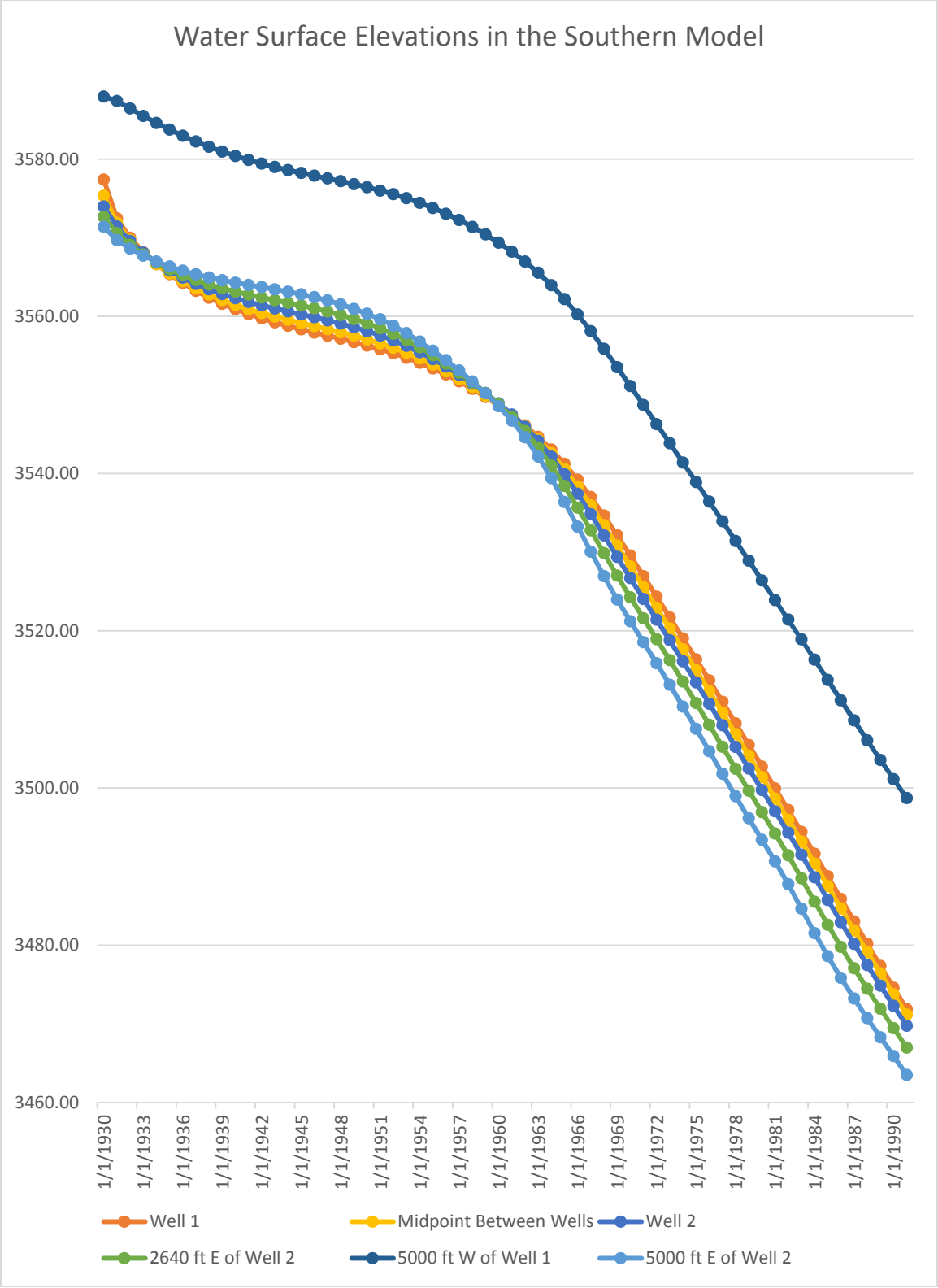

Figure 4.35. Plots of water-surface elevations in the Southern model from 1930-1990.

Figure 4.36. Locations of wells and cells used to generate the water-surface elevation plot in the Southern model.

Efforts were made to use the data extracted from the original GAM to develop a multilayer model, which one might expect to provide more resolution, particularly around the wells where the drawdown is steep during a pumping cycle. Soon after pumping stops, a majority of the rebound is expected. This may be over a few hours or even a few days. The rebound curve would be the reciprocal of the drawdown curve where most of the drawdown occurs soon after the well starts. Figure 4.6 illustrates the cone of depression development. The greatest potential for water to flow to the well occurs when the maximum head difference exists in the cone. The inner cylinders in this figure would fill most rapidly because they have the highest gradient and the smallest volume. Some additional refinement around the well (Figure 4.39) can be realized by increasing the

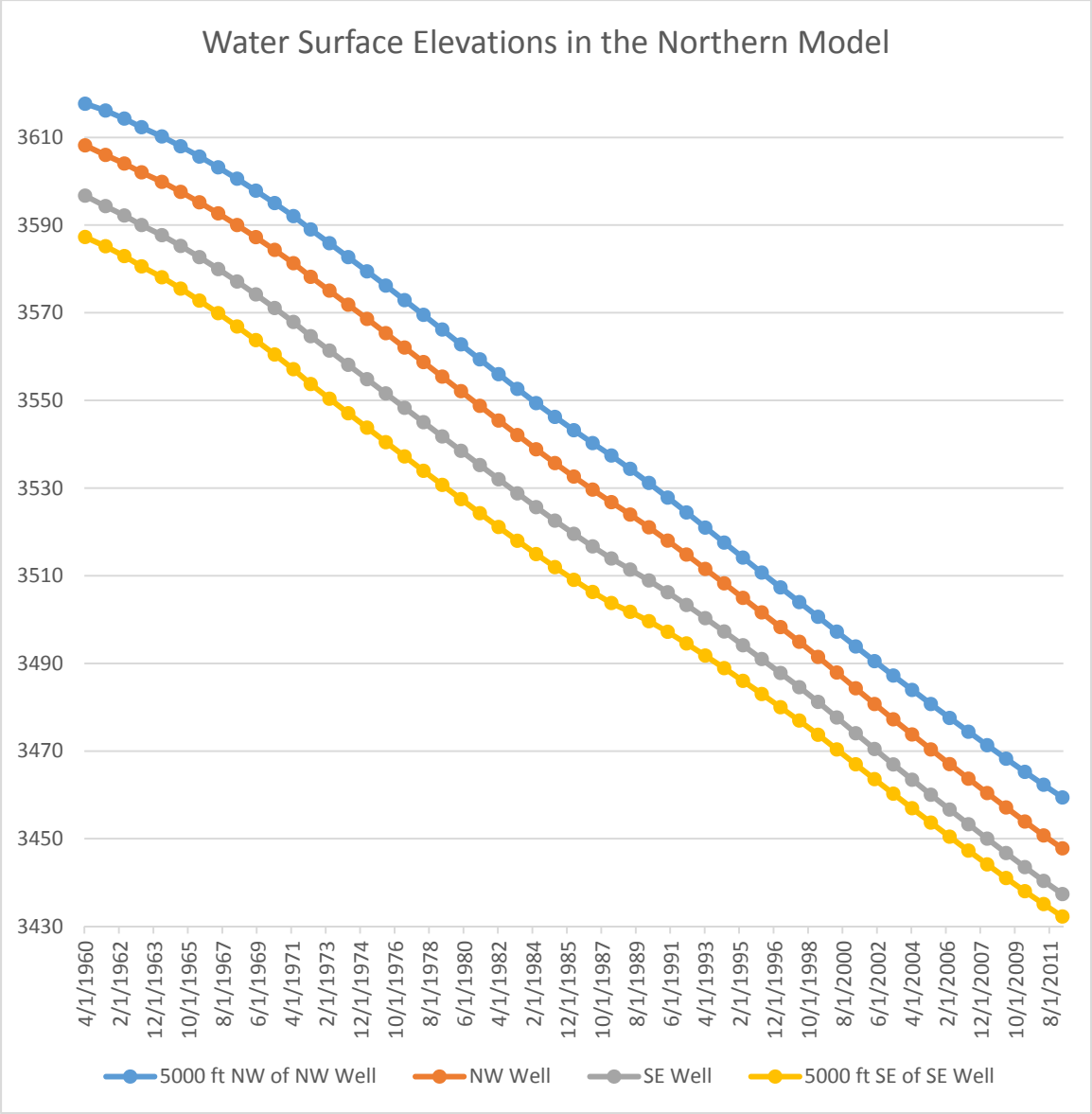

Figure 4.37. Plot of annual water-surface elevations in the Northern model from 1960-2011. Only four wells were pumped to simulate long range water-surface elevations from the wells.

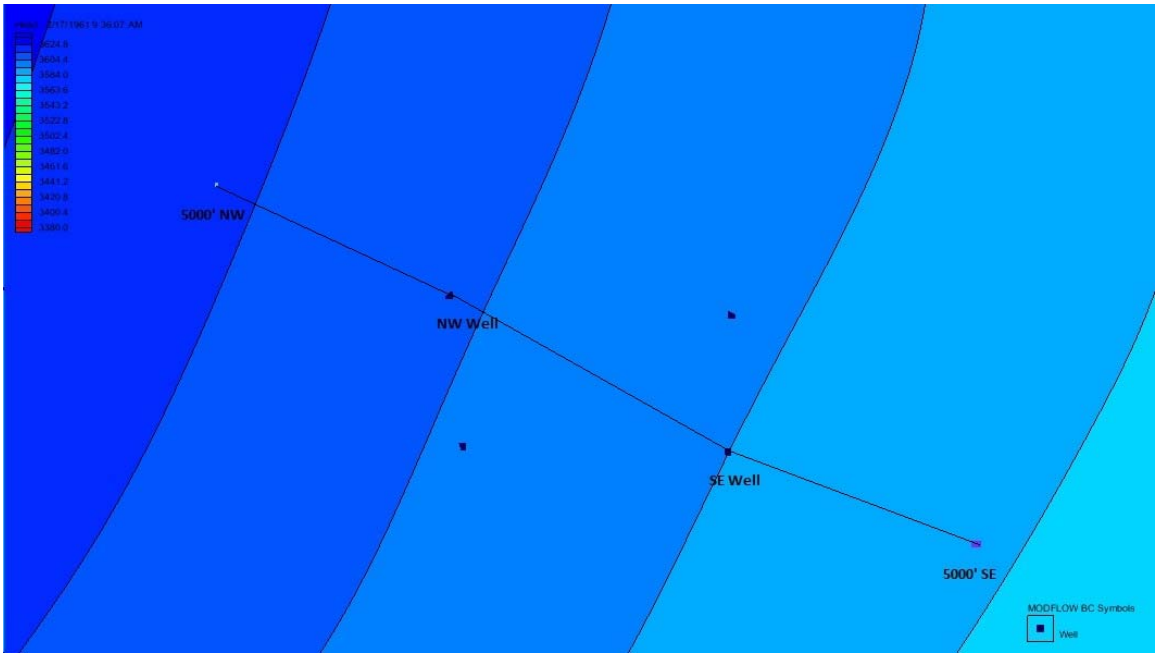

Figure 4.38. Locations of wells and cells used to generate the water-surface elevation plot in the Northern model.

resolution nearest the well. The refinement may help improve the cones near the well. A sensitivity analysis was performed to make this determination. But the fact that this is still a single layer model does not allow enough resolution in the vertical direction. At this time sufficient knowledge of the vertical heterogeneity does not allow for accurate layering of the model. The wells in a given Groundwater District were not all completed at the same time. Water-surfaces have been shown to rebound at a rate slower than previously modeled. For these reasons additional layering may provide a more accurate representation. Additionally, since the nodes used to calculate flows between the cells are centrally located within the cells, this allows for eventual situations where water-surface elevations will be below the nodes. Additional layers would provide a better

understanding in those cells located near the wells which experience substantial changes in saturated thickness during simulations.

Increased layers would present the problem of cells going dry in upper layers. This issue can be resolved by allowing cells to rewet as the cone of depression rebounds. However, efforts to transition this single layer to a multilayer model and allow for rewetting of dry cells failed. As layers were added to the original GAM, upper layers would be pumped dry and mask results in lower layers. Efforts to allow rewetting of cells caused instability during the model run and convergence to a solution was never achieved. Additional iterations and relaxation of acceptance values within the software did not result in convergence of the model. This effort was stopped since no progress was observed and the concern that if the model did successfully run the results would be questionable.

Results shown in this work support the assertion by Ouapo, et al. (2014), who proposed that mounds of water were present to explain the differences between the AWMBA and the WMA. The conceptual model demonstrates that measurement of the water-surface elevations and extrapolating those measurements between wells clearly omits water in these mounds. Local models from both the northern and southern GAM have been shown to support the existence of water mounded between wells. Further, data from the GAMs indicated that the wells do not have sufficient time to achieve a static state before water-surface elevation measurements are made. Measurement of the saturated thickness in the northern model and a visible cone of depression about a well in the southern model provide support that these mounds do exist.

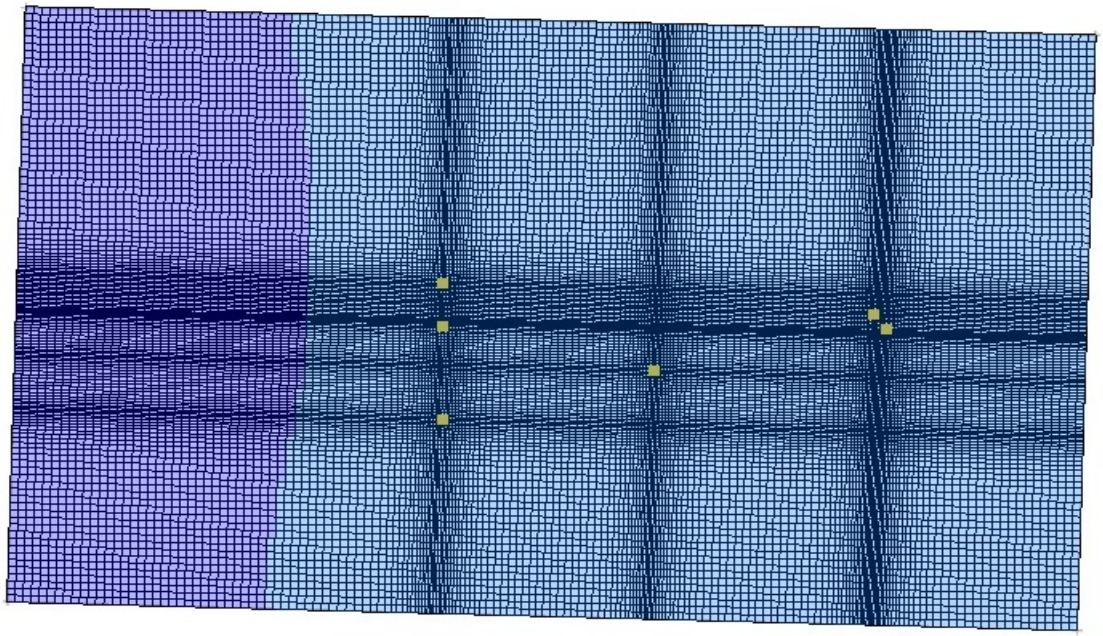

Figure 4.39. Southern model showing increased spatial resolution in the vicinity of the wells.

The model work provided indicates that mounded water can be shown in both the northern and southern models. The mounded water appears to be more abundant in the southern model. The possibility of mounded water in the northern modeled area was presented. In both model areas, the mounds were present when water-surface elevations could be analyzed at some distance from other wells. This leads to the possibility that mounded water may be mostly concentrated in undeveloped areas in the Texas Panhandle.

Chapter V

DISCUSSION

When wells are pumped, a distinct cone of depression will form about the well. As wells continue to be pumped, the cones become more pronounced as the water within the zone of influence is removed. The water adjacent to the well is the first to be removed resulting in a very deep depression at the well head and becoming less pronounced the farther removed from the center of the well. The same phenomenon is portrayed in the model with the cell containing the well having the deepest depression and adjacent cells progressively less so. The depth of the cone decreases as the distance from the well increases as illustrated in Figure 4.6. The well output must be met by water moving through the aquifer at the same rate at which it is removed. In other words, water flow out of the well must equal water flow into the well through the porous media. This implies that for a given flow rate as the saturated thickness decreases velocity through the cells must increase. However, as the distance from the well increases, the rate of flow will not increase in a linear manner. The sides of the cones are curvilinear as they develop. Additionally, as the distance from the central cylinder increases, the depth of the saturated thickness also increases. According to the conservation of mass, the rate of flow through a porous medium will decrease as the thickness of the saturated zone increases. As water moves to fill the central cylinder, the rate of flow through the media

will be at a maximum since this is the area of deepest depression. The rate of flow decreases progressively outward as the surface area of the cylindrical area increases. Also, as the distance from the well increases, the volume of water from which to draw increases. The net result is a cone of depression. Referring to Figure 4.6, after pumping is stopped, the cells with the deepest drawdown will fill first followed by the cells within the next ring and so on. The rates at which the "rings" fill will decrease as the radius from the well increases.

The rate at which the cones of depression would rebound to a water table surface was not known. The assumption was made that wells would need to be pumped a few cycles before an observable and persistent cone of depression would be seen. This was expected because when a well is first drilled it will withdraw the water in adjacent cells first. Small cones of depression would form but would be filled prior to initiation of the next pumping cycle. The recovery process of the water-surface elevation was supported as expected by the model output due to the availability of water during early pumping cycles. In order to confidently report mounded water it was believed that a cone of depression remaining after a complete rebound cycle passed would show that a new water-surface table condition had not been re-established. This would indicate there was insufficient water available to totally fulfill the potential formed in the cone of depression. This leads directly to the implication of mounded water between cells.

Two means of observing the presence of a cone of depression about a well have been presented in this work. When a cone of depression persists through an entire well

rebound period, the saturated thickness between wells will be greater than at the wells. This is the expected mounded water proposed by Ouapo et al. (2014), who suggested an alternative method to estimate the amount of groundwater remaining in the Ogallala aquifer, i.e. the Agronomic Water Mass Balance Approach (AWMBA). The AWMBA used the irrigated crop acreages from the USDA National Agricultural Statistics Service and estimates of the water applied to specific crops to calculate the amount of water withdrawn from the aquifer. When compared to the Well Measurement Approach (WMA), the method commonly used to collect water-surface elevation data, differences were noted between the two methods. Specifically, the AWMBA suggested more water was available than the current groundwater availability model (GAM) indicates. This led to the concept that there must be water remaining in the aquifer that is unaccounted for in the WMA method. The idea that water could be mounded between wells after pumping would account for the additional water. If such mounds were present, then the WMA approach would underestimate the water remaining. The method uses water-surface elevation measurements typically taken in January under the presumption that most of the well rebound has occurred. The water elevations are then extrapolated using tensioned splines applied to measurements made in other wells to develop what is believed to be the current water table. In essence, this method provides a means to look "through" a mound, thus ignoring the water above the "line of sight" between well level measurements. Illustratively this would be looking through a tunnel and dismissing the mountain above it.

The approach undertaken in this work was to use the results from the GAM to determine whether it would be possible to observe the hypothesized mounds of water between pumping wells. Confirmation of this would be the observed persistence of a cone of depression encompassing a well after a full rebound cycle passed, or the indication that an observable head difference between the model cell containing the well and cells located between wells could be noted after a full rebound cycle. This was shown in Figure 4.7. Knowing that the WMA uses measurements of water-surface elevations typically made in January, the focus was placed on time periods after that month. Generally irrigation for corn production begins in May and lasts until the end of August. Using those two months as guides, the time periods of most interest were March and April just prior to the start of the next irrigation cycle. Observations were made in search of a cone of depression that could be observed after allowing for the maximum possible rebound time after pumping. A second criteria used was that the depression would be observable at a later date than when well measurements would be made for the WMA. Meeting these conditions would show that the cones persist and, consequently, the mounds of water between wells would be present.

The two-well model was a very simple conceptual approach used to learn what the software would be capable of producing. Hypothetical model parameters were entered to see if the images produced indicated a cone of depression could be seen. Figures 4.1 and 4.2a show that the software was capable of producing very good results and images of the output. Cones of depression were clearly visible in both the top and profile views. This model output was accomplished with a low pump rate and only one pumping cycle.

Figure 4.2b clearly indicates the water which would be unaccounted for should water-surface elevations be taken.

The northern model presented here did not produce cones of depression in the graphic output as seen in the southern model. Figure 5.1 shows the clear formation of a persistent cone of depression in the southern model. For this reason a high resolution contour was applied and observations were made near one well in the northern model. Results are shown in Figures 5.2 and 5.3. The upper layer is the original water-surface elevation for comparison. Figure 5.2 shows a relatively flat water-surface after a rebound period. The cell containing the well is highlighted. A decrease in the overall head of the aquifer is indicated by the white gap appearing between the upper and lower layers. Figure 5.3 shows the same well after several pumping cycles. Adjustments were made to the contour as needed to follow the decreasing overall head. Slight elevations east and west of the well cell may be present but were not significant enough to conclude the mounds were present. This approach was not pursued since it would require the adjustment of the minimum and maximum head values for each model run for the vicinity near each well.

The alternative approach taken for the northern model was then to select a series of cells, including two wells from west to east across the modeled area. In order to determine whether a possible mound of water persisted after the wells rebounded, several calculations were completed to evaluate the saturated thickness of the aquifer. The plot shown in Figure 4.31 clearly indicates a small mound of water between the wells.

Estimates of the thickness of the mound were applied to an area between four wells. The results indicate that there are an additional 2.28 million gallons or 8.68 ac-ft of water in approximately a one half mile square area. Should this be the case across the entire

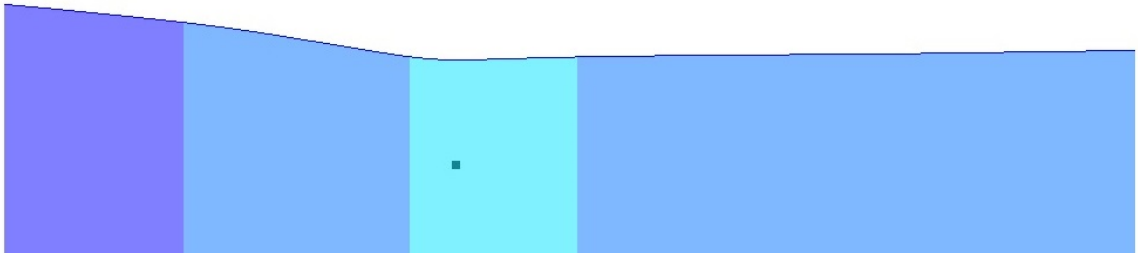

Figure 5.1 Southern model output graphically illustrating the persistent cone of depression after multiple pumping and recovery periods. The decrease zone about the well indicates a depressed head and mounds are noted on either side of the depression.

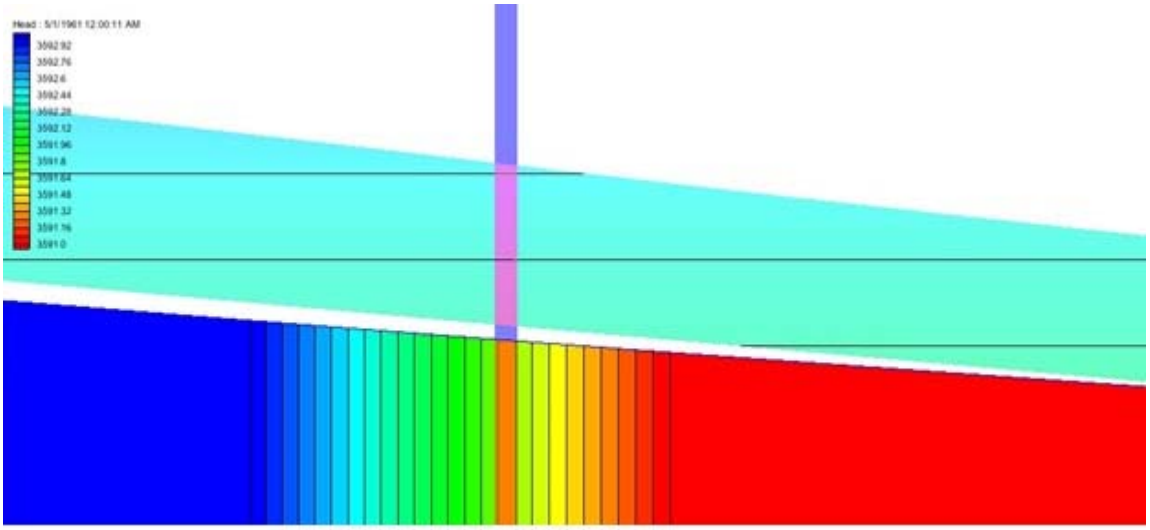

Figure 5.2. High resolution in the northern model area after one pumping cycle. In an effort to visually see the mounded water in the north, this image was generated by narrowing the minimum and maximum head values allowed to generate the color flood image. The upper blue layer is the original starting head for the model. The vertical line rising through the image is the highlighted well cell for reference. No visible cone of depression is seen.

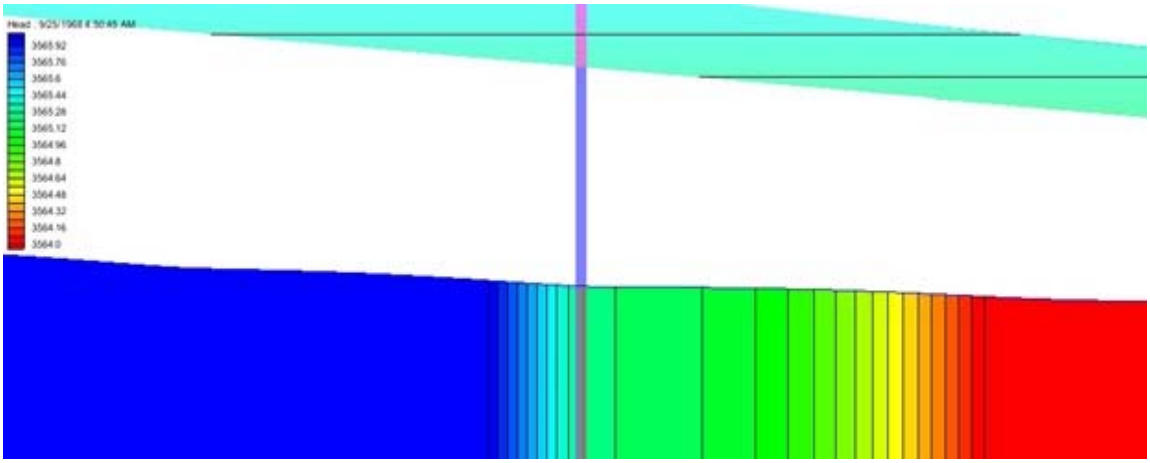

Figure 5.3. High resolution in the northern model after several pumping cycles. The highlighted cell contains the well for reference. After several pumping cycles slight differences in saturated thickness could be noted to the left and right of the well. The upper blue layer is the original starting head of the model for comparison. No clear cone of depression can be seen.

aquifer, it implies that there is slightly more water remaining in this region of the aquifer than previously thought. Table 2.4 shows the North Plains Groundwater Conservation District encompasses 7,324 square miles. If there were 4 wells per square mile, or one well per quarter section resulting in a district wide grid similar to those presented here, there would be an additional 254,300 ac-ft of water available across the northern region. This would not be a significant quantity of water across the district. The NPGCD reports there are approximately one-million irrigated acres within the district. The entire district covers approximately 4.69 million acres (NPGCD, 2016). Using the data in Figure 4.37, there could be a substantial amount of water remaining in rangeland and undeveloped areas of the district. 3.69 million acres are undeveloped and contain up to 2.4 feet of available water, the result would indicate there could be an additional 8.9 million ac-ft of

water in the NPGCD above the WMA estimate. Current water use in the NPGCD is reported to be just under 1.4 million acre-feet (Hallmark, 2016). This would supply an additional 6 years of irrigation district wide at the current rate of application.

Gutentag (1984) proposed a 1 foot per day rate of horizontal movement from west to east under essentially pre-developed aquifer conditions. Figure 5.4 illustrates the pre-pumped aquifer with well cells marked on the east and west sides. The central mark indicates the approximate midpoint between the wells. The distance from the midpoint is approximately 1,360 feet to either well. At a rate of movement of 1 foot per day it would take water 1,360 days, or 3.7 years to move from the midpoint to the well location on the right. As wells are pumped and the gradient is increased, the rate of movement through the aquifer will increase. The well rebound plot in Figure 4.13a illustrates this. The majority of well rebound is realized within days of the pump being stopped. As the gradient declines, the rate of water movement will slow which will decrease the rate of rebound. Figure 5.5 illustrates the effects of pumping on the aquifer. The cells highlighted are the same as those in Figure 5.4. At the midpoint, the rate of horizontal groundwater movement may be essentially unaffected. It is evident that as you approach the depression in water-surface elevations in the well cells that the change in head is much greater. As the potential for water movement increases, the rate of horizontal water movement should also increase. The increased rate of flow through a reduced cross sectional area is explained by the conservation of mass.

Figure 5.6 is an illustration of the flow in a water table aquifer after a pumping cycle and cones of depression are present. On the left side of the figure the saturated flow region is shown as h_1 feet thick and on the right side the same saturated flow region is shown as h_2 feet thick. This difference in saturated flow thickness is $h_1 - h_2$. Referring to the Chapter 2 discussion of Darcy's Law, for flow to be maintained through a reduced cross sectional area, the velocity must increase. The conclusion is that flow of water through an unconfined aquifer is not constant under pumping conditions. As the water moves to fill the cone of depression and the saturated thickness at h_1 approaches the thickness at h_2, the flow velocity will decrease. This will result in a prolonged period of rebound in the region closest to the well.

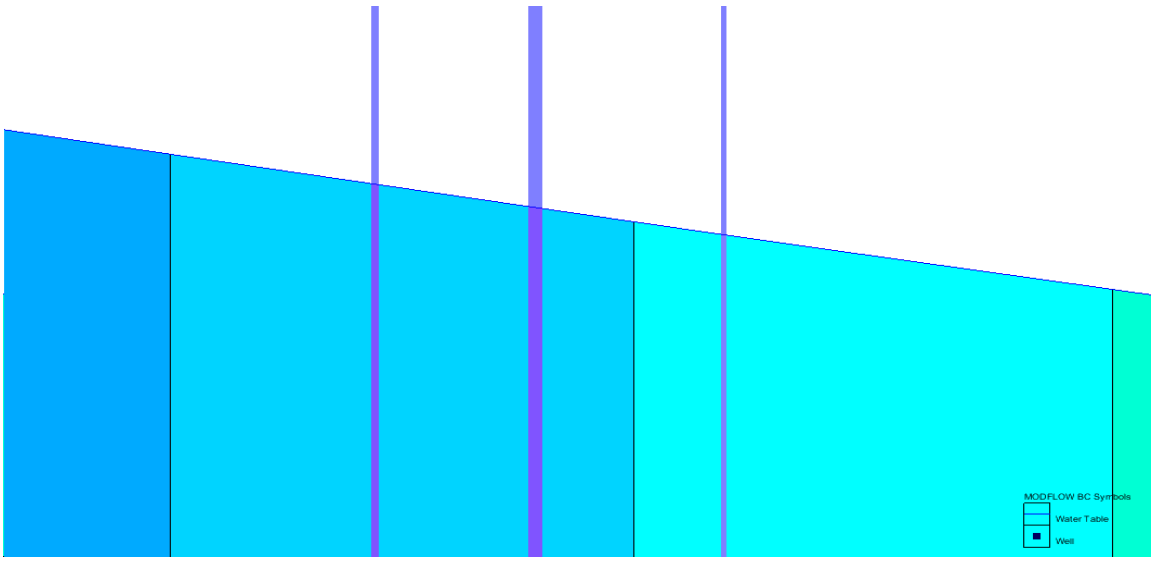

Figure 5.4. Northern model area. Pre-pump water table conditions with slope of water-surface elevation shown. Cells on the right and left are well locations with the approximate center cell shown.

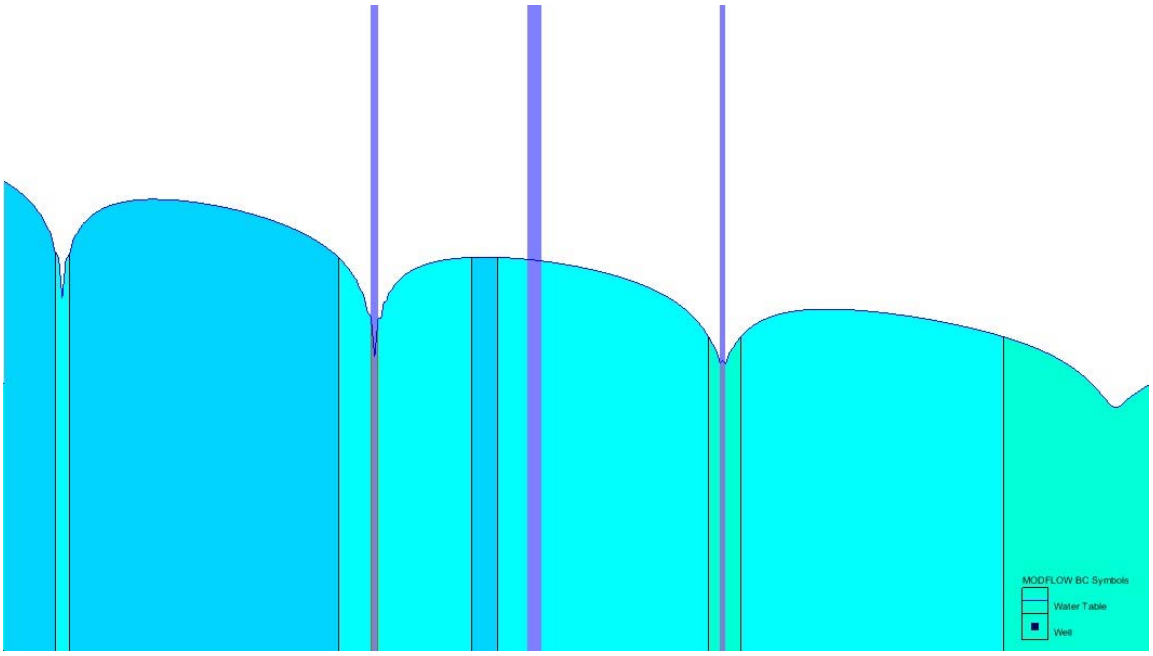

Figure 5.5. Northern model area. Due to drawdown about the wells, flow rates higher than proposed by Gutentag (1984) would be anticipated.

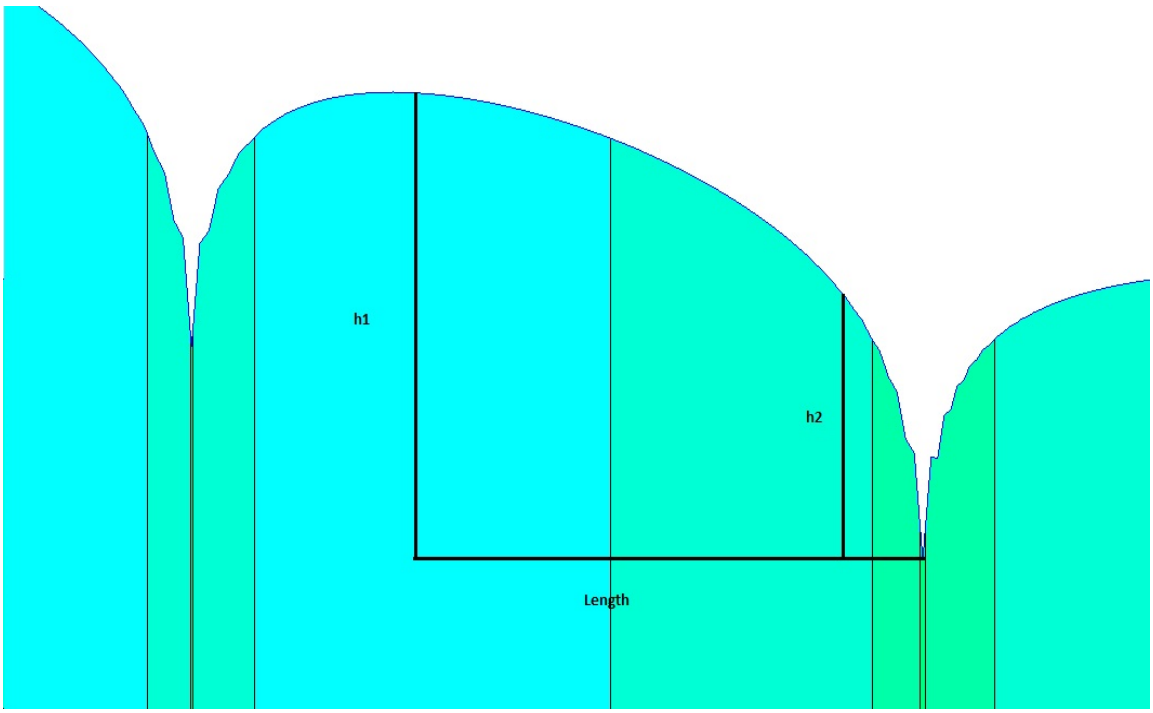

Figure 5.6. Illustration of the Dupuit-Forchheimer flow assumptions. The flow across h_1 will be slower than the flow across h_2. Water flow will be from left to right towards the left cone of depression. As the water moves there is a decreasing saturated thickness through which flow will occur.

The increased rate of movement is shown in Figure 4.13a where the majority of the rebound occurs soon after the pumps stop. Figure 4.14 shows that the rate of rebound is not constant and that a new static water-surface elevation may not be achieved for several years after pumping ceases. The rate of horizontal movement slows and begins to approach that rate proposed by Gutentag. This supports the theory intrinsic with application of the AWMBA method that mounds of water exist in regions of the aquifer. The WMA approach does not allow adequate rebound time of the wells to accurately determine the remaining water in the aquifer. Further, this also explains rebound observed in wells that have not been pumped for several years. The slow, gradual approach towards a new surface elevation equilibrium may take many years.

Figure 5.7 is a series of plots between pumping cycles taken from the model image shown in Figure 4.28. Each curve represents a different time period. Pumping was stopped on 9/1/1980. The wells are located at point NW and NE and are about 2750 feet apart. The NW well has both a higher ground-surface elevation and water-surface elevation since it is the western most well and the slope of the aquifer declines west to east. As can be seen from the plots, the lowest curve in the series is just after pumping is stopped. The series then progresses chronologically up, with each curve from bottom to top representing a date further from pump shutdown. The plot for 9/25/1980 indicates a mound of water is present between the wells. The mound remains visible to the plot on 4/6/1981 which is the last data set prior to the pump starting again on 5/1/1981. Of note is that there are three curves occurring later and above the curve dates 1/24/1981. This

would be about the time the water-surface elevations could appropriately be taken for the WMA. This is construed as evidence that rebound continues to occur which most reasonably can be attributed to mounds of water occurring between the wells.

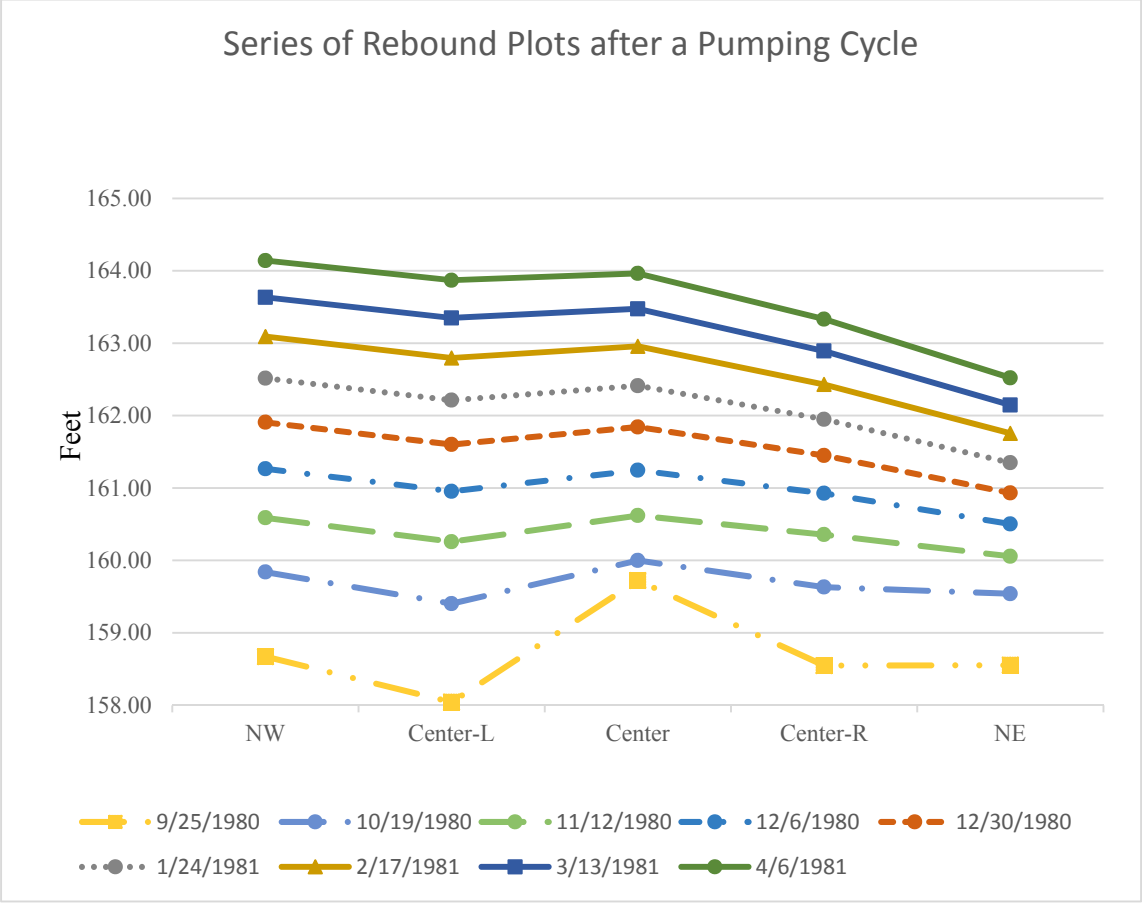

Figure 5.7. Series of rebound curves for the northern model between pumping cycles. The wells are approximately 2750 feet apart. The Center point is equidistant from the wells. Points Center-L and Center-R are equidistant from the wells and the Center points.

The southern model more dramatically demonstrates visually the presence of mounds of water between wells as shown in Figure 4.34. This image clearly shows the presence of an area of decrease saturated thickness about the well. There is a substantial mound to the west and evidence of increase saturated thickness to the east. The cone of depression

appears to be shifted east and the well is not centered in the cone. The slope of the bottom of the aquifer and the resultant slope of the saturated thickness declines from west to east. The observed offset cone falls in line with what would be anticipated. Considering the west is up gradient from the well, a greater potential exists for the water to move from west to fill the cone of depression.

An attempt to monitor the difference in saturated thickness as done with the northern model was tried for the southern model. Figure 5.8 is a plot of the aquifer red bed and the water-surface elevation taken from the model. The water-surface elevation remained fairly steady across the area while the red bed layer shows some decline from west to east. The saturated thickness is determined by taking the difference between the water-surface elevation and the red bed layer. However, with a declining red bed, there will be an increasing saturated thickness across the area. This prevented generating recovery plots similar to those for the northern model.

A plot was developed of the rebound of the southern model and is shown in Figure 5.9. The results are similar to the plots for the northern model showing the gradual increase in water-surface elevation until the next pumping cycle begins. Assuming the WMA well measurements were taken in January, the rebound continues well beyond this time period.

The HPUWCD reports there are approximately 2.2 million irrigated acres within the district (HPUWCD 2015). The entire district covers approximately 7.6 million acres. Using the data in Figure 4.35, there could be a substantial amount of water remaining in

rangeland and non-irrigated areas of the district. If 5.4 million acres are undeveloped and contain up to 5 feet of available water, the result would indicated there could be an additional 27 million ac-ft of water in the HPUWCD above the WMA estimates. Assuming the rate of use is similar to that in the NPGCD, there would be 3.08 million acre-feet of water used for irrigation annually. At this application rate the aquifer could supply an additional 8.8 years of irrigation district wide. The obvious problem would be harvesting the water from where it resides and using it where it would be needed. The areas where the water resides could be developed and water pumped to those areas more suited to agricultural production. Also, surface improvements may allow for some of the undeveloped land to become irrigable.

The Texas Water Development Board reported that irrigated acreage reached a peak in the 39 counties that overlie the Ogallala in 1974. There were 5.98 million acres being irrigated. As of 2000 only 4.6 million acres were being reported as irrigated acres (TWDB 2001). The combined irrigated acreage in the NPGCD and the HPUWCD were reported to be 3.2 million acres in 2015. This is a decrease of 2.78 million acres that were irrigated at the peak in 1974. Efforts to improve the estimated additional water in storage were made based upon these numbers. Combined, there are 12.29 million acres in the northern and southern GAM areas in the Texas Panhandle. From the peak irrigated acreage in 1974 there would be 6.31 million acres of undeveloped or non-irrigated crop land. Since the data is combined form the northern and southern areas, the additional water remaining in storage was determined by using a weighted average. 60 percent of the area is made up of the southern GAM and 40 percent is in the northern GAM. Using

the 5 ac-ft of additional estimated water in the southern area and 2.4 ac-ft in the northern area an estimated 3.96 ac-ft of additional water would be available. This results in an estimated 25 million ac-ft of additional water available in storage that remained unaccounted.

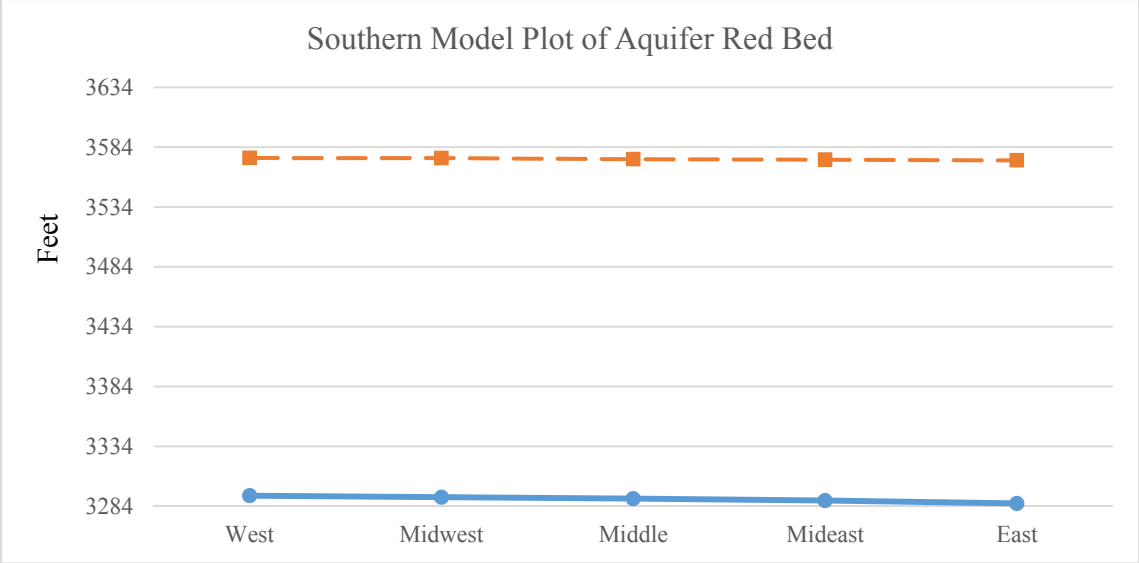

Figure 5.8. Plot of southern aquifer red bed. The upper line is the water-surface elevation. The lower line is the red bed plot. The water-surface elevation remains relatively constant while the elevation of the red bed shows some decline from west to east.

Boundary conditions are critical in model development. Boundaries control the influx and efflux from the model area. These models were developed with a changing head boundary to allow for the water to flow either into or out of the control volume.

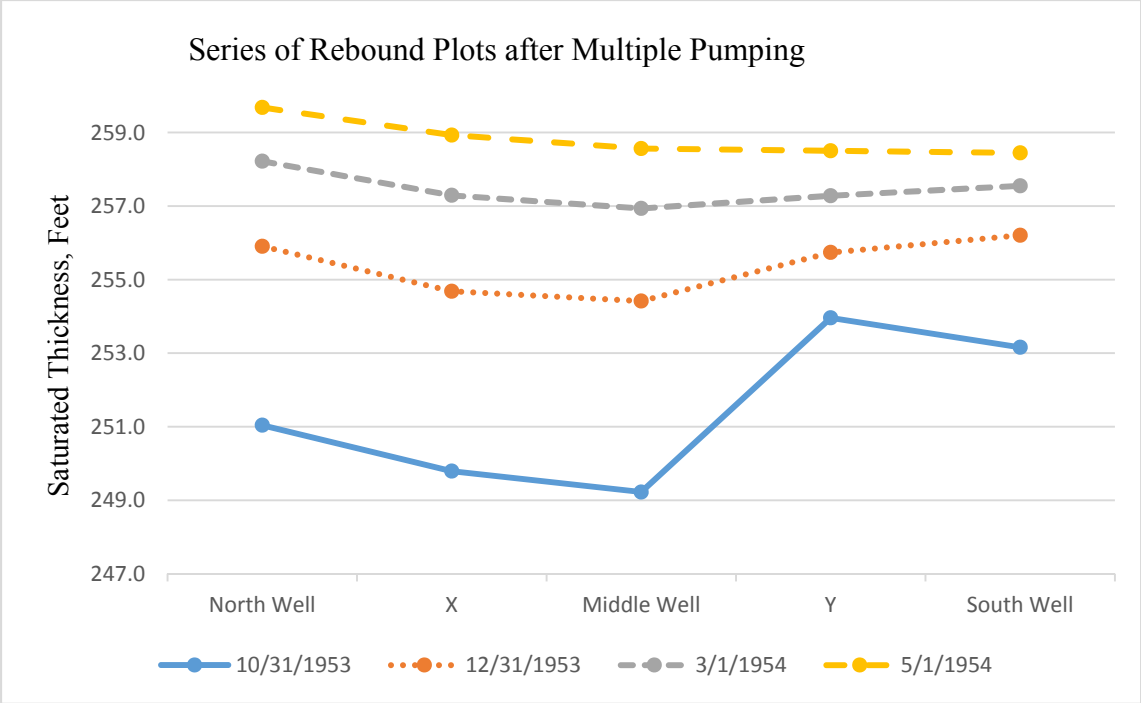

Figure 5.9. Series of rebound curves in the southern model between pumping cycles. Three wells are included. This represents a recovery plot after 23 pumping cycles. Curvature of the plots indicate a zone of depression which would be indicative of the individual cones merging together over time. The elevated levels at point "Y" could be due to a calculation error in the model.

Dutton (2001) proposed that the Ogallala could be modeled as a single layer model by averaging the hydraulic properties across an area. In the same report the author also noted that there is lateral and vertical heterogeneity due to the depositional framework of the Ogallala. The heterogeneity controls properties such as hydraulic conductivity and specific yield. The model assumes the hydraulic conductivity is isotropic in the x and y directions within the cells. Conductivity of the aquifer will vary based upon the type of deposits in the layers. This would result in heterogeneous horizontal flow of water through the model cells. The conductivity of a lower layer could be higher than that of a higher layer. The result could be that the lower layer provides more water to the well

over time. This sets up a situation where the Dupuit-Forchheimer assumptions may not be applicable. Though originally developed for application to shallow aquifers assuming horizontal flow, the assumptions may be used except where the steepness of the gradient is greatest. For the Ogallala the original saturated thickness is well over 100 feet across the Texas Panhandle with some exceptions. As wells are pumped and the cone of depression develops the cells containing the sharp decline in water-surface elevations are violating the assumption of horizontal flow. The finite difference method uses horizontal flow so those cells containing a steep gradient may be contributing to error in the model. Incorporating multiple layers, particularly layers developed based upon the type of stationary media, may provide additional details and support for application of the AWMBA method.

Well pumping rates were based upon the original driller logs reviewed for this study. Since the accuracy of some of the logs may be questionable, the pumping rate was set between 10-20 percent below the rates reported. This resulted in all wells modeled being pumped at 800 gpm. The decision was made to set all the rates the same so the general influence of each well would be constant. The pumping rates were also left constant through all model iterations. The wells were not set to decline in production over time even though wells in aquifers that do not have recharge generally will. This well pumping rate was considered a bounding extreme condition. Actual pumping rates and aquifer response would be less extreme under normal conditions.

Based upon the results obtained through this modeling effort, there is evidence that there are residual mounds of water that will persist. The majority of the mounded water is located in regions that are undeveloped or non-irrigated. Mounds may exist between wells where there is large well spacing. Where the well spacing is concentrated, mounding may not exist. This supports the proposed AWMBA approach as an alternate means of quantifying the remaining groundwater in the aquifer. This also supports the need to model the Ogallala as a multilayer model so that a more detailed analysis can be conducted. Because flow is not constant during well rebound a multi-layer approach would improve the resolution near the wells. This will allow the model cells to more closely follow the conservation of mass and reduce the problem of non-horizontal flow in the cones of depression. Also, this would provide the analysis of the conductivity based upon the horizontal layers of deposition. This would move away from assuming the entire saturated thickness behaves isotropically. The conductivity of layers is not the same throughout the entire saturated thickness which introduces further error into the models. Following the WMA approach does appear to underestimate the remaining water in storage.

A sensitivity analysis of the northern and southern models was conducted. In both models, when the hydraulic conductivity of the model was doubled, the drawdown surrounding the wells was reduced. This means the water flux to the wells was greater and mounds were not as likely to be seen. When the conductivity was reduced, the cones of depression became more pronounced since there was a decline in the flow rate of water to the well. Altering the specific yield of the northern and southern models shows

a more pronounced cone of depression and, consequently, a more pronounced mounding effect. This was due to the removal of more water from storage meaning more water levels were lower leading to a slower rebound. As the specific yield was reduced, the opposite effect was seen.

Figures 5.10 and 5.11 show the effects of altering the hydraulic conductivity and specific yield in the northern model. In Figure 5.10 the hydraulic conductivity was doubled for the simulation. This increased the rate of flow of water to the wells thereby reducing the development of the cone of depression and the corresponding mounds. Figure 5.11 shows the effects of increasing the specific yield by fifty percent. This allows more water to be removed from storage which causes rebound to slow resulting in the formation of cones and mounds.

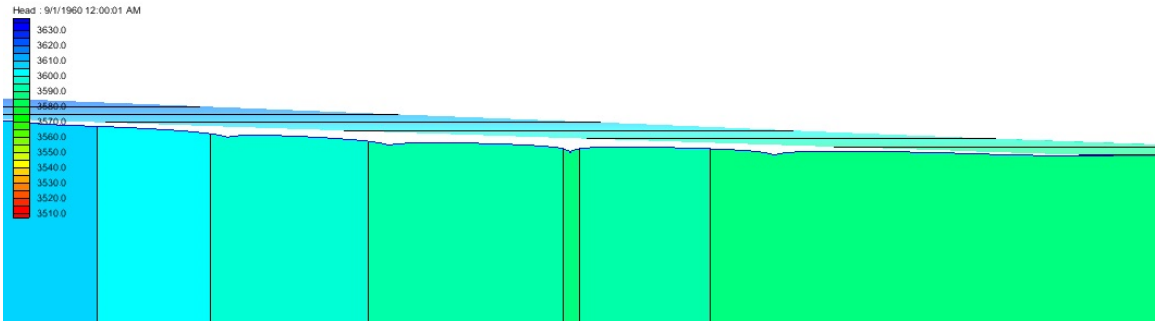

Figure 5.10. Sensitivity analysis of the northern model. Hydraulic conductivity was doubled which allows for greater water flow rates throughout the model. Original values were 23-54.5 ft/day which were increased to 43-109 ft/day. Diminished cones of depression and mounding is observed.

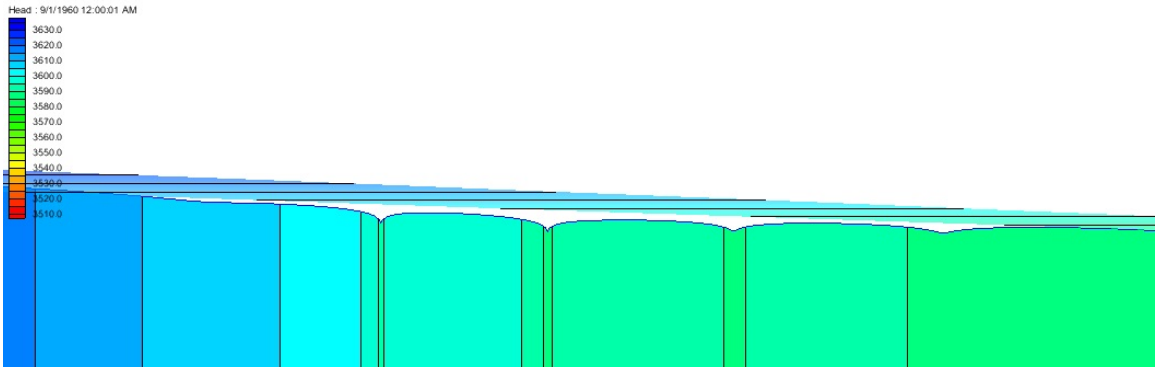

Figure 5.11. Sensitivity analysis of the northern model. Specific yield was increased by fifty percent allowing more water removal from storage within the model cells. Original specific yield was 0.2 which was increased to 0.3. More pronounced cones of depression and evidence of mounding is observed than when hydraulic conductivity was increased.

Figures 5.12 and 5.13 show the effects of altering the hydraulic conductivity and specific yield in the soutehrn model. In Figure 5.12 the hydraulic conductivity was doubled for the simulation. This increased the rate of flow of water to the wells thereby reducing the development of the cone of depression and the corresponding mounds. Figure 5.13 shows the effects of increasing the specific yield by fifty percent. This allows more water to be removed from storage which causes rebound to slow resulting in the formation of cones and mounds.

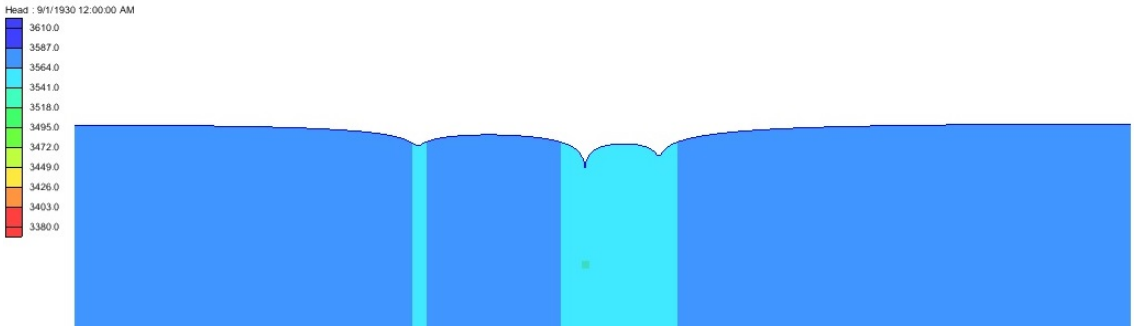

Figure 5.12. Sensitivity analysis of the southern model. Hydraulic conductivity was doubled which allows for greater water flow rates throughout the model. Original values were 4-67 ft/day which were increased to 8-134 ft/day. Diminished cones of depression and mounding is observed.

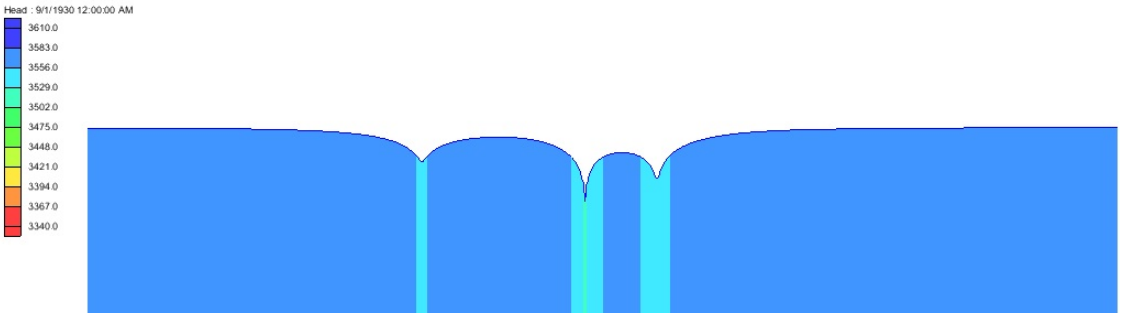

Figure 5.13. Sensitivity analysis of the southern model. Specific yield was increased by fifty percent allowing more water removal from storage within the model cells. Original specific yield was 0.2 which was increased to 0.3. More pronounced cones of depression and evidence of mounding is observed than when hydraulic conductivity was increased.

Figure 5.14 illustrates the cone of depression and the mounds of water just after a pump is stopped. dh_0 represents the water-surface elevation that would be achieved provided the well was allowed to rebound completely. dh_1 represents the height of the mound above the expected water-surface elevation. The radius r_0 represents the radius of the cone of depression which would be filled once a new water table was established. The radius r_1 would represent the radius of water in the mound needed to flow into the cone to establish the new water table level.

The volume of the cone could be determined with the following equation:

$$V = \pi r_0 \int r_0 \, dh_0 \qquad 5.1$$

where:

V is the volume of the cone of depression about the well

r_0 is the radius at which a new water-surface elevation would be established

dh_0 is the difference is elevation from the bottom of the cone to the new water-surface elevation

The volume of water in the mound required to fill the cone of depression could be determined by the equation:

$$V = \pi r_1 \int (r_1 - r_0) \, dh_1 \qquad 5.2$$

where:

V is the volume of the water in the mound which will fill the cone of depression

r_1 is the radius of the mound

r_0 is the radius of the cone of depression

dh_1 is the height of the mounded water

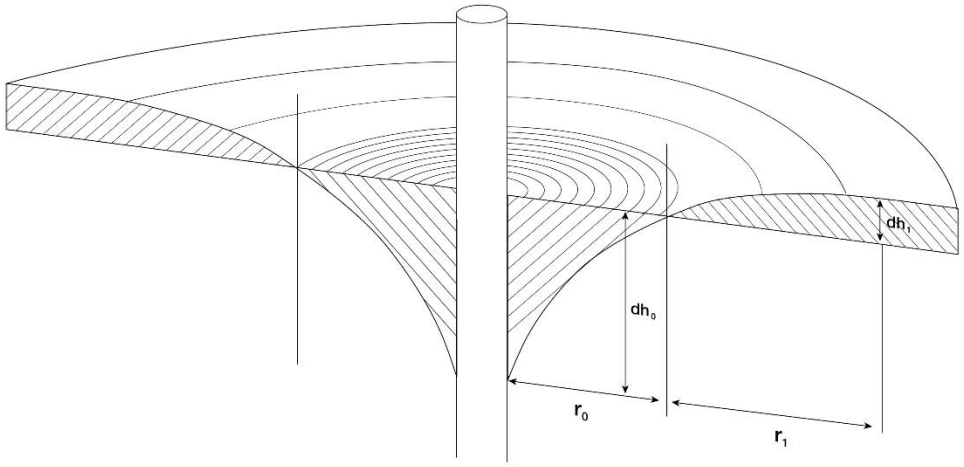

Figure 5.14. Illustration of the cone of depression and the resultant mounds of water about the well. The water will move from the mound into the cone of depression to achieve a new water-surface elevation.

Once the new water-surface elevation is established, the volume of cone filled will equal the volume of water from the mound leading to the following:

$$\pi r_1 \int (r_1 - r_0)\, dh_1 = \pi r_0 \int r_0\, dh_0 \qquad 5.3$$

Which upon simplification gives:

$$(r_1^2 - r_0 r_1) \int dh_1 = r_0^2 \int dh_0 \qquad 5.4$$

The solution to the equilibrium equation, 5.4, would provide a means to more accurately estimate the water available in storage.

The AWMBA illustrates a discrepancy between the volumes of water removed versus the volume of water remaining when compared to the WMA. The existence of mounded water between pumped wells or in undeveloped and non-irrigated areas is a solid explanation for this difference. Further, these modeling efforts indicate water-surface elevations are dynamic for an extended period of time. These could reasonably be extrapolated through the use of Equation 5.4 which would improve the overall modeling effort and provide for an improved model output by accounting for the water that lies within the mounded water within the aquifer.

Analysis of both the northern and southern models developed for this study indicates that there are mounds of water present in the aquifer. The mounds between the wells may be inconsequential. However, the mounds shown to exist in rangeland and non-irrigated land could provide a substantial amount of water for the future. Improved quantitation methods could provide a means for assessing the mounds without excessive additional efforts. These could then be incorporated into a model to improve the overall model output.

Chapter VI

CONCLUSIONS

The need for more accurate measurements of the water remaining in the saturated thickness of the Ogallala is critical, not just in the Texas Panhandle but across the entire area supported by the aquifer. Irrigated agriculture in this area depends upon water withdrawn primarily from the Ogallala aquifer. Long-term agricultural production using irrigation and the regional economic impacts of that production may be in jeopardy. The serious decline of the aquifer, particularly in the southern Texas Panhandle, is well established (McGuire 2014). Because of the number of wells withdrawing water from within the northern and southern portions of the aquifer, availability models make obtaining accurate measures of the remaining water going forward vital.

Based upon the work presented in this modeling effort, the concept that under some circumstances mounds of water develop between pumping wells and will persist through pumping cycles can effectively be argued. Evidence shows that the water surface elevations do not return to a steady state before well water level measurements used for the WMA are collected. Given more time between pumping it is likely that additional rebound of the wells will occur. The work reported herein provides a conceptual model to support the theory proposed by Ouapo et al (2014), as a result of their AWMBA

calculations that mounded water does exist between wells. Continued model improvement going forward would improve the accuracy of the groundwater availability estimates.

The WMA is an easy method for monitoring the rough drawdown of the water levels in the aquifer. This process, though, may substantially underestimate the amount of water remaining in the aquifer. The small regional models presented in this work do support concepts gleaned from application of the AWMBA approach and the supposition that there is additional water as yet not inventoried. The WMA also depends upon the presence of wells to obtain data. In undeveloped rangeland there may not be wells with which to measure the water-surface elevations. Non-irrigated farmland may also lack wells for data collection. As shown in this study there may be substantial mounding in those areas. The southern area appears to have more potential for mounded water than the northern model.

The exclusion of recharge to the aquifer was justified due to the normal rates of evapotranspiration and the rate of water ingress during a rainfall event, but given the evidence provided here, the recharge would not likely explain the estimated water available, even in small mounds. It is generally assumed that any significant recharge attributed to rainfall would be in areas such as lakes and streams or deep sand soils where the water is concentrated and has some residence time. It should be noted that recharge will not occur in these areas unless there is adequate potential for recharge.

Application restrictions by groundwater conservation districts will alleviate some concern that additional water in the aquifer will cause increased pumping. On the contrary, the imposed restrictions coupled with more available water will extend the life of the aquifer for some time. As shown in the limited simulations presented there is potentially enough water to maintain current application rates for several years beyond the projected economic life span of the aquifer.

Going forward, there are many steps to be taken to advance this conceptual model. First, the need for actual field data to support this conclusion needs to be gathered. This would require, at a minimum, several monitoring well installations and careful water surface measurements over time. Additional monitoring efforts could confirm the amounts of mounded water shown in these models. When considering the large areas of undeveloped land and non-irrigated areas within the two districts, there could be as much as 36 million ac-ft of additional water available in storage that is not accounted for in the WMA. As much as 5 feet of additional water is available in the southern model and 2.5 feet of additional water is available in the northern model area. Using a more conservative approach and the irrigated acreage in 1974 as a bounding condition, an estimated 25 million ac-ft of water may be unaccounted within the Texas Panhandle.

The second need would be to develop a multilayer model to provide more resolution of the aquifer behavior. The current single layer model does not adequately address the Dupuit-Forchheimer assumptions, particularly when drawdown occurs in the vicinity of wells. Since this single-layer modeling effort assumes horizontal flow, the steepness of

the gradient about pumped wells presents some problems when calculating water flux. Further, the correlation of layers with the various geological formations could be a tedious undertaking, but one which would improve the modeling effort by allowing each layer to behave independently from others. Certain layers will have higher or lower hydraulic conductivity than what is currently allowed in the single layer model. A sensitivity analysis studying the impacts of changing the hydraulic conductivity shows that, in the single layer model, the effects on water withdrawal are not as significant as changing specific yield values. This would also be important to understand the vertical flow component of the aquifer, often considered unimportant. All assumptions are that the primary flow of groundwater is horizontal. However, given the varied layering of the aquifer strata, there is reason to believe some layers will be more conductive than others. Dutton (2004) alludes to the fact that lower layers tend to be composed of more course-grained sediment resulting in higher hydraulic conductivity than in upper layers. A layer with lower conductivity overlying a layer with higher conductivity could have more vertical flow potential than horizontal flow potential.

Based upon the three models investigated in this work, there is adequate evidence to pursue additional work to better quantify the mounded water between wells. The approach undertaken here was not directed at full quantification of the mounds but to study whether or not they likely exist. Two approaches have been provided to show that the mounds are present. Larger mounds of water have been shown to exist in areas of the GCDs that are undeveloped. This water is unaccounted in the current WMA approach. Continued development of the mathematical approach as suggested could improve future

modeling efforts. Combined with improved irrigation techniques and water management, the longevity of the aquifer could be extended by many years beyond current expectations.

REFERENCES

Alley, W. M., T. E. Reilly, and O. L. Franke, 1999, Sustainability of Ground-Water Resources: U. S. Geological Survey Circular 1186, 86 p. http://pubs.usgs.gov/circ/circ1186/index.html Accessed June 21, 2015.

Amosson, S. H., Gurrero, B., Dudensing, R., 2015, The Impact of Agribusiness in the High Plains Trade Area, Amarillo Chamber of Commerce Report, 12p.

Amosson, S. H., Almas, L. K., Bretz, F., Gaskins, D., Guerrero, B., Jones, D., Marek, T. H., New, L., Simpson, H., 2005, Water Management Strategies for Reducing Irrigation Demands in Region A. Report to the Panhandle Water Planning Group, Amarillo, TX, January. http://www.panhandlewater.org [14 June 2015].

Andrews, R., 1984, First Status Report of Regional Groundwater Modeling of the Palo Duro Basin: Houston, Texas, INTERA Environmental Consultants, 252 p.

Barnes, J.R., W. C. Ellis, E.R. Legget, R. A. Scalapino, W. O. George, 1949, Geology and Ground Water in the Irrigated Region of the Southern High Plains of Texas,

progress report No. 7: Texas Board Water Engineers, 106 p.

Beattie, B.R., 1981, Irrigated agriculture and the Great Plains—Problems and management alternatives: Western Journal of Agricultural Economics, v. 6, no. 2, p. 289–299.

Bell, A. E., and S. Morrison, 1979, Analytical study of the Ogallala aquifer in Carson County, Texas, projections of saturated thickness, volume of water in storage, pumpage rates, pumping lifts, and well yields: Texas Department of Water Resources Report 242, 64 p.

Bell, A. E., and S. Morrison, 1981, Analytical study of the Ogallala aquifer in Hartley County, Texas, projections of saturated thickness, volume of water in storage, pumpage rates, pumping lifts, and well yields: Texas Department of Water Resources Report 261, 70 p.

Bennett, Julie. “Re: Permitted Wells in PGCD.” Message to Glen Green. 19 July 2016. E-mail.

Blanford, T. N., Blazer, D. J., Calhoun, K. C., Dutton, A. R., Naing, T., Reedy, R. C., Scanlon, B. R., Groundwater Availability of the Southern Ogallala Aquifer in Texas and New Mexico: Numerical Simulations Through 2050, Report prepared for the Texas Water Development Board, 2003, 69p.

Bossler, J. D., 1984, United States Federal Geodetic Control Committee, Standards and Specifications for Geodetic Control Networks, http://www.ngs.noaa.gov/FGCS/tech_pub/1984-stds-specs-geodetic-control-networks.htm, Accessed August 2016.

Bragg v Edwards Aquifer Authority. Fourth Court of Appeals. 14 Feb. 2002. http://www.search.txcourts.gov/SearchMedia.aspx?MediaVersionID=88cef3c2-8ca6-41f2-9637-eb471dc21b13&MediaID=d5ce49aa-44b2-4042-98fb-faac1ea3cd53&coa=" + this.CurrentWebState.CurrentCourt + @"&DT=Opinion, Accessed December 2016.

Coleman, Jason. "Re: Permitted Wells in District." Message to Glen Green. 6 July 2016. E-mail.

Claborn, B. J., Austin, T. A., and Wells, D. M., 1970, Numerical model of the Ogallala as a management tool, *in* Mattox, R. B., and W. D. Miller, eds., Ogallala Aquifer Symposium: Texas Tech University, International Center for Arid and Semi-Arid Land Studies, Special Report Number 39, p. 89–110.

Deeds, N. E., Jigmond, M., Intera Incorporated, eds., 2015, Final Numerical Model Report for the High Plains Aquifer System Groundwater Availability Model, Prepared for the Texas Water Development Board, 640 p.

Domenico, P. A. and Schwartz, F. W., 1990, Physical and chemical hydrogeology: New York, John Wiley, 824 p.

Dongarra, J., 1995, Iterative Methods, http://www.netlib.org/linalg/html_templates/node9.html, Accessed August 2016.

Dorman, T. M., 1996, The Texas High Plains Aquifer System—modeling and projections for the southern region: Master's Thesis, Civil Engineering Department, Texas Tech University, Lubbock, Texas.

Dutton, A. R., Mace, R. E., and Reedy, R. C., 2001, Quantification of spatially varying hydrogeologic properties for a predictive model of groundwater flow in the Ogallala aquifer, northern Texas Panhandle, *in* Lucas, S. G., and Ulmer-Scholle, D. S., Geology of the Llano Estacado: New Mexico Geological Society Guidebook, 52nd Field Conference, p. 297–307.

Dutton, A. R., and Reedy, R. C., 2000, Comparison of water in storage in the Ogallala aquifer versus projected amounts of withdrawal from 1998 to 2050 in Planning Region A, Letter Report (rev. 1): The University of Texas at Austin, Bureau of Economic Geology, prepared for Panhandle Water Planning Group (PWPG) under contract number UTA99-0230, 15 p.

Dutton, A. R., Reedy, R. C., and Mace, R. E., 2001, Saturated thickness in the Ogallala aquifer in the Panhandle Water Planning Area—Simulation of 2000 through 2050 withdrawal projections: The University of Texas at Austin, Bureau of Economic Geology, topical report prepared for the Region A Panhandle Water Planning Group, Panhandle Regional Planning Commission under Contract number UTA01-462, 130 p.

Dutton, A. R., Adjustment of Parameters to Improve the Calibration of the Og-n Model of the Ogallala Aquifer, Panhandle Water Planning Area: The University of Texas at Austin, Bureau of Economic Geology prepared for Freese and Nichols, Inc. and Panhandle Water Planning Group, June 2004.

Fetter, C. W., 2001, Applied Hydrogeology, 4th Ed. Upper Saddle River, New Jersey, Prentice Hall.

Freese and Nichols, Inc., 2000, Current and projected population and water demand for the region: topical report prepared by Freese and Nichols, Inc., Texas Agricultural Experiment Station, and Texas Agricultural Extension Service for Panhandle Regional Planning Group, Amarillo, Texas, 20 p.

Freeze, R. A. and Cherry, J. A., 1979, Groundwater, Upper Saddle River, New Jersey, Prentice Hall.

Frye, J. C., 1970, The Ogallala Formation-A review, *in* Mattox, R. B., and Miller, W. D., eds., Ogallala aquifer, A symposium: Texas Tech University, Lubbock, 1970,

International Center for Arid and Semi-arid Land Studies Special Re[port no. 39, p. 5-14.

Gilbert, G. K., 1896, The underground water of the Arkansas Valley in eastern Colorado: U. S. Geological Survey 17th Annual Report, pt. 2, p. 551-601.

Gollehon, N. and Winston, B. 2013, Groundwater Irrigation and Water Withdrawals: The Ogallala Aquifer Initiative. *U.S. Geological Service REAP Report.* 2013.

Gutentag, E. D., Heimes, F. J., Krothe, N. C., Luckey, R. R., and Weeks, J. B., 1984, Geohydrology of the High Plains aquifer in parts of Colorado, Kansas, Nebraska, New Mexico, Oklahoma, South Dakota, Texas, and Wyoming: U.S. Geological Survey Professional Paper 1400-B, 57 p.

Guthrie, Janet. "Re: Permitted Wells in District." Message to Glen Green. 16 July 2016. E-mail.

Hallmark, D., 2014, Hydrology and Groundwater Resources 2013-2014, North Plains

Groundwater Conservation District Annual Report, 45 p. http://www.northplainsgcd.org/news/latest-news/88-2013-hydrology-and-groundwater-resources.html

Harbaugh, A.W., 2005, MODFLOW-2005, The U.S. Geological Survey modular ground-water model—the Ground-Water Flow Process: U.S. Geological Survey Techniques and Methods 6-A16, 253 p.

Harbaugh, A. W., Banta, E. R., Hill, M. C., and McDonald, M. G., 2000, MODFLOW-2000, The U. S. Geological Survey Modular Ground-Water Model-User Guide to Modularization Concepts and the Ground-Water Flow Process: U.S. Geological Survey Open-File Report 00-92, 130 p.

Harkins, D., 1998, The future of the Texas High Plains aquifer system—modeling and projections: Texas Tech University, Ph.D. dissertation, 278 p.

Havens, J. S., 1966, Recharge Studies on the High Plains in Northern Lea County, New Mexico: U.S. Geological Survey Water Supply Paper 1819-F, 52 p.

High Plains Underground Water Conservation District No. 1 (HPUWCD), 2005. Ogallala Aquifer. http://hpwd.com/aquifers/ogallala-aquifer, Accessed September 2016.

High Plains Underground Water Conservation District No. 1 (HPUWCD), 2015. https://static1.squarespace.com/static/53286fe5e4b0bbf6a4535d75/t/56675b030ab377ddbc90f318/1449614083127/AGENDA+ITEM+7+2015+Annual+Report.pdf, Accessed October 2016.

Hill, M. C., 1990, Preconditioned conjugate-gradient 2 (PCG2), a computer program for solving ground-water flow equations: U.S. Geological Survey Water-Resources Investigations Report 90-4048, 43 p.

Houston & T. C. Ry. Co. v. East, 98 Tex. 146, 81 S.W. 279 (1904).

Dutton, A., INTERA, Inc., 2010, Northern Ogallala Update to Support 2011 State Water Plan, 106 p.

Johnson, W. D., 1901, The High Plains and their utilization: U. S. Geological Survey 21st Annual Report, pt. 4-C, p. 601-741.

Knowles, T. R. 1981, Evaluating the ground-water resources of the High Plains of Texas, ground-water simulation program GWSIM-III: Texas Department of Water Resources, UM- 36, 84 p.

Knowles, T. R., 1984, Assessment of the ground-water resources of the Texas High Plains, *in* Whetstone, G. A., ed. Proceedings, Ogallala Aquifer Symposium II: Texas Tech University Water Resources Center, p. 217–237

Knowles, T. R., Nordstrom, Philip, and Klemt, W. B., 1984, Evaluating the ground-water resources of the High Plains of Texas: Texas Department of Water Resources, Final Report LP-173, v. 1, 174 p.

Leake, S. A., Prudic, D. E., Techniques of Water-Resources Investigations of the United States Geological Survey; Documentation of a Computer Program to Simulate Aquifer-System Compaction Using the Modular Finite-Difference Ground-Water Flow Model, Book 6, Chapter A2, 1991, 25p.

Luckey, R. L., and Becker, M. F., 1999, Hydrogeology, water use, and simulation of

flow in the High Plains aquifer in northwestern Oklahoma, southeastern Colorado, southwestern Kansas, northeastern New Mexico, and northwestern Texas: U.S. Geological Survey Water- Resources Investigations Report 99-4104, 68 p.

Luckey, R. R., and Stephens, D. M., 1987, Effect of grid size on digital simulation of ground- water flow in the southern High Plains of Texas and New Mexico: U.S. Geological Survey Water-Resources Investigations Report 87-4085, 32 p.

Mace, R. E., and Dutton, A. R., 1998, Numerical modeling of groundwater flow in the Ogallala aquifer in Texas, *in* Castellanos, J. Z., Carrillo, J. J., and Yanez, C. H., eds., Memoria del Simposio Internacional de Aguas Subterraneas: Sociedad Mexicana de la Ciencia del Suelo, p. 98–109.

McAda, D. P., 1984, Projected water-level declines in the Ogallala aquifer in Lea County, New Mexico: U.S. Geological Survey Water-Resources Investigations Report 84-4062, 84 p.

McDonald, M. G.; and A. W. Harbaugh, 1988, A modular three-dimensional finite-

difference ground-water flow model: U. S. Geological Survey Open-File Report 83-875, 588 p.

McGuire, V. L., 2014, Water-level Changes and Change in Water Storage in the High Plains Aquifer, Predevelopment to 2013 and 2011 to 2013, U. S. Geological Survey Scientific Investigations Report 2014-5218, 14p. *http://dx.doi.org/10.3133/sir20145218.*

McGuire, V.L., Johnson, M.R., Schieffer, R.L., Stanton, J.S., Sebree, S.K., and Verstraeten, I.M., 2003, Water in storage and approaches to ground-water management, High Plains aquifer, 2000: U.S. Geological Survey Circular 1243, 51 p.

Mitchell, R. J.,Lecture 21: Groundwater: Hydraulic Conductivity, http://geology.wwu.edu/rjmitch/L21_groundwater2.pdf Accessed January 3, 2016.

Mullican, W. F., III, 1995, A technical review of the Canadian River Municipal Water Authority application for permit to transport water from Roberts and Hutchinson Counties: Panhandle Ground Water Conservation District, variously paginated.

Mullican, W. F., III, Johns, N. D., and Fryar, A. E., 1997, Playas and recharge of the Ogallala aquifer on the southern High Plains of Texas—an examination using numerical techniques: The University of Texas at Austin, Bureau of Economic Geology Report of Investigations No. 242, 72 p.

Narasimhan, B., R. Srinivasan, S. Quiring, and J. Nielsen-Gammon (2008), Digital climatic atlas of Texas, *Report 2005-483-5591*, Texas Water Development Board Contract, Texas A&M University, TX.

National Weather Service. Data obtained by author

Nativ, Ronit, and Riggio, Robert, 1989, Meteorologic and isotopic characteristics of precipitation events with implications for ground-water recharge, southern High Plains: Atmospheric Research v. 23, p. 51-82.

Nativ, Ronit, and Smith, D. A., 1987, Hydrogeology and geochemistry of the Ogallala aquifer, southern High Plains. Journal of Hydrology v. 91,217-253.

North Plains Groundwater Conservations District, 2016, http://northplainsgcd.org/conservationprograms/agricultural-conservation/, Accessed December 2016.

Osterkamp, W. R., and Wood, W. W., 1987, Playa-lake basins on the southern High Plains of Texas and New Mexico: part I. hydrologic, geomorphic, and geologic evidence for their development. Geological Society of America Bulletin v. 99, 215-223.

Oupao, C. Z., Stewart, B. A., DeOtte, Jr., R. E., 2014. Agronomic Water Mass Balance vs. Well Measurement for Assessing Ogallala Aquifer Depletion in the Texas Panhandle. Journal of the American Water Resources Association (JAWRA) 50(2): 483-496. DOI: 10.1111/jawr.12134.

Panhandle Water Planning Group. http://panhandlewater.org/ Accessed 2015.

Peckham, D. S., and J. B. Ashworth, 1993, The High Plains aquifer system of Texas; 1980 to 1990 overview and projections: Texas Water Development Board 341, p. 1–13.

Qi, S.L., Scott C. 2010. Assessing groundwater availability in the High Plains aquifer in parts of Colorado, Kansas, Nebraska, New Mexico, Oklahoma, South Dakota, Texas,

and Wyoming. Albuquerque (New Mexico): U.S. Geological Survey. Fact Sheet FS-2010-3008.

Rossman, N. R., Zlotnik, V. A., 2013, Review: Regional groundwater flow modeling in heavily irrigated basins of selected states in the western United States, Hydrogeology Journal, 21, 1173-1192, doi: 10.1007/s10040-013-1010-3.

Ryder, P.D., 1996, Ground Water Atlas of the United States-Segment 4: Oklahoma, Texas, ed. 1.0, Hydrologic Investigations Atlas HA 730-E, Reston, VA, Published by USGS. http://pubs.usgs.gov/ha/ha730/ch_e/E-text5.html, Accessed June 2016.

Schultz, G. E., 1977, The Ogallala Formation and its vertebrate faunas in the Texas and Oklahoma Panhandles, *in* Schultz, G. E., ed., Field conference on Late Cenozoic biostratigraphy of the Texas Panhandle and adjacent Oklahoma, August 4-6, 1977, Guidebook: West Texas State University, Department of Geology and Anthropology, Killgore Research Center Special Publication no. 1, p. 5-104.

Schwarz, C. R., and Wade, E.B., 1990, The North American datum of 1983, Project Methodolgy and Execution, Journal of Geodesy, v. 64, p. 28-62.

Simpkins, W. W., and Fogg, G. E., 1982, Preliminary modeling of groundwater flow near salt- dissolution zones, Texas Panhandle, *in* Gustavson, T. C., and others, Geology and geohydrology of the Palo Duro Basin, Texas: The University of Texas at Austin, Bureau of Economic Geology Geological Circular 82-7, p. 130–137.

Snyder, J.P., 1987, Map Projections, A Working Manual, U.S. Geological Survey Paper 1395.

Stovall, J. N., 2001, Groundwater Modeling for the Southern High Plains: Texas Tech University, Ph.D. dissertation, 307 p.

Texas Administrative Code. Title 31, Part 10, Chapter 356, Subchapter A, Ruler 356.10 (7), Desired Future Conditions. http://texreg.sos.state.tx.us/public/readtac$ext.TacPage?sl=R&app=9&p_dir=&p_rloc=&p_tloc=&p_ploc=&pg=1&p_tac=&ti=31&pt=10&ch=356&rl=10, Accessed October 2016.

Texas Constitution Online. Article 1. Bill of Rights. Section 17, Taking, Damaging, or Destroying Property for Public Use; Special Privileges and Immunities; Control of Privileges and Franchises. http://www.statutes.legis.state.tx.us/SOTWDocs/CN/htm/CN.1.htm, Accessed October 2016.

Texas Constitution. Article 16, Section 59. General provisions. 1917. http://www.statutes.legis.state.tx.us/Docs/CN/htm/CN.16.htm , Accessed August 2016.

Texas Legislature Online, 1997, http://www.capitol.state.tx.us/BillLookup/History.aspx?LegSess=75R&Bill=SB1 , Accessed August 2016.

Texas Water Development Board, 1996, Surveys of irrigation in Texas 1958, 1964, 1969, 1974, 1979, 1984, 1989, and 1994: Austin, Texas, Report 347, 59 p.

Texas Water Development Board, 2001, Surveys of irrigation in Texas, 1958, 1964, 1969, 1974, 1979, 1984, 1994, and 2000: Texas Water Development Board, Report 347,

https://www.twdb.texas.gov/publications/reports/numbered_reports/doc/R347/R347.pdf, Accessed December 2016.

Texas Water Development Board, 2016, Ground water database: Texas Water Development Board, http://www.twdb.texas.gov/groundwater/management_areas/index.asp , Accessed October 2016.

Theis, C. V., 1937, Amount of Ground Water Recharge in the Southern High Plains: Am. Geophys. Union Trans., 18th Ann. Mtg., p. 564-568.

United Nations, 2012, The Millennium Development Goals Report, 72 p., http://www.un.org/millenniumgoals/pdf/MDG%20Report%202012.pdf, Accessed June 2016.

U.S. Department of Agriculture, Natural Resources Conservation Service. National soil survey handbook, title 430-VI. http://www.nrcs.usda.gov/wps/portal/nrcs/detail/soils/ref/?cid=nrcs142p2_054242 accessed October 5, 2016.

U.S. Geological Survey, 1997, Modeling Ground-Water Flow with MODFLOW and Related Programs, Fact Sheet FS-121-97, https://pubs.usgs.gov/fs/FS-121-97/fs-121-97.pdf, Accessed June 2016.

U.S. Geological Survey, 2014, High Plains Water-Level Monitoring Study, http://ne.water.usgs.gov/ogw/hpwlms/, Accessed June 2016.

U.S. Geological Survey, 2015, URL: http://water.usgs.gov/ogw/aquiferbasics/ext_hpaq.html Page Contact Information: Contact the USGS Office of Groundwater , Page Last Modified: Tuesday, 14-Apr-2015 14:28:12 EDT

Van der Heijde, P., Bachmat, Y., Bredehoeft, J., et al. (1985), Groundwater management: the use of numerical models, 2nd Ed. American Geophysical Union, Washington, DC, 180 p.

Ward, Odell. "Re: Wells in District." Message to Glen Green. 1 July 2016. E-mail.

Weeks, J. B., Gutentag, E. D., Heimes, F. J., and Luckey, R. R., 1988, Summary of the High Plains Regional Aquifer-System Analysis in parts of Colorado, Kansas, Nebraska, New Mexico, Oklahoma, South Dakota, Texas, and Wyoming: U.S. Geological Survey Professional Paper 1400-A, 39 p.

Weeks, J. B., Gutentag, E. D., 1981, Bedrock geology, altitude of base, and 1980 saturated thickness of the High Plains aquifer in parts of Colorado, Kansas, Nebraska, New Mexico, Oklahoma, South Dakota, Texas, and Wyoming: U. S. Geological Survey Hydrologic Investigations Atlas HA-648.

Wirojanagud, P., Kreitler, C. W., Smith, D. A., 1986, Numerical Modeling of Regional Groundwater Flow in the Deep-Basin Brine Aquifer of the Palo Duro Basin, Texas Panhandle: The University of Texas at Austin, Bureau of Economic Geology Report of Investigations No. 159, 68 p.

APPENDICES

APPENDIX 1

COPYRIGHT PERMISSON

From: Robert Mitchell <Robert.Mitchell@wwu.edu>
Sent: Wednesday, March 16, 2016 4:29 PM
To: rggreen1
Subject: RE: Permission to use images

Hi Glen-

Feel free to use the images. Could you please send me the url for the site where you accessed them, because I haven't had lectures available online for quite some time.

Good luck with your dissertation.

Regards,

-Bob

Robert Mitchell, Ph.D., L.HG.
Professor
Geology Department
Western Washington University
516 High Street
Bellingham, WA
360-650-3591
robert.mitchell@wwu.edu

WESTERN WASHINGTON UNIVERSITY
GEOLOGY DEPARTMENT

From: rggreen1 [mailto:rggreen1@buffs.wtamu.edu]
Sent: Wednesday, March 16, 2016 12:41 PM

To: Robert Mitchell <Robert.Mitchell@wwu.edu>
Subject: Permission to use images
Dr. Mitchell,

I am a graduate student at West Texas A&M University in Canyon, Texas. I am working on a conceptual groundwater model on a very small scale within the Ogallala Aquifer in the Texas panhandle.

While doing some research on hydraulic conductivity, I came across your Powerpoint (as PDF), Lecture 21: Groundwater: Hydraulic Conductivity. Within that lecture, I saw several images of interest. Specifically, they are the images on slides 39-45 where you illustrate the formation of the cone of depression and demonstrate the influences on the cone.

I wanted to ask for your permission to include those images within my dissertation. They will be referenced as your images and left unchanged. I wasn't sure how to go about doing this since they were from a lecture posted online. I thought the best way to approach this would be to simply ask for permission.

I would be grateful for your consideration of this request.

Thank you,

Glen Green